# CLIMATE CHANGE IMPACTS ON SURFACE WATER BUDGET COMPONENTS USING HIGH-RESOLUTION REGIONAL CLIMATE DATA FOR SNOW-DOMINATED BASINS IN TÜRKİYE

A THESIS SUBMITTED TO
THE GRADUATE SCHOOL OF NATURAL AND APPLIED SCIENCES
OF
MIDDLE EAST TECHNICAL UNIVERSITY

BY

BUSE KARAKÖSE

IN PARTIAL FULFILLMENT OF THE REQUIREMENTS
FOR
THE DEGREE OF MASTER OF SCIENCE
IN
CIVIL ENGINEERING

DECEMBER 2023

Approval of the thesis:

CLIMATE CHANGE IMPACTS ON SURFACE WATER BUDGET COMPONENTS USING HIGH-RESOLUTION REGIONAL CLIMATE DATA FOR SNOW-DOMINATED BASINS IN TÜRKİYE

submitted by **Buse KARAKÖSE** in partial fulfillment of the requirements for the degree of **Master of Science** i**n Civil Engineering, Middle East Technical University** by

Prof. Dr. Halil Kalıpçılar
Dean, **Graduate School of Natural and Applied Sciences** _____

Prof. Dr. Erdem Canbay
Head of the Department, **Civil Engineering** _____

Prof. Dr. İsmail Yücel
Supervisor, **Civil Engineering, METU** _____

**Examining Committee Members:**

Assoc. Prof. Dr. Tuğrul Yılmaz
Civil Engineering, METU _____

Prof. Dr. İsmail Yücel
Civil Engineering, METU _____

Assoc. Prof. Dr. Koray Kamil Yılmaz
Geological Engineering, METU _____

Assoc. Prof. Dr. Ali Ercan
Civil Engineering, METU _____

Assoc. Prof. Dr. Sertaç Oruç
Civil Engineering, Çankırı Karatekin University _____

Date:11.12.2023

**I hereby declare that all information in this document has been obtained and presented in accordance with academic rules and ethical conduct. I also declare that, as required by these rules and conduct, I have fully cited and referenced all material and results that are not original to this work.**

Name Last name : Buse Karaköse

Signature :

# ABSTRACT

## CLIMATE CHANGE IMPACTS ON SURFACE WATER BUDGET COMPONENTS USING HIGH-RESOLUTION REGIONAL CLIMATE DATA FOR SNOW-DOMINATED BASINS IN TÜRKİYE

Karaköse, Buse
Master of Science, Civil Engineering
Supervisor: Prof. Dr. İsmail Yücel

December 2023, 124 pages

In recent years, there has been an increasing global concern regarding the issue of climate change. As a result of this phenomenon, there has been a noticeable trend towards water scarcity, often accompanied by extreme weather events, floods, and droughts. This thesis focuses on the impacts of climate change on surface water budget components of seven snow-dominated basins (Tigris, Euphrates, Aras, Coruh, Western Black Sea, Eastern Mediterranean, and Susurluk) in Türkiye. A comparative analysis was conducted between a 20-year reference period (1995-2014) and a corresponding pseudo-future period (2081-2100), examining the observed changes between the two intervals. The high resolution (4 km) data used in this study were obtained by Weather Research and Forecasting (WRF) simulations using ERA5 reanalysis data for the 1995-2014 and using perturbed ERA5 reanalysis data by the Pseudo Global Warming (PGW) method (with 13 Coupled Model Intercomparison Project Phase 6 (CMIP6) Global Climate Models (GCMs) under Shared Socio-Economic Pathway, SSP5-8.5 emission scenario) for 2081-2100. This study is the first water budget analysis conducted in Türkiye using high spatial

resolution data (4 km) obtained with the latest version of GCMs and high emission scenario.

Firstly, precipitation, Evapotranspiration (ET), and Snow Water Equivalent (SWE) maps for the reference period throughout Türkiye and anomaly maps showing the difference between the future and reference periods were created. Secondly, water budget analyses were carried out for the catchments selected in this study. With this analysis, the relationship of the water budget variables, both within themselves and with each other, could be observed inter and intra-years. According to the water budget analysis, a 1.4%, 4%, and 1% decrease in precipitation is expected in the Tigris, Eastern Mediterranean, and Susurluk basins, respectively. In comparison, an increase of 6.3%, 33%, 29%, and 3.8% is expected in the Euphrates, Aras, Coruh, and Western Black Sea basins. Thirdly, focusing on the SWE variable, the changes in the average SWE values and inter-annual variability were examined. It has been determined that there will be a substantial decrease in peak SWE values and a shrinkage of approximately 20%-40% in all selected basins during the snow season.

Additionally, the study scrutinized how terrestrial water storage anomaly (TWSA) is influenced by variables such as snow water equivalent anomaly (SWEA) and soil water storage anomaly (SWSA). Based on TWSA graphs, it has been predicted that the impact of snow will be substituted by soil water storage. Moreover, the Eastern Mediterranean and Tigris basins will experience the most significant reduction in peak storage values in March, with a decline of 36% and 25%, respectively. Finally, the evaluation of surface runoff fraction values indicates that peak values occurred earlier in the future, especially in the Tigris and Euphrates basins. These findings suggest that snowmelt periods will occur earlier in the future period, and precipitation type will change from snow to rain.

Keywords: Climate Change, Water Budget, Weather Research and Forecasting Model, Pseudo Global Warming, Coupled Model Intercomparison Project Phase 6 Global Climate Models

# ÖZ

## TÜRKİYE'DE KAR HAKİM HAVZALAR İÇİN YÜKSEK ÇÖZÜNÜRLÜKLÜ BÖLGESEL İKLİM VERİLERİ KULLANILARAK YÜZEY SUYU BÜTÇESİ BİLEŞENLERİ ÜZERİNDE İKLİM DEĞİŞİKLİĞİ ETKİLERİ

Karaköse, Buse
Yüksek Lisans, İnşaat Mühendisliği
Tez Yöneticisi: Prof. Dr. İsmail Yücel

Aralık 2023, 124 sayfa

Son yıllarda iklim değişikliği konusunda küresel ölçekte artan bir endişe söz konusudur. Bu olgunun bir sonucu olarak, genellikle aşırı hava olayları, seller ve kuraklıkların eşlik ettiği su kıtlığına doğru gözle görülür bir eğilim olmuştur. Bu tez, iklim değişikliğinin Türkiye'deki kar ağırlıklı yedi havzanın (Dicle, Fırat, Aras, Çoruh, Batı Karadeniz, Doğu Akdeniz ve Susurluk) yüzey suyu bütçesi bileşenleri üzerindeki etkilerine odaklanmaktadır. Bu çalışmada, 20 yıllık referans dönem (1995-2014) ile buna karşılık gelen sözde gelecek dönem (2081-2100) arasında karşılaştırmalı bir analiz yapılmış ve iki aralık arasında gözlenen değişiklikler incelenmiştir. Bu çalışmada kullanılan yüksek çözünürlüklü (4 km) veriler, 1995-2014 dönemi için ERA5 yeniden analiz verileri kullanılarak Hava Durumu Araştırma ve Tahmin (WRF) simülasyonları ve 2081-2100 dönemi için Sözde Küresel Isınma (PGW) yöntemiyle (Paylaşımlı Sosyo-Ekonomik Rotalar, SSP5-8.5 emisyon senaryosu altında 13 Birleşik Model Karşılaştırma Projesi Aşama 6 (CMIP6) Küresel İklim Modelleri (GCM'ler) ile) pertürbe edilmiş ERA5 yeniden

analiz verileri kullanılarak elde edilmiştir. Bu çalışma, GCM'lerin son versiyonu ve yüksek emisyon senaryosu ile elde edilen yüksek mekânsal çözünürlüklü veriler (4 km) kullanılarak Türkiye'de yapılan ilk su bütçesi analizidir.

İlk olarak, Türkiye genelinde referans dönem için yağış, evapotranspirasyon (ET) ve kar suyu eşdeğeri (SWE) haritaları ve gelecek dönem ile referans dönem arasındaki farkı gösteren anomali haritaları oluşturulmuştur. İkinci olarak, bu çalışmada seçilen havzalar için su bütçesi analizleri gerçekleştirilmiştir. Bu analiz ile su bütçesi değişkenlerinin hem kendi içlerinde hem de birbirleri ile olan ilişkileri yıllar arası ve yıl içi olarak gözlemlenebilmiştir. Su bütçesi analizine göre, Dicle, Doğu Akdeniz ve Susurluk havzalarında yağışlarda sırasıyla %1,4, %4 ve %1 oranında azalma beklenmektedir. Buna karşılık, Fırat, Aras, Çoruh ve Batı Karadeniz havzalarında sırasıyla %6,3, %33, %29 ve %3,8'lik bir artış beklenmektedir. Üçüncü olarak, SWE değişkenine odaklanılarak, ortalama SWE değerlerindeki değişimler ve yıllar arası değişkenlik incelenmiştir. Kar sezonu boyunca seçilen tüm havzalarda pik SWE değerlerinde önemli bir düşüş ve yaklaşık %20-%40 oranında bir küçülme olacağı tespit edilmiştir.

Çalışmada ayrıca karasal su depolama anomalisinin (TWSA) kar su eşdeğeri anomalisi (SWEA) ve toprak su depolama anomalisi (SWSA) gibi değişkenlerden nasıl etkilendiği incelenmiştir. TWSA grafiklerine dayanarak, karın etkisinin toprak su depolaması ile ikame edileceği öngörülmüştür. Ayrıca, Doğu Akdeniz ve Dicle havzaları mart ayında sırasıyla %36 ve %25'lik bir düşüşle pik depolama değerlerinde en önemli azalmayı yaşayacaktır. Son olarak, yüzey akış fraksiyonu değerlerinin değerlendirilmesi, özellikle Dicle ve Fırat havzalarında pik değerlerin gelecekte daha erken gerçekleşeceğini göstermektedir. Bu bulgular, gelecek dönemde kar erime dönemlerinin daha erken gerçekleşeceğini ve yağış türünün kardan yağmura doğru değişeceğini göstermektedir.

Anahtar Kelimeler: İklim Değişikliği, Su Bütçesi, Hava Durumu Araştırma ve Tahmin Modeli, Sözde Küresel Isınma, Birleşik Model Karşılaştırma Projesi Aşama 6 Küresel İklim Modelleri

To my youth…

## ACKNOWLEDGMENTS

First of all, I would like to express my endless gratitude to my advisor, Prof. Dr. İsmail Yücel, for guiding me and always supporting me in this long and challenging journey. His encouragement has been invaluable and served as a motivating force to me. I am sincerely grateful for the impact he has had on my academic and personal growth.

Committee members: Assoc. Prof. Dr. Tuğrul Yılmaz, Assoc. Prof. Dr. Koray Kamil Yılmaz, Assoc Porf. Dr. Ali Ercan and Assoc. Prof. Dr. Sertaç Oruç guided me with their vast knowledge and experience. I express my gratitude to them for sparing their valuable time and assisting me in improving my thesis.

I want to thank Soner Çağatay Bağçacı for providing the necessary data for this study and for patiently answering all my questions.

I wish to thank Eren Düzenli and Berkin Gümüş for always taking the time to generously share their knowledge and experiences with me, regardless of the circumstances. Their motivation and encouragement were invaluable to me, and I am truly grateful for their unwavering help. I am also thankful to Ali Cem Çatal for his time, constant help, and efforts in solving the technical problems I encountered.

I cannot express enough gratitude towards my parents, Serap Karaköse, Osman Karaköse, and my brother Fırat Karaköse, who have been my biggest supporters. I consider myself extremely fortunate to have such a wonderful family. They always believe in me more than I believe in myself and have been my constant support system, picking me up every time I fall. I owe all my success to them, and I could not have accomplished anything without their endless love and support.

I would like to thank Hanife Barut and Hande Barut for being there with me through every moment of this challenging process. I am deeply thankful to these amazing

women who have played the role of spiritual sisters and even mother in my life and for making me believe in myself with their support.

I would like to thank my other sister, Zelal Köksal. I am grateful for her friendship as she has been by my side since the beginning of my undergraduate life, facing every challenge with me and being my unwavering source of support and motivation.

I would also like to thank Sertaç Fatih Ünal. I am grateful to him for being a colleague and friend who always listens to me patiently, calms me down when necessary, and always makes me feel his support.

## TABLE OF CONTENTS

## LIST OF TABLES

TABLES

## LIST OF FIGURES

FIGURES

## LIST OF ABBREVIATIONS

ABBREVIATIONS

| | |
|---|---|
| CMIP6 | Coupled Model Intercomparison Project 6 |
| DJF | December-January-February |
| ESM | Earth System Model |
| ET | Evapotranspiration |
| GCM | Global Climate Model |
| JJA | June-July-August |
| LSM | Land Surface Model |
| MAM | March-April-May |
| NWP | Numerical Weather Prediction |
| PGW | Pseudo Global Warming |
| RCM | Regional Climate Model |
| RCP | Representative Concentration Pathway |
| SFROFF | Surface Runoff |
| SON | September-October-November |
| SSP | Shared Socioeconomic Pathway |
| SWE | Snow Water Equivalent |
| SWS | Soil Water Storage |
| TWS | Terrestrial Water Storage |
| TWSA | Terrestrial Water Storage Anomaly |

| | |
|---|---|
| WPS | WRF Preprocessing System |
| WRF | Weather Research and Forecasting |

# CHAPTER 1

# INTRODUCTION

In this section, a general introduction is made about the main subjects of the study, namely climate change, water budget, and terrestrial water storage, and the purpose of the study is mentioned.

## 1.1 Introduction

Climate change is one urgent global issue that has received much attention recently. Its effects are felt worldwide, affecting people, the environment, and the economy. Scientists, policymakers, and the public increasingly know that rising temperatures, extreme weather, and long-term disruption of natural systems are all linked.

The amount of greenhouse gases released into the atmosphere may significantly impact the Earth's surface's global warming over the following decades, according to the Intergovernmental Panel on Climate Change (IPCC) (Molina et al., 2020).

Climate models predict an even more pronounced shift in the future than the one that has already been observed (Kundzewicz, 2008). By 2100, models predict a 2-degree increase in global mean surface temperature over 1990 levels, based on the IPCC's mid-range emission scenario and the best estimate of climate sensitivity. However, a projected warming of roughly 3.5 degrees arises when combining the highest IPCC emissivity scenario with a high climate sensitivity (Frederick & Major, 1997). However, there is still much uncertainty about how and when the climate will change, as well as how this will impact the supply and demand for water at the river basin and watershed levels, despite recent advancements in the science of climate change (Frederick & Major, 1997).

The water cycle is predicted to change due to climate change (Haddeland et al., 2014). Frederick and Gleick (1999) stated that while variations in precipitation have an impact on runoff patterns, groundwater recharge characteristics, and the timing and intensity of floods and droughts, temperature variations have an impact on cloud characteristics, soil moisture, snowfall, and snowmelt regimes, and the rate at which water evaporates from the earth's surface or transpires from plants. Previous studies showed that increased precipitation causes an increase in mean river flow, while increased temperature causes a decrease in flow (Claessens et al., 2006; Frederick & Gleick, 1999).

The National Research Council (NCR) emphasized an increasing need to predict how watersheds will respond to global climate change, as climate change can significantly impact a watershed's hydrology. (Claessens et al., 2006). The effects of climate change and human activity on water resources can be understood by examining changes in an area's water budget over time (Molina et al., 2020) since a water budget is necessary for consistent budget component estimates (Zhang et al., 2018). The water budget analysis includes measuring inputs, outputs, and changes in water storage to provide helpful information regarding managing total water resources.

Water budgets can be evaluated many times and on different space scales. However, as these scales shrink (like until the river basin), more detail can be added to the analysis until it can provide information on the values of overland runoff, subsurface flow, soil moisture storage, and evapotranspiration losses from soil and vegetation on a daily, weekly, and monthly basis (Hanson, 2001). Therefore, water budget analysis is a sound basis for water management (Mollema et al., 2012).

The latest generation of comprehensive Earth system models (ESMs) are used in Phase 6 of the Coupled Model Intercomparison Project (CMIP6), which is driven by historical greenhouse gas concentrations and followed by different future greenhouse gas and aerosol concentrations based on the Shared Socioeconomic Pathways (SSP) scenarios (Tokarska et al., 2020). It expands on the previous phase 5 (Taylor et al.,

2012) and provides new opportunities (Grose et al., 2020). CMIP6 models are recently organized experiments in global climate modeling designed to provide insight into various climate responses and mechanisms, and they generally have finer resolution with improved dynamical processes (Chen et al., 2020).

Previous studies show that the performance of CMIP6 models is better than CMIP5 models. Bagcaci et al. (2021) compared the temperature and precipitation changes obtained with the CMIP5 and CMIP6 models for all Türkiye located in the Mediterranean region called climate hotspots. They emphasized that in the results obtained with CMIP6, the error for temperature and precipitation is lower, and the correlation for precipitation is higher than CMIP5.

LSMs (land surface models) (Pokhrel et al., 2021; Pokhrel et al., 2015) and GHMs (Global hydrological models) (Pokhrel et al., 2021; Doll et al., 2014; Hanasaki et al., 2018) have better represented terrestrial water storage (TWS) thanks to recent modeling advances, and the Gravity Recovery and Climate Experiment (GRACE) satellite mission (Pokhrel et al., 2021) has given an additional opportunity to enhance and validate TWS simulations in these models (Pokhrel et al., 2021). These gravity maps can infer sea level change, ice loss, and global and regional variations in terrestrial water storage (Girotto & Rodell, 2019). The terrestrial carbon sink is significantly impacted by the interannual variations in terrestrial water storage, both globally and regionally (L. Guo et al., 2021;Fang et al., 2017; Humphrey et al., 2018).

## 1.2 Scope of the Study

Türkiye is a crucial area for investigating the changes in the components of the surface water budget due to its diverse climate, geography, and hydrological features. Furthermore, the country is highly vulnerable to climate change as it is located in the Mediterranean hotspot region worldwide.

Bagcaci et al. (2021) found that the CMIP6 climate models outperformed the CMIP5 models in predicting precipitation and temperature in Türkiye. In a subsequent study, Bagcaci et al. (2023) conducted very high-resolution (4km) regional climate simulations for Türkiye using the Weather Research and Forecasting (WRF) model and an ensemble of CMIP6 climate models.

In this study of climate simulations, the WRF model replicated the historical period (1995-2014) by using data from ECMWF ERA5 reanalysis. For the future projection spanning 2081-2100, the WRF model employed a pseudo global warming method, which involved adjusting the historical ERA5 forcings based on future climate changes derived from the ensemble of CMIP6 models under the SSP5 8.5 emission scenario. Given the access to detailed regional climate simulations of Türkiye using the latest climate projections from CMIP6, it is crucial to revise the effects of climate change on the elements of surface water budgets for various significant snow-dominated basins in Türkiye. Hence, the objective of this thesis is to evaluate the various elements of the monthly surface water budget and explore the potential effects of climate change on these components in the future, specifically in snow-dominated high mountainous basins. The surface water budget elements in WRF historical and future projections include precipitation, snow water equivalent (SWE), columnar soil moisture, evapotranspiration (ET), surface runoff, and interflow. These are provided at a resolution of 4 kilometers and in hourly intervals for analysis.

In reaching the goal of this thesis study, the following objectives are carried out:

- To achieve the lowest residual values using the water budget equation and assess the equilibrium among the elements.
- To investigate the variations in precipitation, evapotranspiration, and snow water equivalent within Türkiye on a yearly and seasonal basis.
- To gain a main understanding of the impact of climate change and to compare the values of the water budget components between the reference period and its simulated future pseudo period on different snow-dominated basins.

- To compare the terrestrial water storage values between two time periods, analyze their fluctuations, and evaluate the efficacy of snow and soil moisture within a specific basin.
- To identify the periods of snow accumulation and melting throughout the water year using daily average snow water equivalent values and to assess how these patterns may change in the future.
- To understand the alteration in the timing of snowmelt runoff in basins as a result of climate change.

The findings may affect water resource management, planning, and climate change adaptation in Türkiye.

# CHAPTER 2

# LITERATURE REVIEW

This section explains the concept of the surface water budget and its components, examples of other studies conducted in this field, and the difficulties and gaps are mentioned.

## 2.1 Water Budget Concept and Components

The water budget can be explained as the conservation equation. It represents a method for quantifying the entirety of water inflows, outflows, and alterations in water storage within a specified study area (Levin et al., 2023). In simpler terms, the system's inflow, outflow, and water storage should balance each other (Bales et al., 2010). Although the equation of the water budget is simple and flexible (Healy et al., 2007), developing an accurate water budget can be a challenging endeavor (Maven, 2020), and its outputs are of great importance. Because it provides an understanding of historical conditions and facilitates comprehension of the potential impacts on water resources within the area stemming from future alterations in supply, demand, hydrology, population, land use, and climate (Maven, 2020).

Water budget components are the individual factors that contribute to the water balance in a specific area. An example illustration of water budget components is given in Figure 2.1. These components may vary on a study basis, depending on the study area's climatic characteristics, the study's purpose, or data availability. Khan et al. (2018) stated that a water budget may include some, all, or none of the components depicted in this diagram (Figure 2.1), depending on each item's specific needs and importance for a given area. The land and surface water systems would be

the only emphasis of the water budget in an area devoid of groundwater (Khan et al., 2018).

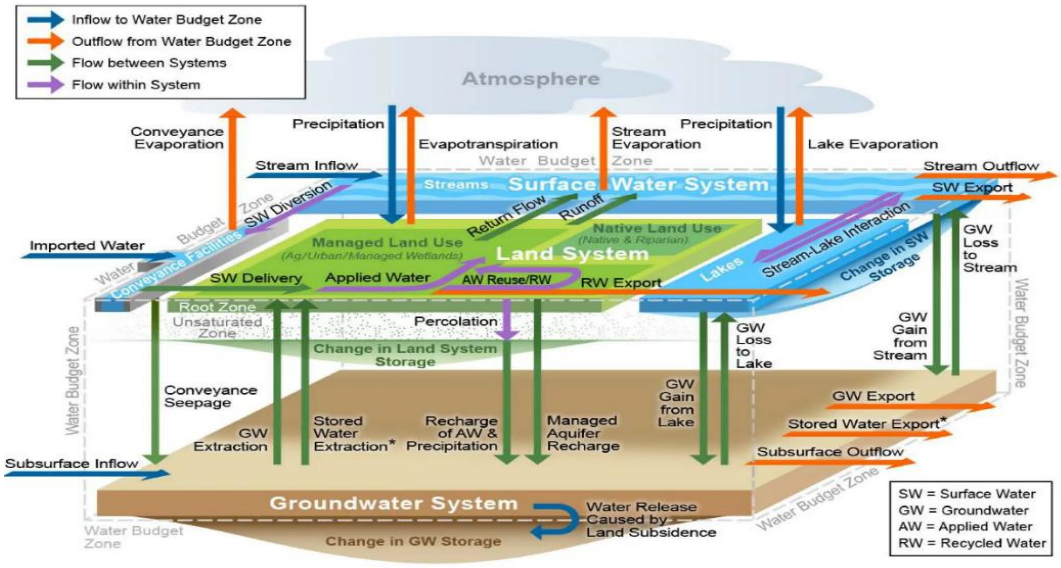


Figure 2.1. Conceptual water budget (Handbook for Water Budget Development, 2018).

This study uses precipitation, surface runoff, interflow, evapotranspiration, snow water equivalent, and soil moisture variables. Detailed information about these components is given in the Water Studies section.

## 2.2 Water Budget Studies

Fersch et al. (2020) focused on evaluating a fully coupled atmospheric-hydrological model in various parts of the water and energy cycle. In this context, in the area covered by the Ammer and Rott river basins in southern Bavaria, Germany, they made monthly water budget analysis by using precipitation, evapotranspiration, surface and subsurface runoff, and soil variation for WRF_SA (standalone WRF), WRF-H_FC (fully coupled WRF-Hydro), WRF-H_SA (standalone WRF-Hydro) simulations. According to the authors, the analysis of sub-basin water budgets revealed a clear link between precipitation, soil infiltration, evapotranspiration, and

discharge deviations. They also pointed out that the other terms of the water balance equation, soil water storage change, and percolation, did not show distinct trends between the standard and coupled simulations, which could be attributed to inter-sub catchment variations in infiltration and percolation parameters.

Zheng et al. (n.d.) conducted a Terrestrial Water Budget study based on the Land Surface Model (LSM). They simulated the monthly Terrestrial Water Budget from 1980 to 2015 at a spatial resolution of 1/8° over the continental United States (CONUS). As an extension to the NLDAS-2 four-LSM, they set up a 48-member perturbed-physics ensemble based on the Noah LSM utilizing multi-physics options (Noah-MP). Their main concern was the assessment of the estimated TWSA, soil moisture, SWE, and ET about the NLDAS ensemble. At the end of the study, they mentioned that the Noah-MP perturbed-physics ensemble helps improve water budget estimations over CONUS and identify model deficiencies.

(Duzenli, 2022) obtained monthly water budget graphs over the Arhavi basin in the Eastern Black Sea (EBS) and the Kemer basin in the Mediterranean (MED) with three models, which are WRS-SA, WRF-Coup, WRF-SM-Coup. They stated that the coupled model's interflow contribution is higher in spring because they yield more snowmelt than the standalone WRF. They realized that for all models of the EBS region, underground runoff contributes primarily to the total streamflow. Also, infiltrated water was distributed to the lower elevations with the coupled model's subsurface routing options. For the Kemer basin, they found that both coupled models reduce the precipitation predicted by WRF-SA because of the influence of surface energy exchanges under semi-arid climate conditions. Also, because of the increased soil moisture deficit, the infiltration of the soil causes the streamflow to be mainly contributed to by the interflow, whereas the precipitation occurs in the spring. Luo et al. (2023) evaluated water budget closure residual error (ΔRes) over China. They used precipitation (P), evapotranspiration (ET), streamflow (R), and terrestrial water budget storage change (TWSC) as components of the water budget. They evaluated the accuracy of water budget closure in satellite/reanalysis-based hydrological data products. As a P product, GPM IMERG, TRMM 3B43,

PERSIANN-CDR, ERA5, GLDAS, and FLDAS, and multiple datasets for other components were used in the study. End of the study, the authors determined that the ΔRes changes between ±15 mm. Because the selected datasets of additional budget components (ET and R) are also derived from reanalysis datasets, reanalysis P products such as GLDAS and FLDAS showed better water budget closure.

Yoon et al. (2019) used a suite of uncoupled LSM simulations forced with prescribed meteorology to investigate the errors and uncertainties in key terrestrial water budget variables such as precipitation, evapotranspiration, runoff, terrestrial water storage, and snow cover over HMA. They found that the uncertainty and spread of P (precipitation), ET (evapotranspiration), and R (runoff) were significantly more significant when they compared mean annual estimates of surface water balance components with global estimates from previous studies. Additionally, they discovered that the input meteorology plays a crucial role in water budget characterization over HMA when comparing changes in ET, snow cover rate, and TWS (terrestrial water storage) estimates with remote sensing-based references.
It is important to note that to ensure the conservation of mass, the evapotranspiration (ET) must be equal to the total precipitation minus the net runoff minus the change in total terrestrial water storage (TWS), as explained by Rodell et al. (2011). To estimate the mean ET, they used a combination of satellite and ground-based observations and calculated it as a residual of the water budget. They demonstrate that although the uncertainty in the mean annual cycle is small enough to make it feasible to evaluate other ET products, the uncertainty in the water budget-based estimates of monthly ET is frequently too large for those estimates to be useful.

### 2.3 The Effect of Climate Change on Water Resources in Türkiye

Bagcaci (2023) evaluated current and future climate projections for Türkiye and the large-scale EMBS (Eastern Mediterranean Black Sea Region). This study involved several different components, including a comparison of the performance of CMIP6 and CMIP5, future climate projections for both medium-range SSP2-4.5 and high-

range SSP5-8.5 scenarios, testing of various RCM physics options through dynamic downscaling of ERA5-reanalyses, obtaining a retrospective hourly dataset with the WRF model at a 4 km resolution, and future climate projections using PGW under the CMIP6 SSP5-8.5 emission scenario. It has been observed that CMIP6s have better performance than CMIP5s, especially for precipitation data. Future and current period precipitation differences were examined seasonally, and it was stated that, in general, an increase in precipitation was expected in the northern part of Türkiye and a decrease in the southern part. According to the author, this study is critical because the data obtained are the highest resolution data known for Türkiye. It also pioneers the research of extreme weather conditions, snow cover loss, etc., and so understanding the effects of climate change in Türkiye.

Fujihara et al. (2008) explored the potential impacts of climate change on the hydrology and water resources of the Seyhan River Basin in Türkiye. A dynamical downscaling method, the pseudo global warming method (PGWM), was used to connect the outputs of GCMs and river basin hydrologic models. MRI-CGCM2 and CSR/NIES/FRCGC-MIROC under the SRES A2 scenario were used as GCMs, and the two 10-year time slices that the downscaled data represented were the present (1990s) and the future (2070s). It was concluded that the temperature and precipitation data, which were downscaled dynamically via bias correction, showed good agreement with the observed data. According to various models, the study predicted that until 2070, the average annual temperature will rise by 2.0–2.7°C, and annual precipitation will fall by 157–182 mm. The PGWM, when coupled with bias correction, was deemed an effective method for producing input data for hydrologic simulations.

Yilmaz & Yazicigil (2011) üuexamined the effects of climate change in two groups, investigating the degree of climate change effects observed in the past and the potential impact of climate change on water resources. According to the authors, the Mediterranean climate region (west and south of Türkiye) will see the most significant changes due to rising temperatures and falling precipitation. After much consideration, they concluded that summer and annual minimum temperatures will

increase while winter precipitation will fall. Additionally, they discovered that variations in atmospheric variables impact groundwater levels and stream flow, indicating that water scarcity may arise in numerous areas.

Durdu (2010) focused on the impact of climate change on water resources in the Büyük Menderes River basin in western Türkiye. According to the data, there has been a significant increase in temperature of about one °C over the past 45 years. Additionally, the annual precipitation trend in the Afyon and Uşak regions has declined, leading to water shortages in the Aydın area. The streamflow of the Çine and Akçay rivers has also shown a downward trend between 1985 and 1998. The author concluded that climate change may have impacted temperature, precipitation, and streamflow changes in the Büyük Menderes River basin.

Yilmaz & Imteaz (2014) evaluated the impact of climate change on hydrometeorology and water resources in Türkiye. It is predicted that temperatures will increase by 2-6°C across the country in the 21st century, and rainfall will decrease in most parts of Türkiye. The Mediterranean and snow-dominated Eastern regions are defined as the most vulnerable regions to climate change. They pointed out that summer temperatures, especially maximum temperatures, may increase significantly, causing more frequent and severe droughts and floods with increased precipitation in the Northern Black Sea region. Finally, they stated that future climate projections show decreased stream flow in water basins in Türkiye.

Özdoğan (2011) studied how climate change would affect the water the Euphrates-Tigris basin mountains store in their seasonal snowpack. It used two scenarios for greenhouse gas emissions, thirteen general circulation models, and two time periods to evaluate possible changes. The findings showed that climate change could significantly reduce the amount of water stored in the snowpack (between 10 and 60 percent), putting more strain on the region's water-dependent societies. The research also revealed that the lowest elevation bands would see the most significant changes (more than 50 percent) in snow water equivalent (SWE). In contrast, the lower basin zones would see a quicker decline in snow accumulation.

Yilmaz et al. (2019) used a high-resolution regional climate model to simulate the effects of irrigation-induced changes in land use and land cover on the regional water and energy balances in the Euphrates-Tigris basin. Three land cover distributions representing the rise in irrigation and water surfaces were used to run historical simulations. The result showed that evapotranspiration increases dramatically as irrigation coverage increases. The authors noted that a significant reduction in sensible heat flux results in local cooling of approximately 0.4 °C under current and 0.8 °C under future irrigation conditions. Conversely, a rise in latent heat flux led to an increase in evapotranspiration and, in turn, in water vapor concentration in the atmosphere. Finally, they concluded that enhanced water loss through evapotranspiration has the potential to alter the water budget of the GAP region significantly.

Bozkurt & Sen (2013) used various GCMs and emissions scenarios to investigate the future climate change impacts in the Euphrates-Tigris basin. They stated that winter temperatures will increase more in the highlands, although winter precipitation decreases in the highlands and northern parts and increases in southern parts. They determined that snow water equivalent will decrease by 55-87% because of warming. They found declines in the annual surface runoff and temporal shifts to earlier days (18-39 days) in the surface runoff timing in the headwater's region. Also, they pointed out that the region's most vulnerable to climate change within the basin will be the lands of Türkiye and Syria.

Yucel et al. (2015) conducted a study to investigate the potential impact of snowmelt on runoff changes in the Euphrates, Tigris, Aras, and Coruh basins. According to their findings, the average temperature increase across all stations is 1.3 ∘C, and the annual precipitation is 7.5%. They predicted that by the end of the current century, the yearly surface runoffs of the Aras, Euphrates, and Tigris basins would decrease by 10% to 30%. In comparison, the annual surface runoff of the Coruh basin would slightly increase (by roughly 4%). They also noted that the timing of peak flows would continue to shift earlier by about four weeks per century in response to further

warming, which could increase the winter flow rate while decreasing the spring flow rate over the year in all these basins.

## 2.4 Challenges and Gaps in Water Budget Studies

The hydrological cycle is a complex journey, and water strives to navigate through this cycle. Thus, monitoring the hydrologic cycle for specific geographic features of interest, like watersheds, reservoirs, or aquifers, presents a formidable challenge to humans (Healy et al., 2007).

Also, Gonzalez et al. (2016) stated that data accessibility is significantly restricted in certain regions, and observational data availability is inconsistent. As a result, constructing a water budget becomes a challenging task.

Extensive literature discusses techniques and detail levels in estimating the hydrological cycle's components. However, there is frequently a lack of information regarding the uncertainty linked to these estimates, which poses a challenging issue for water managers (Levin et al., 2023).

# CHAPTER 3

# METHODOLOGY

The methodology section of the study explains the covered area, the data used, the variables employed for water budget analysis, and how these variables were obtained. Additionally, information is given about the Noah LSM used and the TWSA analysis performed. Figure 3.1 shows the surface water budget analysis flowchart and Figure 3.2 shows the TWSA analysis flowchart.

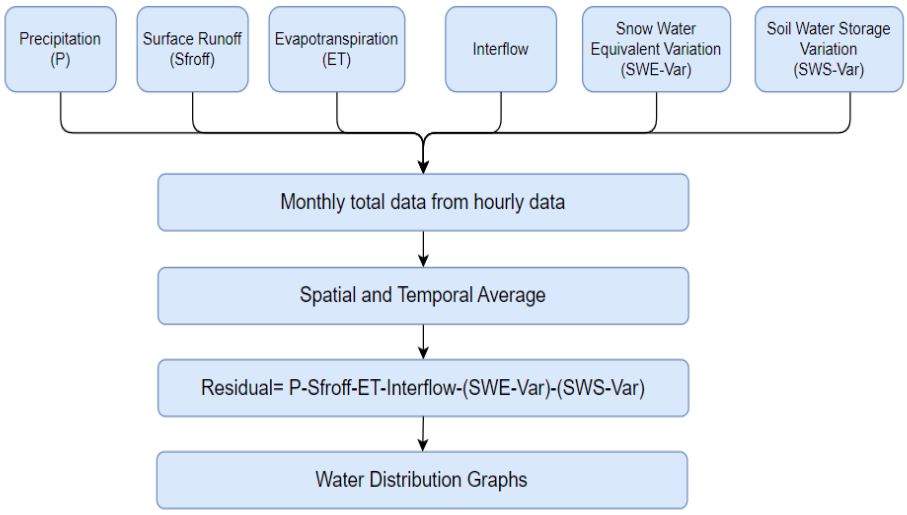


Figure 3.1. The surface water budget analysis flowchart

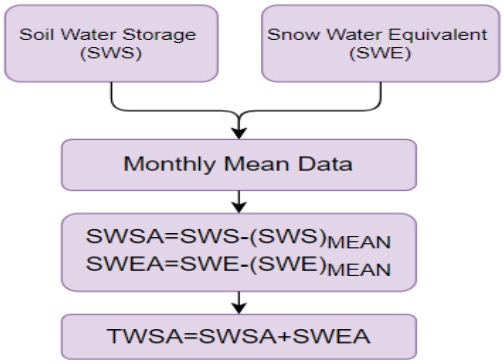


Figure 3.2. TWSA analysis flowchart

## 3.1 Study Area

Türkiye is a country with diverse topography and climate due to its geographical location. The country is surrounded by sea on three sides; coastal areas enjoy a temperate climate, while the mountains running parallel to the coast do not allow the influence of the coast to reach the interior. As a result, different regions in Türkiye can experience varying climatic conditions simultaneously.

The climate zones in Türkiye can be classified under three main headings: Black Sea, Mediterranean, and Continental Climate. The Black Sea Region and the parts of the Marmara region coastal to the Black Sea have a Black Sea climate. In the Black Sea climate, summers are cool, and winters are warm since it rains throughout the year. However, it is snowy and cold in the higher elevations. Most of the Aegean Region, the southern portion of the Taurus Mountains, and the western portion of Central Anatolia experience the Mediterranean climate, characterized by hot, dry summers and rainy winters. Similar to the climate of the Black Sea, snowfall occurs at higher elevations but does not fall along the coast. The continental climate is the climate type with the highest seasonal temperature differences. In general, summers are hot and dry, and winters are snowy. It is dominant in Eastern Anatolia, Southeastern Anatolia, Central Anatolia, and the inner parts of Thrace. Different from the previously mentioned climate types, the southern part of the Marmara region and the northern portion of the Aegean region experiences a transitional climate. This climate type can be expressed as a combination of these three climate types.

In this study, analyses were conducted for seven basins in Türkiye. These are the Tigris, Euphrates, Aras, Coruh, Eastern Mediterranean, Western Black Sea, and Susurluk basins, and are showed in Figure 3.3. These basins are specifically selected because they are represented by highly elevated mountains that receive significant snow during winter and contribute to streamflow with their snowmelt runoff. Moreover, assessing the indication of climate change's effect on snow is a priority for mountainous basins.

The cumulative height frequency curve for a given basin area is called the hipsometric curve. This curve is a graph that plots relative area versus relative height to show the proportion of land area at various elevations. The elevation value indicates the median elevation of that basin in this curve, which corresponds to 50% of the area. As a result, we can better comprehend the basin's topography and climate. Figure 3.4 shows the hypsometric curves of these basins through their median height values. The median heights of these selected basins are represented with an elevation greater than 600 m. Thus, these basins, particularly those in the eastern Anatolia region, are mostly snow-dominated.

The area of the Tigris basin makes up about 7% of Türkiye's total surface area and has a 54.695,7 $km^2$ rainfall area. The median height of the Tigris basin is 1250 m. The basin drained by the Tigris River and its tributaries covers the southeastern part of the Eastern Anatolia region and the eastern part of the Southeastern Anatolia region (Elmastas, 2000). While the southwestern part of the basin experiences a Mediterranean climate, the interior parts experience a continental climate.

The Euphrates basin is quite broad as it covers the Euphrates River and its surroundings and constitutes approximately 16% of Türkiye's surface area. The basin's median height is 1439 m. While summers are hot and dry in the rest of the Southeastern Anatolia region and winters are cold, summer temperatures decrease towards the Eastern Anatolia region, and winter months are freezing and snowy.

The Aras basin, which has a 2013 m median height, covers approximately 3.57% of Türkiye's surface area and has a rainfall area of 28.114 $km^2$. The Aras River, with a length of 548 km, is one of the largest rivers of the Caucasus and is located within the borders of Türkiye. A continental climate prevails in the basin located in the Eastern Anatolia region. This basin contains the highest mountain in Türkiye, Mount Ararat, and the province with the least rainfall, Iğdır.

Coruh basin covers 2.3% of Türkiye's surface area, and its median height is 1910 m. The basin has a transitional climate between the continental and Black Sea climates because it is situated between the Eastern Anatolia and Eastern Black Sea regions.

Regions at higher elevations experience heavy snowfall; springtime brings the most rainfall.

The total rainfall area of the Eastern Mediterranean basin, which constitutes 2.8% of the country, is 21.807 $km^2$. The median height of the basin is 1239 m. The Eastern Mediterranean basin is in the Mediterranean basin and is influenced by the Mediterranean climate in many regions. However, due to the abundance of mountainous areas in the basin, the continental climate prevails in the higher parts, and therefore snowfall is observed (Koçyigit et al., 2021). One of Türkiye's climatically hottest regions, the Mediterranean receives the most sunlight and, consequently, the most radiation. In the basin, the average monthly general temperature is 17.78 °C.

The Western Black Sea basin has a rainfall area of 28.855 $km^2$, making up 3.7% of Türkiye's total surface area. Its median height is 879 m. The basin is generally mountainous, and while the Black Sea climate dominates the coastline, the Black Sea climate is replaced by a continental climate towards the interior. The basin's average annual total precipitation is 822.95 mm.

Susurluk basin constitutes 3.1% of Türkiye and has a rainfall area of 24.319 $km^2$. The median height of the basin is 603 m. The climate of the Susurluk Basin is a transitional climate. The west experiences a Mediterranean climate, the east experiences a continental climate, and the north experiences a Black Sea climate (Ceribasi et al., 2021; Bulut and Saler, 2018; Albayrak, 2019; Ceribasi and Ceyhunlu 2020a, b). In high-altitude locations like Uludağ, winters are snowy and chilly even though snowfall and frost are uncommon in the Marmara Sea's coastal regions.

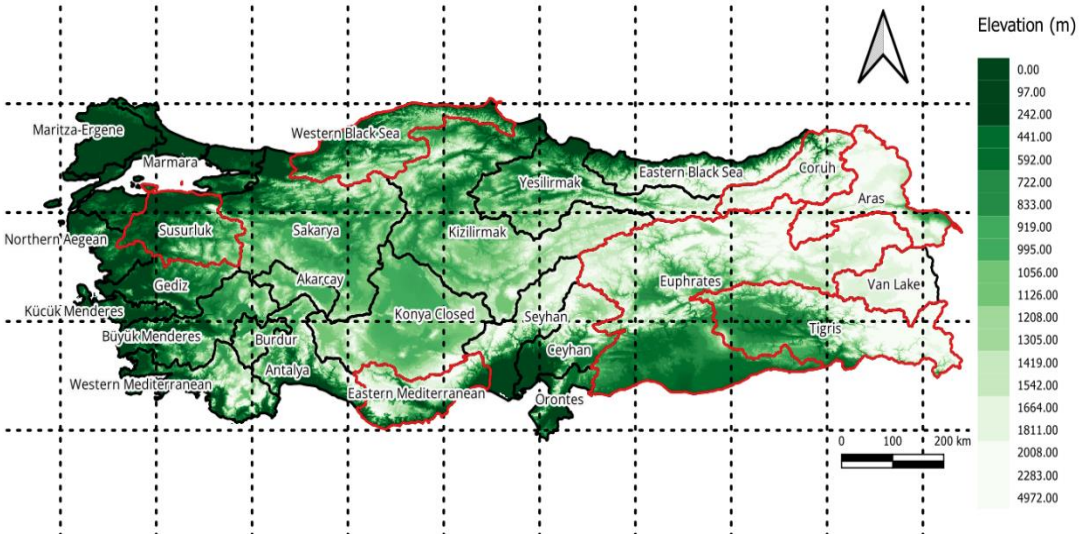


Figure 3.3. Basins of Türkiye. The basins selected within the scope of the study are marked in red.

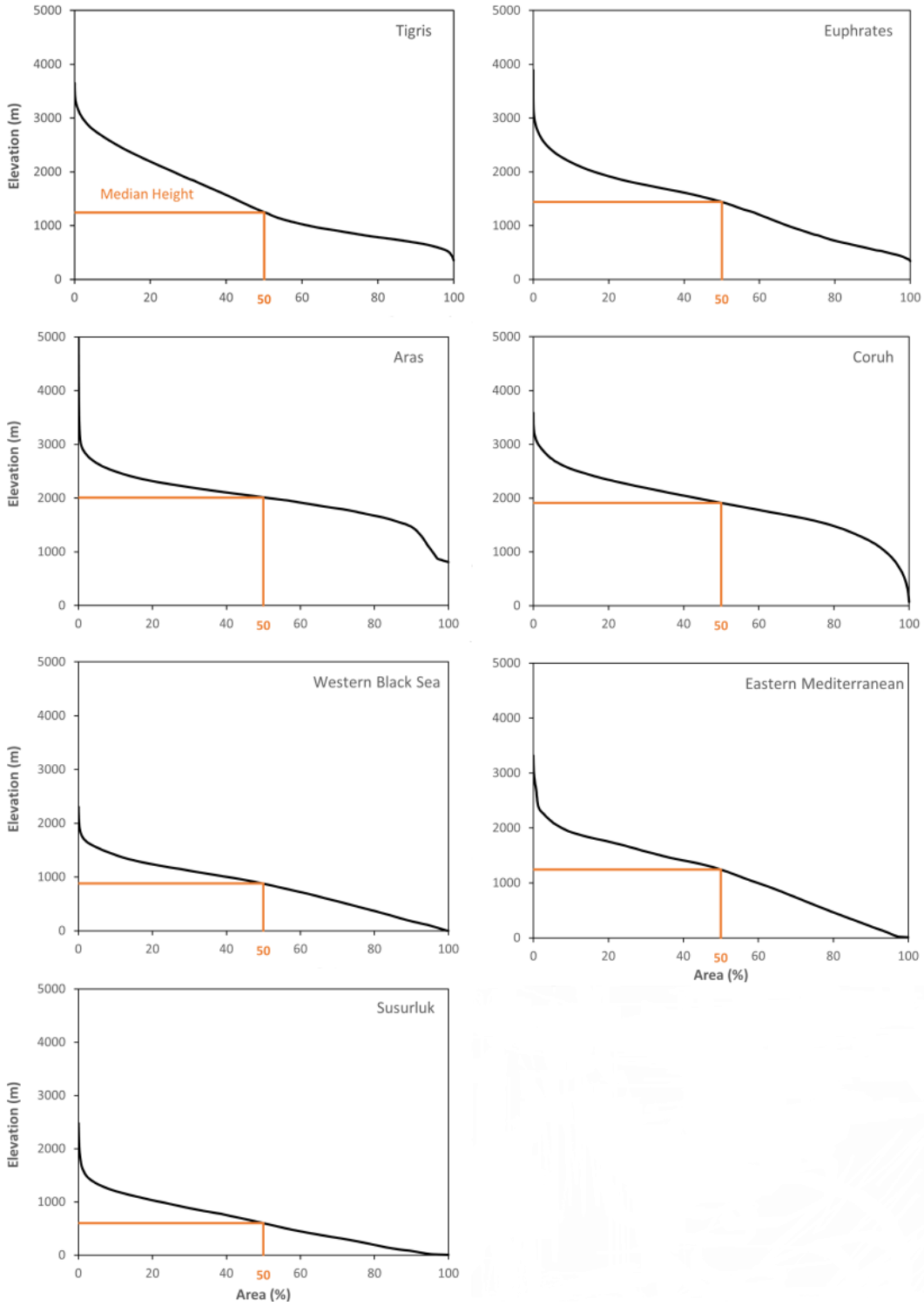


Figure 3.4. Hypsometric curves of selected basins

## 3.2 Models and Data

The required data to perform surface water budget analyses are obtained from 4-km high-resolution climate simulations of Türkiye established by Bagcaci (2023) and Bagcaci et al. (2021). WRF model is used to dynamically downscale the ERA5, the fifth-generation atmospheric reanalysis generated by the European Centre for Medium-Range Weather Forecast (ECMWF) (Bell et al., 2021) for historical climate simulation from 1995 to 2015 while the far future projection from 2081 to 2100 is established using the pseudo global warming approach that involves perturbation of ERA5 forcing data in WRF using the ensemble climate signals from CMIP6 climate models under the SSP5-8.5 high emission scenario.

An international team recently created Shared Socioeconomic Pathways (SSPs) to give the climate change research community a set of tools to perform integrated, multidisciplinary analyses: the CMIP6, the most recent set of climate model experiments, employed scenarios based on SSP. The findings of these climate model experiments served as a basis for the Intergovernmental Panel on Climate Change's (IPCC) Sixth Assessment Report (AR6), which assessed both past and future climate change.

SSPs are predicated on five narratives (see Figure 3.5) that depict alternative socio-economic developments: middle-of-the-road development, inequality, sustainable development, regional competitiveness, and fossil fuel development (Riahi et al., 2017). Figure 3.6 illustrates the $CO_2$ emissions, $CO_2$ concentrations, total anthropogenic radiative forcing and temperature change for 21$^{st}$ century scenarios.

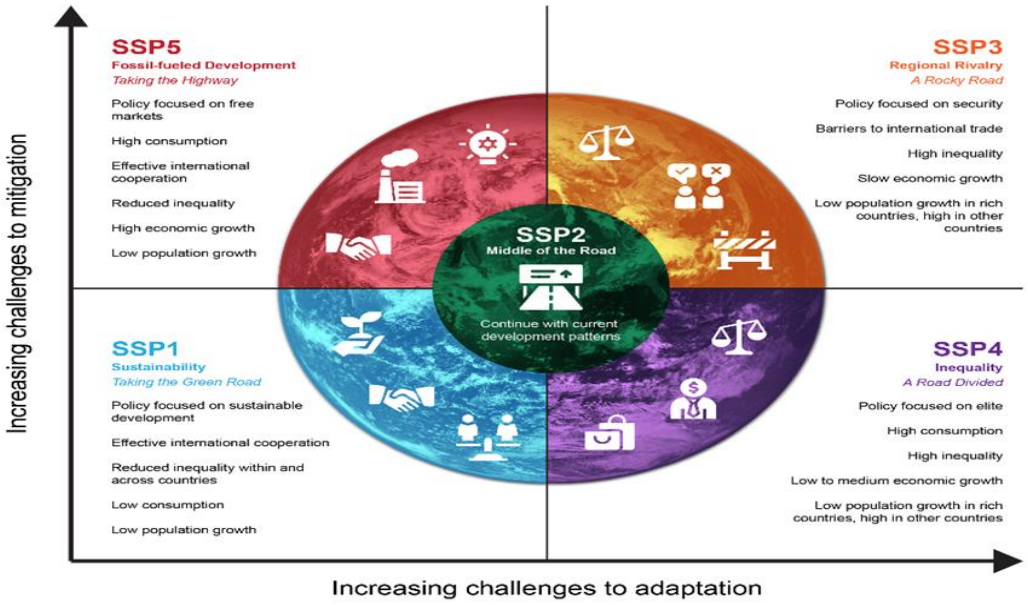


Figure 3.5: The five narratives of SSPs (ClimateData.ca)

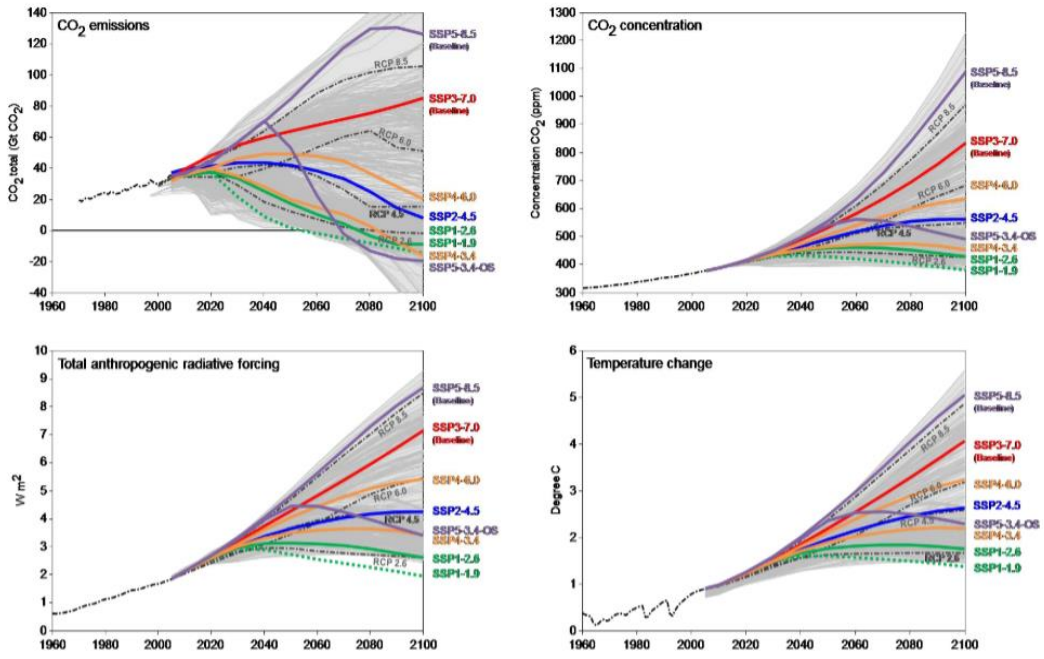


Figure 3.6: 21st century scenarios (ScenarioMIP), CO2 emissions, $CO_2$ concentration, total anthropogenic radiative forcing, temperature change (O'Neill et al., 2016)

Representative Concentration Pathways (RCPs) and previous emission scenarios were designed to allow the climate model community to explore the impacts of different emission scenarios or concentrations. On the other hand, SSPs build upon RCPs to facilitate a consistent comparison of social and economic decisions and their associated levels of climate change.

The main CMIP6 activity that will produce multi-model climate projections based on alternative scenarios of future emissions and land use changes generated with integrated assessment models is the Scenario Model Intercomparison Project or ScenarioMIP. Four combinations have been agreed upon worldwide as standard scenarios (or "Tier 1") for ScenarioMIP. These pairings are SSP1-2.6, SSP2-4.5, SSP3-7.0, and SSP5-8.5 (O'Neill et al., 2016).

- SSP1-2.6: The 2 ºC scenario of the socioeconomic family SSP1 focuses on "sustainability" with a nameplate 2100 radiative forcing level of 2.6 $W\,m^{-2}$. This scenario roughly matches scenario generation RCP 2.6 (Meinshausen et al., 2020).
- SSP2-4.5: This scenario updates the RCP4.5 pathway with an additional radiative forcing level of 4.5 $W\,m^{-2}$ by the year 2100 and represents the middle portion of the range of possible future forcing pathways (O'Neill et al., 2016).
- SSP3-7.0: This scenario falls in the upper-middle range of all scenarios, with 7 $W/m^2$ by 2100. It was recently released, bringing RCP6.0 and RCP8.5 closer together after the RCP scenarios.
- SSP5-8.5: It can be interpreted as an update to the CMIP5 scenario RCP8.5, adding 8.5 $W\,m^{-2}$ of additional radiative forcing by 2100. This scenario denotes the upper bound of the range of scenarios documented in the literature (O'Neill et al., 2016).Most global warming is projected by SSP5-8.5, which makes it easier to distinguish the climate change signal from the background noise of natural climate variability. Given that the climate signal is strongest under this emissions scenario, SSP5-8.5 may be the best choice

for research applications where the objective is to determine a correlation between climate change and some other event.

### 3.2.1 High-Resolution Historical Climate Data

Regional Climate Models (RCM) are crucial tools for addressing regional-local scale climate variability, changes, and impacts (Liang et al., 2012; Giorgi & Mearns, 1999; Giorgi et al., 2001; Leung et al., 2003; Wang et al. 2004; Giorgi, 2006; Fowler et al., 2007; Christensen et al., 2007; Bader et al., 2008; Liang et al. 2008 a,b). Reanalysis data combines observations and past short-term weather forecasts and is used to get state-of-the-art climatologies to assess forecast-error anomalies, to measure progress in modeling and assimilation capabilities, and to evaluate the effect of monitoring system changes (Hersbach et al., 2020). ERA5 reanalysis estimates a wide range of atmospheric, land, and oceanic climate variables hourly and includes uncertainty information. Bagcaci (2023) used the ERA5 reanalysis as the parent model for the retrospective dynamic downscaling simulations via the WRF RCM (Skamarock et al., 2008). WRF was developed for use in operational forecasting as well as atmospheric and climate research. The hydrometeorological cycle's interactions with precipitation, temperature, surface runoff, soil moisture/temperature, and specific humidity can be closely monitored using the WRF model. Figure 3.7 shows the WRF model physic interactions. The twenty-year WRF historical simulation from 1995 to 2015 using the ERA5 initial and boundary conditions over Türkiye was made at 4 km resolution and hourly time intervals.

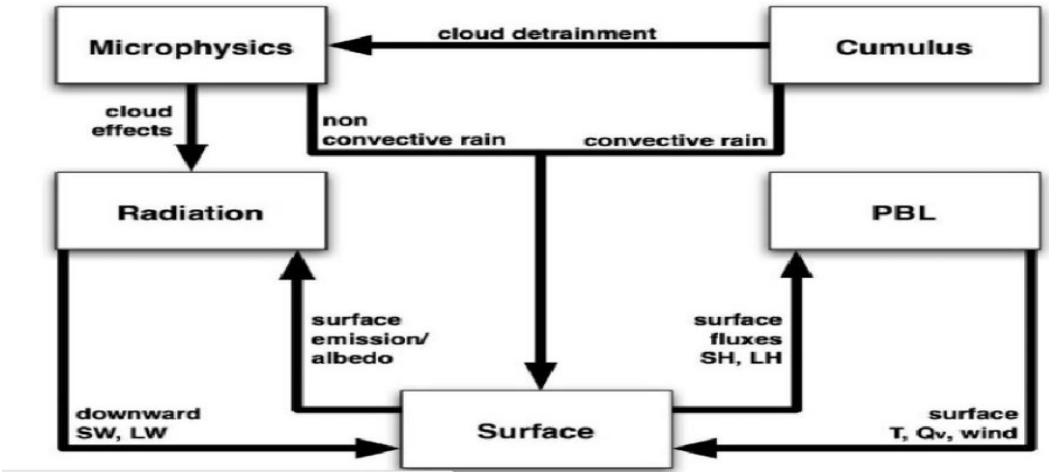


Figure 3.7. WRF model physics interactions (Dudhia, 2015)

### 3.2.2 High-Resolution Climate Projection Data

Bagcaci (2023) used the Pseudo Global Warming (PGW) approach with the WRF model to downscale the CMIP6 GCM ensemble dynamically to a high resolution (4 km) in the high-emission range for the far future period. In regional climate modeling, the phrase "pseudo-global warming" (PGW) designates a simulation strategy (Brogli et al., 2023). The strategy entails changing the boundary conditions of a control regional climate simulation, which typically represents current circumstances, to directly impose large-scale changes on the climate system (Brogli et al., 2023).

Some advantages that make the PGW method preferred are as follows:

- It prevents GCM biases, provides simulation design flexibility, and reduces computing requirements (Brogli et al., 2023).

- PGW Method enables the estimation of the effects of global warming for a particular year (Fujihara et al., 2008). The authors mentioned that the precipitation data of a current year can be compared with its corresponding future pseudo period under global warming.

- Numbers of GCM can be used with the PGW method, which can reduce model uncertainties (Bagcaci, 2023).

Although PGW can provide solutions to some problems encountered in other dynamically downscaling methods, it also has disadvantages, which are given below:

- A lateral boundary forcing imbalance could be introduced by adding the climate change signal to the reanalysis field (Li et al., 2019; Misra & Kanamitsu, 2004).
- It cannot predict future changes in storm frequency, intensity, and track positions because it does not fully account for the nonlinear interaction between changes in atmospheric circulation and global warming (Li et al., 2019; Sato et al., 2007).

An ensemble of 13 CMIP6 GCMs operating under the SSP5-8.5 emission scenario was employed in the perturbation process for PGW-based downscaling (Bagcaci, 2023). Table 3.1 shows these 13 CMIP6 GCMs selected based on their performances (Bagcaci, 2023).

Table 3.1. Ensemble members of 13 CMIP6 GCMs (Bagcaci, 2023)

| CMIP6 GCM | Ens. used | Resolution (x°,y°) |
|---|---|---|
| AWI-CM-1-1-MR | r1i1p1f1 | 0.94x0.94 |
| BCC-CSM2-MR | r1i1p1f1 | 1.10x1.10 |
| CMCC-CM2-SR5 | r1i1p1f1 | 1.25x0.94 |
| CMCC-ESM2 | r1i1p1f1 | 1.25x0.94 |
| CNRM-CM6-1-HR | r1i1p1f2 | 0.50x0.50 |
| EC-Earth3 | r1i1p1f1 | 0.70x0.70 |
| EC-Earth3-CC | r1i1p1f1 | 0.70x0.70 |
| EC-Earth3-Veg | r1i1p1f1 | 0.70x0.70 |
| FGOALS-f3-L | r1i1p1f1 | 1.25x1.00 |
| GFDL-ESM4 | r1i1p1f1 | 1.30x1.00 |
| HadGEM3-GC31-MM | r1i1p1f3 | 0.80x0.60 |
| MPI-ESM1-2-HR | r1i1p1f1 | 0.90x0.90 |
| MRI-ESM2-0 | r1i1p1f1 | 1.13x1.12 |

In Bagcaci (2023), two WRF simulations from 1995-2014 and their corresponding pseudo-future period of 2081-2100 were set up. Firstly, to obtain retrospective

simulations at the targeted 4-km resolution, the model was forced using the 6-hourly ~0.25° ERA5 reanalysis data. Then, to create pseudo future period simulations, they perturbed the ERA5 reanalysis data using the climate change signal derived from the GCM ensemble (13 CMIP6 GCMs shown in Table 3.1) under the SSP5-8.5 emission scenario. For these calculations, the following formulas were used in Bagcaci (2023):

- $PGW_{forcing} = ERA5_{1995-2014} + \Delta CMIP6_{SSP585-historical}$
- $\Delta CMIP6_{SSP585-historical} = CMIP6_{2071-2100} - CMIP6_{1985-2014}$

$\Delta CMIP6_{SSP585-historical}$ refers to 30- years Multi-Model Ensembe mean monthly differences.

Figure 3.8 shows the WRF setup flowchart. More detailed information about the PGW method and its application steps, together with the design of the WRF model for climate simulations, are addressed in the studies of Bagcaci (2023) and Bagcaci et al., (2021).

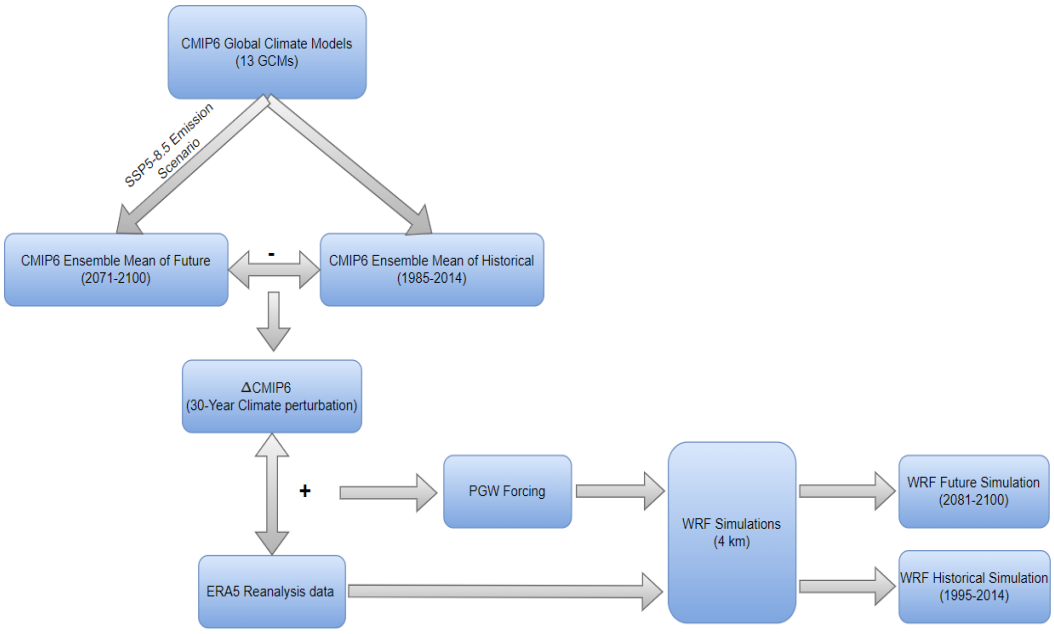


Figure 3.8. WRF setup flowchart. The figure is formed based on Ma et al. (2022)

### 3.2.3 NOAH Land Surface Model (NOAH LSM)

In the global forecast system (GFS) and climate forecast system (CFS), land surface simulates interactions between land and atmosphere by acting as a lower boundary forcing. Gaining better weather and seasonal prediction abilities requires understanding the physics behind land models (Dong et al., 2017). Zheng et al. (n.d.) stated that land surface models are suitable for generating physically consistent terrestrial water budgets over an extended period and a large domain. Also, an essential aspect of estimating annual cycles is using LSM parameterizations; the spread in the annual cycle determines the overall ensemble spread of soil moisture and runoff (Zheng et al., n.d.).

As a lower boundary condition, the Noah Land Surface Model (Chen & Dudhia, 2001) used in the WRF atmospheric model is a well-known LSM applied extensively in hydrological and atmospheric research. The primitive canopy model, the multilayer soil model, and the diurnally dependent Penman potential evaporation approach are the basis of the Noah LSM (Nair & Indu, 2016). It uses calculations for soil heat flux based on Pan & Mahrt (1987) and vertical soil water movement through soil layers based on Pan & Mahrt (1984) and Samuel & Chakraborty (2023).

In addition to the one-layer vegetation canopy model, snow prediction, evapotranspiration, and soil drainage and runoff, the Noah LSM also includes four soil temperature and soil moisture layers (Campbell et al., 2019). The thicknesses of these four layers are 0.1, 0.3, 0.6, and 1 m from top to bottom (Samuel & Chakraborty, 2023), as shown in Figure 3.9. Thus, with Noah LSM, more detailed information about soil moisture and characteristics can be obtained than with a single-layer model.

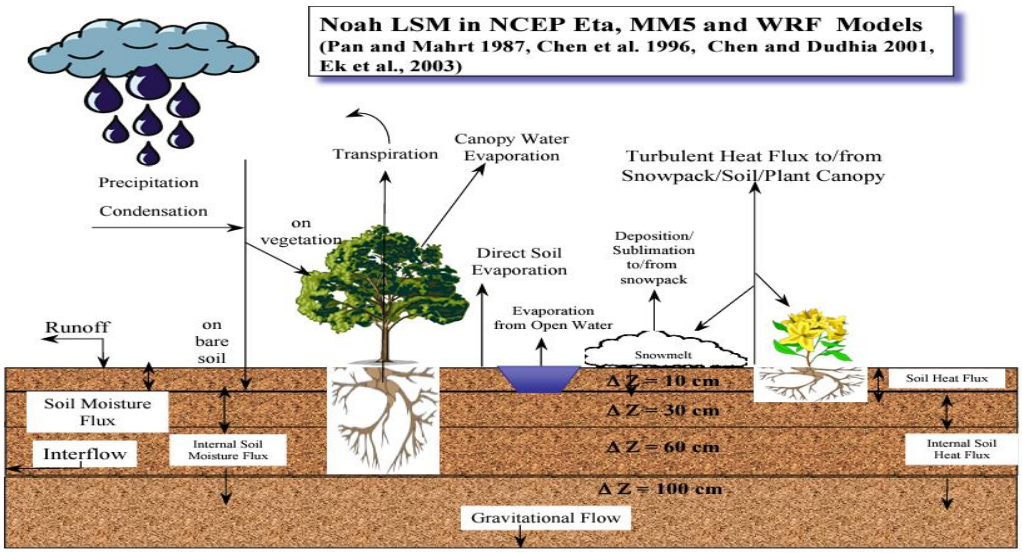


Figure 3.9. Noah Land Surface Model (Pan & Mahrt, 1987; Chen et al., 1996; Chen and Dudhia, 2001; Ek et al., 2003)

Cho et al. (2022) stated that one frequently used to generate comprehensive estimates of snow water equivalent (SWE) and hydrological variables on a broad scale is using land surface models (LSMs). Snowfall events are directly interpreted by numerical weather prediction models, whereas LSMs evaluate snow cover fraction, snow albedo, and snow depth through interaction with atmospheric conditions (Lim et al., n.d.).

Noah LSM computes snowfall minus the total of sublimation and snowmelt using a one-layer snow model to simulate SWE. Several unknown and constrained factors affect the accuracy of the LSM-based SWE outputs, including uncertainties in the model physics and meteorological boundary conditions (Cho et al., 2022).

According to Barlage et al. (2010), the Noah LSM displayed an excessively early end to the snow period and an excessively low and early seasonal maximum snow water equivalent. Previously conducted studies have discovered an inclination toward negative bias in the Noah model's representation of snow cover extent, total snow water equivalent (SWE), and the timing of snow depletion in the spring (Barlage et al., 2010).

Barlage et al. (2010) also stated that in the presence of snow, Noah considers a combined layer of snow, vegetation, and soil. Then, using a basic snow parameterization from Koren et al. (1999), Noah simulates the accumulation, sublimation, melting, and heat exchange at the interfaces between snow, atmosphere, and soil. Neither independent snow layers nor a canopy snow interception component is present in Noah (Barlage et al., 2010).

### 3.2.4 Terrestrial Water Storage (TWS) and Anomalies (TWSA)

Terrestrial water storage, or TWS, is the total amount of water stored on and below the surface of the Earth, including that in lakes, rivers, artificial reservoirs, wet areas, soil, and groundwater reservoirs (Ni et al., 2018). It is a dynamic element of the hydrological cycle that significantly influences water, energy, and biogeochemical fluxes. As a result, TWS significantly impacts the Earth's climate system (Girotto & Rodell, 2019).

TWS change (TWSC) substantially affects human beings, terrestrial ecosystems, and even sea level. For optimal management of water resources and sustainable use, it is crucial to monitor the geographical and temporal variations in TWSC (Li et al., 2021).

To monitor TWS variations, several in situ systems have been developed, including wireless sensors, ground-penetrating radar (GPR), and soil moisture sensors. However, in-situ measurements focus on one-point measurements with high costs and significant labor intensity. Furthermore, the absence of a comprehensive worldwide monitoring network makes it difficult to monitor and quantify global TWS variations with high spatial precision (Jin & Zhang, 2016).

Terrestrial Water Storage Anomaly (TWSA) is a collective term that encompasses several components, including groundwater storage (GWS), canopy water storage (CWS), snow water equivalent (SWE), surface water storage (SWS), and soil moisture storage (SMS) (Koycegiz et al., 2023; Pan et al., 2016; Tregoning et al.,

2012). The literature contains numerous studies demonstrating The Gravity Recovery and Climate Experiment mission (GRACE) and Global Land Data Assimilation System (GLDAS) datasets used in TWSA calculations, and these data are commonly used in hydrological studies (Koycegiz et al., 2023; Zhang et al., 2019; Long et al., 2016; Awange et al., 2014; Hu et al., 2021; Hu et al., 2022). According to Tapley et al. (2004), GRACE satellites have produced observations of terrestrial water storage anomalies (TWSAs) that are incredibly accurate. However, since this study aimed to analyze the WRF data and used water budget elements we had, data such as GRACE and GLDAS were not included.

For the TWS calculation, Zheng et al. (n.d.) employed the following formula;

$$TWS = SWE + W_{gw} + \sum_{i=1}^{N\,soil} W_{soil,i} \quad (1)$$

TWS = Terrestrial Water Storage

SWE = Snow Water Equivalent

$W_{gw}$ = Groundwater Storage

$W_{soil,\,i}$ = Soil Water Storage (SWS) (Detailed formula is given in Methodology/Soil Moisture part)

According to Koycegiz et al. (2023), to find anomaly values, the mean value of the time series should be subtracted from the monthly data:

$$SWEA = SWE - \overline{SWE} \quad (2)$$

$$SWSA = SWS - \overline{SWS} \quad (3)$$

The LSM lower boundary is frequently considered zero flux, or the soil moisture content is fixed at a constant value. This mass-conservative approach misses processes that can change runoff, water quantity, quality, and surface fluxes (Maxwell & Miller, 2005). Also, the effects of groundwater are not considered by the Noah Land Surface Model (Noah LSM) (Samuel & Chakraborty, 2023). Therefore, the groundwater term is neglected in this study.

The final formula which is used for terrestrial water storage anomaly (TWSA):

$$TWSA = SWSA + SWEA \quad (4)$$

## 3.3 Surface Water Budget Calculation Using Data from WRF and NOAH LSM

Surface water budget analyses are performed for the selected basins. Human-induced water consumption is not considered since the primary purpose here is to see changes in the hydrological water balance because of climate change. As mentioned above, the equations used vary depending on the purpose of water budget calculations. In this study, the variables selected to be used in the water balance equation are as follows: Precipitation, evapotranspiration, snow water equivalent, surface runoff, interflow, and columnar soil moisture. The accuracy assessment of these variables is not carried out because this study focuses on relative changes in these variables solely due to climate change from the current to the future. Hence, any possible error in calculating these variables may exist in historical and future WRF simulations.

The budget analysis was based on monthly total data acquired from WRF's original hourly data. This method allows for the direct calculation of values for precipitation, surface runoff (sfroff), interflow, and evapotranspiration (ET); however, it is impossible to find monthly total values for soil moisture and snow water equivalent. Since it is possible to store snow and soil moisture, the data set includes instantaneous values rather than incremental values. As a result, hourly variation values for these two variables were used to generate monthly total change data.

The spatial average was determined because the goal is to comprehend the water balance throughout the basin. Also, the water year (starting from October 1 of the current year) was considered for the analysis, so the data set, which covers 20 calendar years, was organized, and temporal averages were calculated. Finally, each variable's average monthly total values were calculated for each month.

The residuals were created using the monthly values found using the equation below:

Residual = P - ET - Sfroff - (SWE – Var) - (SWS – Var) – Interflow ( 5 )

In this equation, it is aimed that the residual is minimized and the optimum value is zero for a perfect water balance closure. The handling of these elements within the WRF-NOAH model is shown in Figure 3.6. Detailed information about these variables is explained below.

### 3.3.1 Precipitation

In hydrologic modeling, precipitation is a crucial forcing that affects several hydrologic components, including runoff, evaporation, and infiltration of the water budget (J. Guo et al., 2004). For many years, determining precipitation's temporal and spatial distribution has been complex. This difficulty persists in present attempts to quantify the water and energy cycle over the cold regions, which include high-elevation and high-latitude regions (Ye et al., 2012; Woo & Steer, 1979; Goodison & Yang, 1995; Walsh et al., 1998).

Bagcaci (2023) validated the precipitation outputs of a historical WRF simulation that was run for the 1995–2015 period using the ERA5 initial and boundary conditions. Figure 3.10 a presents daily correlations' spatial distribution between the WRF simulations and the stations in 1995-2014. Over southeastern of Türkiye, values of daily correlations differ between 0.5 and 0.83. When it comes to the easternmost Mediterranean coasts and northeastern Türkiye, these values differ in the range of 0.5 and 0.6, and over the Aegean coasts and northwestern part of the country, daily correlations vary between 0.6 – and 0.7. These correlations usually appear homogeneously.

Figure 3.10 b presents the same attributes as in Figure 3.10 a but for wet seasons. The range of the daily correlations' values between WRF simulations and stations is 0.7 – 0.9. Despite all of this, there is no steady spatial pattern in these correlations.

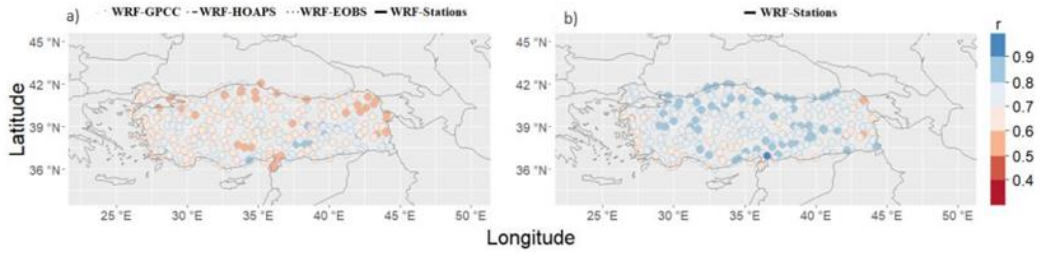


Figure 3.10. a) The spatial correlations of daily precipitation between WRF and ground observations for 1995-2014 in Türkiye. b) As in a, but for the wet season (NDJFM) (Bagcaci, 2023)

### 3.3.2 Evapotranspiration (ET)

Water vapor loss from cropped soil to the atmosphere is known as evapotranspiration. Both evaporation from the top soil layers and transpiration, the vaporization of water that plants draw from the soil, are included in this water loss (Rijtema, n.d.). The evaporation process requires latent heat, or energy, making evapotranspiration one of the essential components of the energy balance (Karimi & Bastiaanssen, 2015).

One of the parameters commonly used in drought studies is the evapotranspiration (ET) parameter. After precipitation data, this parameter is the most critical component of the hydrological budget (Yilmaz & Bulut, 2015; Hanson, 1991).

In this study, evapotranspiration was calculated with hourly temperature and latent heat flux as shown in the following equation:

$$LH = Latent\ Heat\ Flux\ (Wm^{-2})$$

$$\lambda(latent\ heat\ vaporization) = \left(2.501 - 0.00237 * T(℃)\right) * 10^{6}(Jkg^{-1})$$

$$ET = LH/\lambda * 3600\ \ (kg\ m^{-2}\ s^{-1}) \qquad (6)$$

ET is multiplied with 3600 to obtain values in mm per hour.

### 3.3.3 Snow Water Equivalent (SWE)

Snow water equivalent (SWE) is a crucial metric utilized in hydrology, water resources, and the effects of climate change (Yao et al., 2018). One important source of water, especially in mountain basins, is accumulated snow (Carroll et al., 2019). Moreover, the amount of water in the snow is determined by its snow water equivalent or SWE. Accurate SWE data is required to evaluate climate effects from GCMs, calibrate hydrological models, estimate freshwater runoff from large and poorly gauged catchments, and improve decision-making in water supply, hydroelectric power, flood forecasting, and other areas (Yao et al., 2018; Rutter et al., 2009).

Fontrodona-Bach et al. (2023) created a graph of daily SWE values for one year in Figure 3.11 and explained the terms related to the snow season. According to the authors, the longest stretch of continuous snow cover (meaning SWE is greater than 0) during a snow year is known as the annual snow season. Peak SWE has the highest snow water equivalent value during the annual snow season. The snowmelt onset date coincides with the final day of peak SWE, which divides the snowmelt and accumulation seasons.

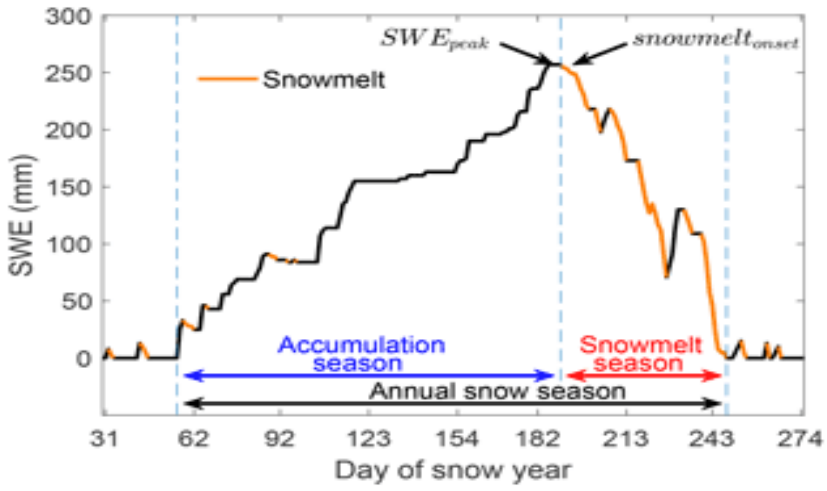


Figure 3.11. Terms of snow season (Fontrodona-Bach et al., 2023)

### 3.3.4 Surface Runoff

One of the main components of the water cycle is surface runoff, which is the movement of water over the land surface caused by precipitation, melting snow, or other sources. It is an essential process of interest in hydrology that can be generated at various scales, from small pools of excess water that spread downward to large catchment-draining stream networks (Guo et al., 2019).

Also, surface runoff is one of the critical elements in a groundwater recharge balance because it acts as a conduit between groundwater-surface water interactions and surface flow conditions on the surface (Weatherly et al., 2021).

### 3.3.5 Soil Water Storage (SWS)

Soil moisture is the total volume of water in an unsaturated soil. It influences evapotranspiration and regulates the flux of solar radiation at the surface (the albedo effect) and the flux of momentum at the surface (the roughness effect) by affecting the vegetation structure (Mintz & Serafini, 1992).

While soil moisture gives the volume of water in a single layer in $m^3/ m^3$, soil water storage can express the total amount of water that the soil can hold within the entire soil profile at a given time in mm. Therefore, soil water storage values were calculated using soil moisture values for a 2 m soil profile for surface water budget analysis. As mentioned before, NOAH LSM is based on a 2-meter soil profile and examines this profile in four layers of thicknesses: 0.1, 0.3, 0.6, and 1 meter. The following formula is used to obtain soil water storage:

$$SWS = \rho_{wat} * w_i * \Delta z_i \; for \; i = 1,2,3,4 \qquad (7)$$

$w_i \; is \; volumetric \; content \; (m^3 m^{-3})$

$\rho_{wat} = 1000 \; kg \; m^{-3}$ (density of water).

$\Delta z_1 = 0.1 \; m, \Delta z_2 = 0.3 \; m, \Delta z_3 = 0.6 \; m, \Delta z_4 = 1 \; m$

### 3.3.6 Interflow

The portion of rainfall known as infiltration enters the soil first and flows laterally without connecting to the water table, streams, rivers, or ocean (Balasubramanian, n.d.). It depends on permeability contrasts and is typically transient due to perched conditions or a water table that fluctuates seasonally (Carroll et al., 2019). According to Caroll et al. (2019), when there is a drought, there is a decrease in interflow, which leads to an increase in plant water use and a rise in the proportion of groundwater to streams.

# CHAPTER 4

# RESULTS

## 4.1 Spatial Distributions of Precipitation, ET, and SWE over Türkiye

This section shows precipitation, ET, and SWE maps prepared for Türkiye. While monthly total values were used for precipitation and ET, SWE maps were obtained from monthly average values.

The maps created as follows:

- Annual maps were created for the historical period (1995-2014), and the distribution and change of the water budget variable over the years were examined.
- Secondly, seasonal and 20-year average maps were created for the historical period, and the spread of variables on a seasonal basis was examined.
- Thirdly, the differences between the seasonal and 20-year average values between 1995-2014 and corresponding pseudo-future period values were found, and the change was examined.
- Finally, standard deviation maps of 20-year average values were created for historical and pseudo-future periods.

### 4.1.1 Precipitation Maps

Figure 4.1 shows the spatial distribution of annual total precipitation for the reference period. The maps show that the Eastern Black Sea and Mediterranean regions (especially the Antalya basin) are among the places that receive the most precipitation. The Western Mediterranean basin, the mountainous parts of the

Euphrates-Tigris and Seyhan-Ceyhan basins, and the northern parts of the Coruh and Aras basins can be listed among the regions that receive high rainfall.

In the year-by-year analysis, it was seen that precipitation decreased significantly in 1999, especially in the inner regions, and that there was an increase in precipitation in the Antalya region in 2001. Sari & Demirkaya (2012) stated that 1892 mm of precipitation fell in Antalya in 2001, the most precipitation of the observation year (Sari & Demirkaya, 2012). Precipitation was found to have increased in the Eastern Black Sea region in 2004, but nationwide levels decreased in 2008 and then increased once more in 2009. The "2009 Climate Data Evaluation Report" of the Turkish State Meteorological Service pointed out that the amount of precipitation in the 2008-2009 water year increased by 10% compared to average precipitation and by 20.2% compared to the previous year (TSMS, 2010). Again, the 2012 Climate Assessment Report regarding the increase in precipitation in 2012 stated a 16% increase compared to the precipitation norms. In 2013, precipitation started falling and has continued to fall through 2014.

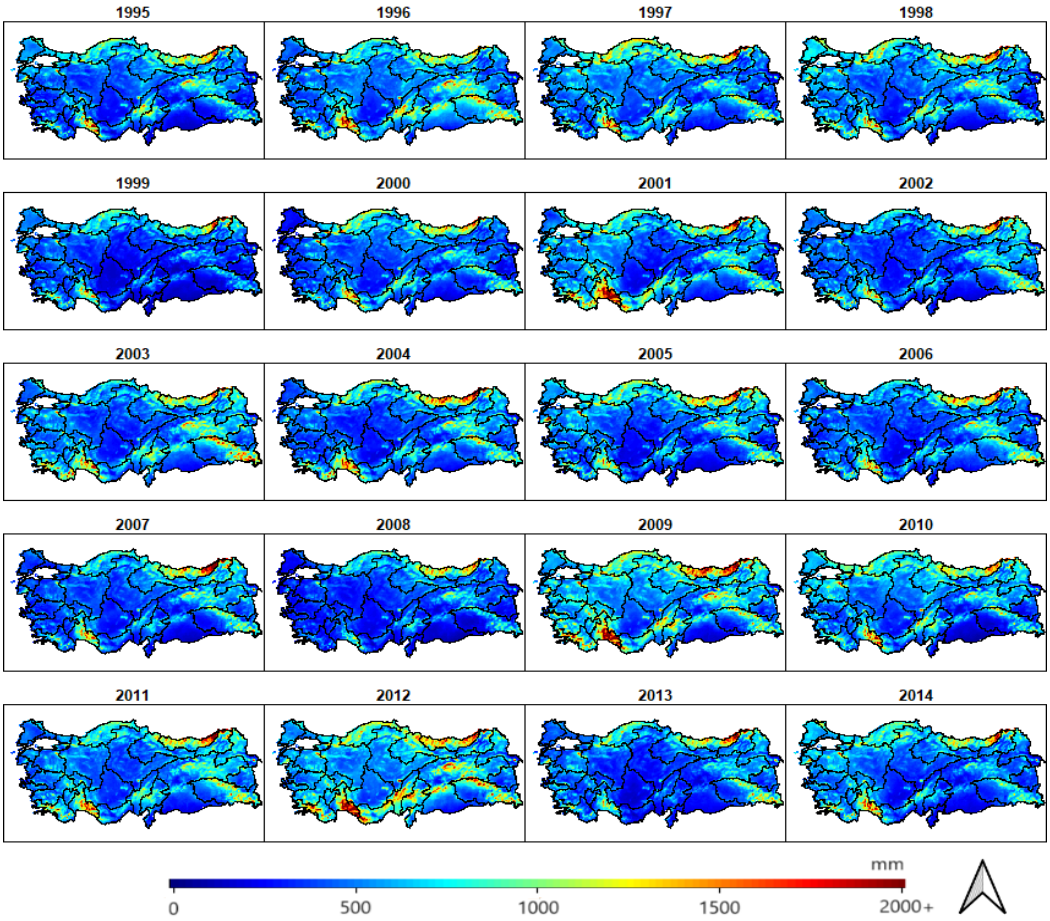


Figure 4.1. Spatial distribution of the annual total precipitation during the historical period (1995-2014).

In Figure 4.2, while the first column shows the twenty-year average of seasonal and annual total precipitation for the reference period, the second column consists of anomaly maps illustrating the differences between the future and reference periods. Based on the analysis of the reference period, it can be observed that the winter months receive the highest amount of precipitation. Although precipitation tends to cover more areas during spring, it is also possible to observe regions with higher precipitation levels during autumn. The Eastern Black Sea basin, in particular, draws attention due to the quantity of rainfall on the Black Sea coast, which experiences four distinct seasons of precipitation. The Mediterranean region is the region that receives the most rainfall in the winter season.

The anomaly maps show that while the precipitation in the Mediterranean region and the coastal part of the Aegean region will decrease in the winter season, the precipitation will increase significantly in the eastern Black Sea region. The precipitation increase in the Eastern Black Sea region has been determined to reach its maximum in the summer. Gumus et al. (2023) conducted a study targeting the period between 2015 and 2100 to examine the extreme climate in Türkiye, and in this study, they used CMIP6 models with SSP5-8.5 and SSP2-4.5 emission scenarios. The authors noted that the Aegean and Mediterranean regions of Türkiye experience a 20% reduction in total precipitation under the SSP5-8.5 scenario, which indicates more severe water stress than the SSP2-4.5 scenario (Gumus et al., 2023).

Total maps indicate increased precipitation, particularly in the northeastern part of the Eastern Black Sea, Aras, and Coruh basins and the southern part of the country except for a part of Seyhan, Ceyhan, and Eastern Mediterranean basins. The Aegean and Marmara regions, the Central Black Sea region, the north of the Tigris basin, and the south of the Euphrates basin are the areas where the highest rainfall decrease is expected.

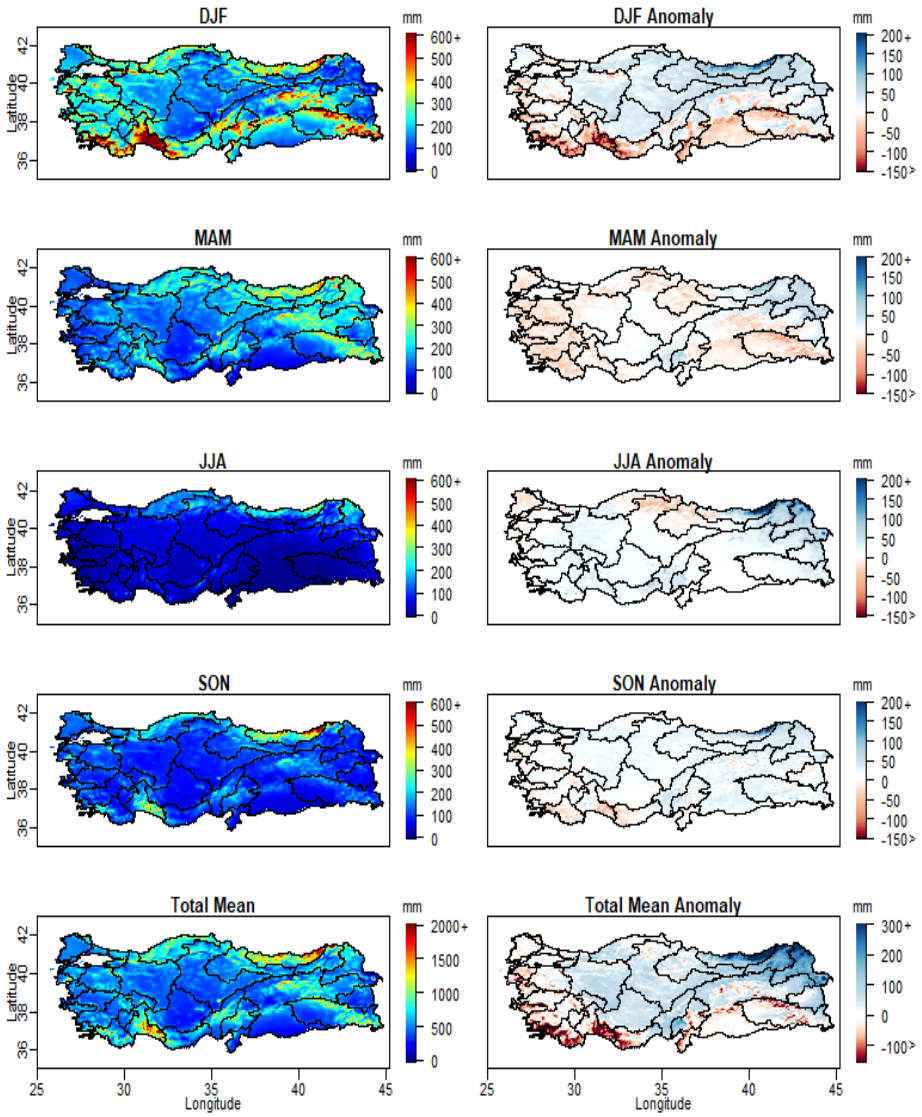


Figure 4.2. Spatial distributions of the seasonal and the total mean precipitation during 1995-2014 (historical) (first column), seasonal and total mean change between future (2081-2100), and historical period (1995-2014) (second column).

Spatial distributions of standard deviation of annual precipitation for both historical and future periods calculated over 20-year periods are shown in Figure 4.3. Overall, the deviation or variability from the mean increases for the projection period, particularly in areas with higher annual mean precipitation. The higher deviation values with warmer climates in the future period indicate more significant year-to-year variability from the mean annual precipitation. When we look at the standard deviation maps for precipitation, the mountainous regions of the Eastern Black Sea, Seyhan - Ceyhan and Euphrates - Tigris basins, and the west of the Western Black Sea basin are examples. Although precipitation will decrease in the Antalya basin, it maintains its difference from the average.

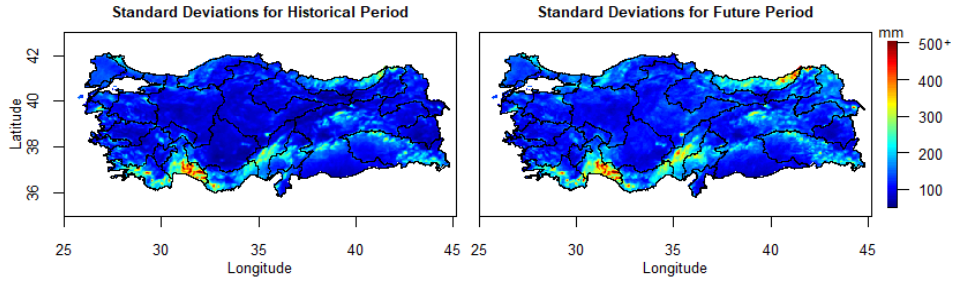


Figure 4.3. Spatial distributions of standard deviations of annual precipitation for historical and corresponding pseudo future period.

### 4.1.2 ET Maps

Spatial distributions of annual ET values for each year from 1995 to 2014 are shown in Figure 4.4. Year-to-year ET variability for each catchment across the country is clearly shown. Specific drought and wet years are evident within this 20-year historical period. The condition of high actual ET explains both the availability of high energy (temperature) and the abundance of water for a region. Accordingly, the lower ET values indicate relatively dry areas (southeastern Anatolia and southern inner Anatolia), while higher ET values (Black Sea region, Antalya basin) refer to

wet regions. For example, the years 2001 and 2007 were drier for western basins in the Aegean region than the other years in the historical period.

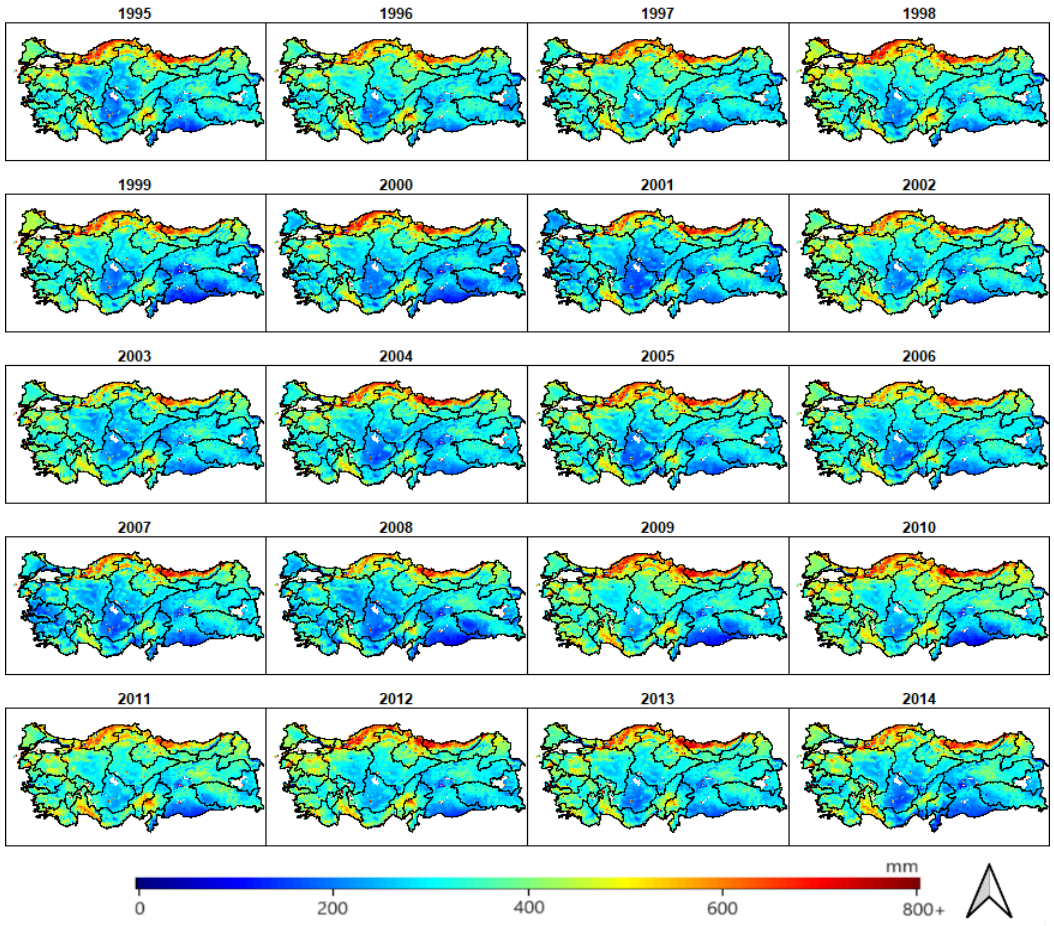


Figure 4.4. Spatial distribution of the annual total evapotranspiration (ET) during the historical period (1995-2014).

Seasonal and annual spatial distributions of ET values calculated from a 20-year historical period and their anomaly changes calculated between future projection and historical periods are shown in Figure 4.5. When higher temperatures and water availability exist in the spring and summer seasons across the country, the actual ET values are higher. However, the summer season shows more spatial ET variability than spring, depending on the availability of precipitation. Since southeastern Anatolia, inner Anatolia, and western Aegean Sea regions receive less precipitation during summer, these regions have the smallest actual ETs. However, these regions

are represented with relatively higher actual ET values in the spring season. With increased projected warming, the highest anomaly increases in the projection period occurred in the spring season across the country, particularly for the entire eastern Anatolia. Moreover, the coast of the Aegean Sea and Marmara region (Trachea) show a decrease in ET values in the summer season in the future periods. Summer drying is seen especially for these regions, and over the lower Euphrates, Yesilirmak basin, and Hatay province also influences annual ET values of these regions represented with negative anomalies.

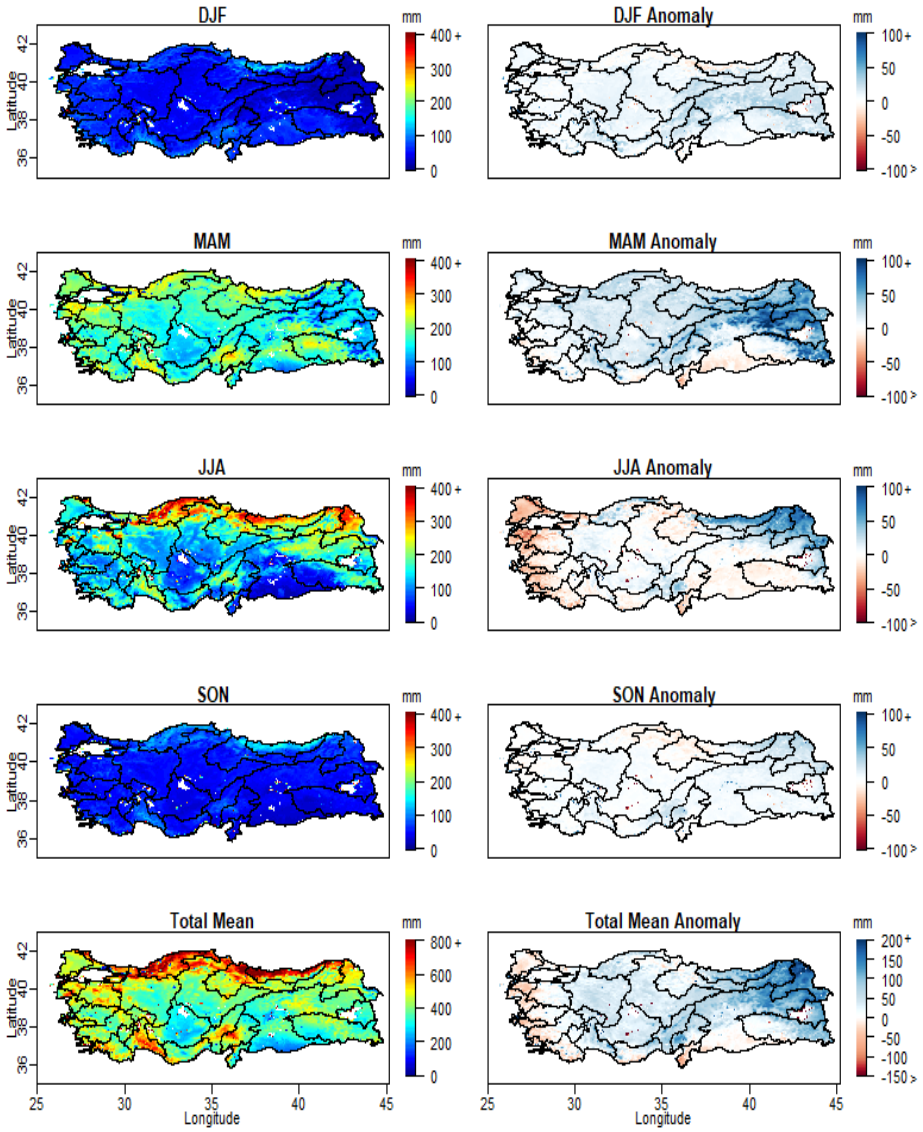


Figure 4.5. Spatial distributions of the seasonal and the total mean ET during 1995-2014 (historical) (first column), seasonal and total mean change between future (2081-2100) and historical period (1995-2014) (second column).

Figure 4.6 shows the spatial distributions of standard deviations of ET for historical and corresponding pseudo-future periods. According to maps, there is expected to be an increase in variability in the future period, particularly in the country's coastal regions, especially in the Aegean part. For future projections, ET's deviation from its 20-year mean annual value is much higher than the deviation of the reference period (see Figure 4.6). It seems that a warmer climate in the future period increases the year-to-year variability in evaporative losses across the country.

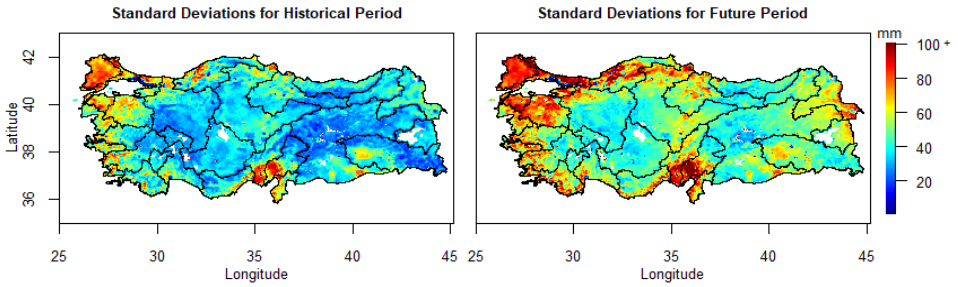


Figure 4.6. Standard deviations of ET for historical and corresponding pseudo-future periods.

### 4.1.3 SWE Maps

Figure 4.7 shows the spatial distribution of the annual mean snow water equivalent for the reference period (1995-2014). Among the places with the most snowfall are the Eastern Anatolia region, the Western Black Sea basin, the high mountains such as the Taurus Mountains in the Mediterranean, and the Southeast Anatolian region. It has been observed that SWE maps exhibit similar outcomes to those of precipitation and evapotranspiration. The annual maps show a decrease in SWE during 1996, 1998-1999, 2001, 2006-2007, 2011, and 2013-2014. These periods also correspond to periods of drought in Türkiye.

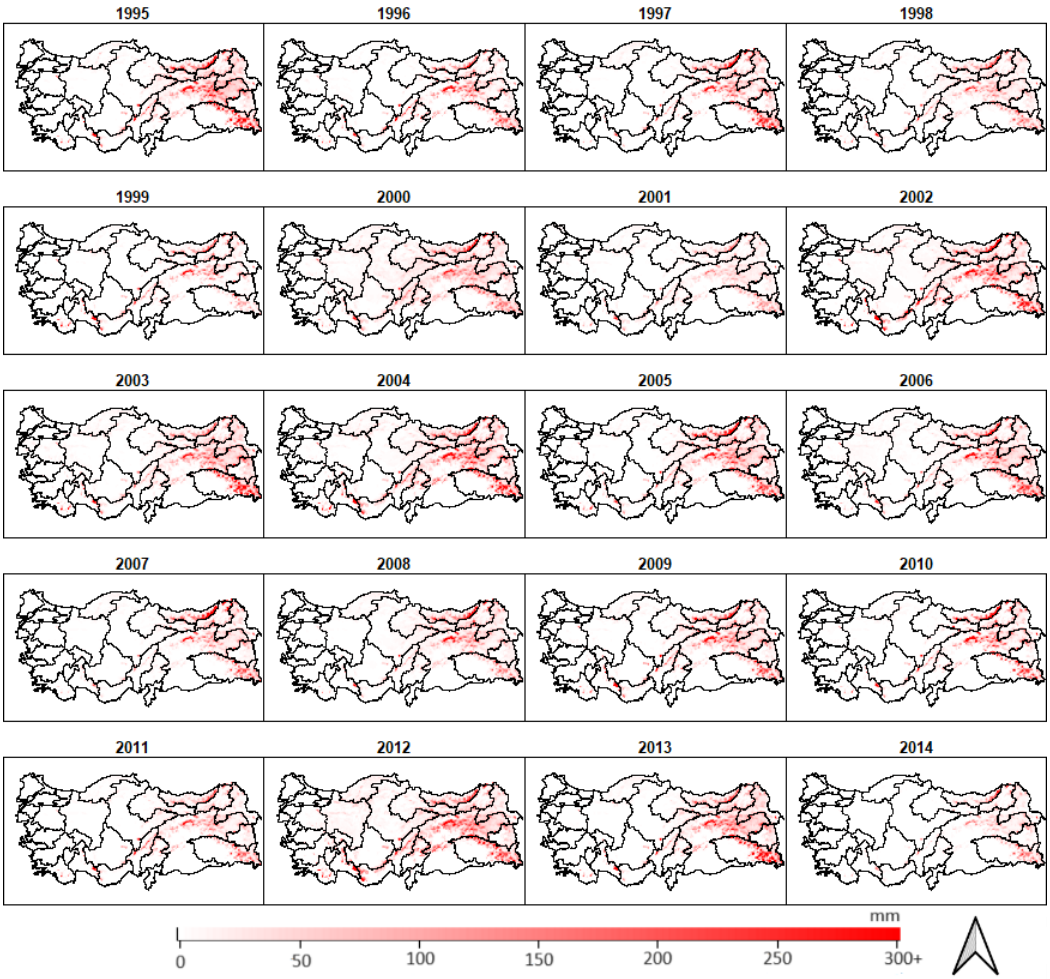


Figure 4.7. Spatial distribution of the annual mean snow water equivalent (SWE) during the historical period (1995-2014).

Seasonal and annual spatial distributions of mean SWE values calculated from a 20-year historical period and their anomaly changes calculated between future and historical periods are shown in Figure 4.8. It is seen that SWE values are at their maximum in winter and spring, while they have no or very low values in summer and autumn. When the differences between the future period and the reference period for SWE were examined, it was observed that there would be no rise in snowfall during the future period. Furthermore, upon comparing the reference period and change graphs, it is evident that snowfall will decline across almost all regions.

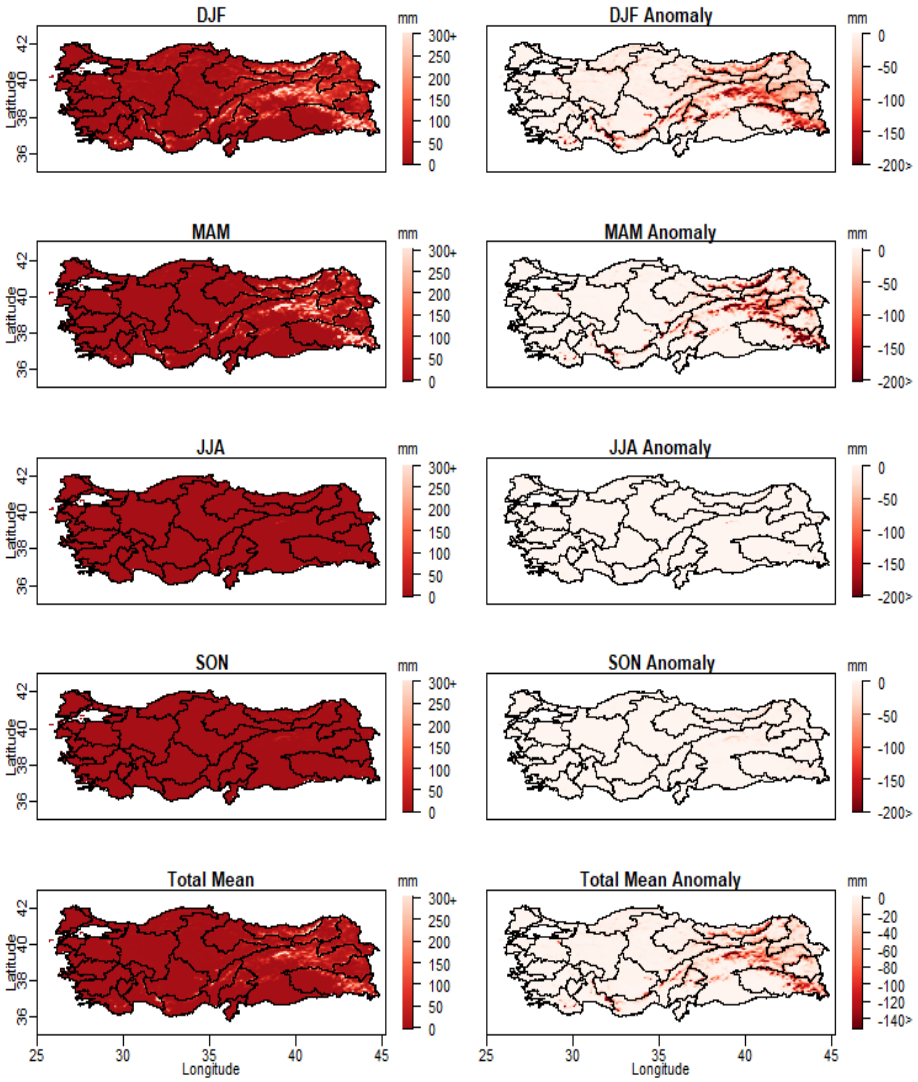


Figure 4.8. Spatial distributions of the seasonal and the total mean SWE during 1995-2014 (historical) (first column), seasonal and total mean change between future (2081-2100) and historical period (1995-2014) (second column).

Figure 4.9 shows the spatial distributions of standard deviations of mean SWE for historical and corresponding pseudo-future periods. Since SWE values will decrease in the future regardless of location, the average value will also decrease, so no noticeable difference in standard deviation is observed.

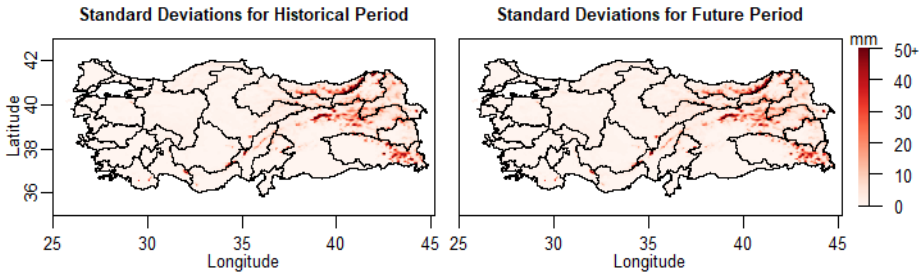


Figure 4.9. Spatial distributions of standard deviations of mean SWE for historical and corresponding pseudo future period.

## 4.2 Surface Water Budget Analysis for Selected Catchments

A water budget analysis was conducted using monthly total values for selected seven basins. Negative values are seen in the graphs because variation values are used for snow water equivalent and soil water storage. When it comes to snow water equivalent and soil water storage, negative values are indicative of certain processes. In the case of snow water equivalent, negative values typically signify melting, while negative values in soil water storage are associated with evaporation. Graphs were started in October since the analysis was conducted based on the water year to achieve better results and visualize the variable distributions (snow accumulation-melting period, etc.). The analysis included all grids within the basin, so spatial and temporal averages were calculated for water budget analysis.

Firstly, the 20-year monthly total time series used in water budget analysis for the reference periods of the basins (1995-2014) is given. In these graphs, the trends in the variables and their relationships with each other are seen. Secondly, each basin's water budget analysis results are given as water distribution graphs since they allow the interpretation of the interactions between the budget variables and the monthly distribution of the water entering and leaving the basin. Thirdly, the seasonal and annual differences between future and reference periods are provided in tables. Change values are presented in millimeters and percentages. Percentage values are obtained by dividing the difference between future and reference values by the reference value. Since snow water equivalent (SWE) and soil water storage (SWS) have negative values, their differences are given monthly averages rather than monthly totals to avoid confusion and to facilitate a more straightforward interpretation of the results.

### 4.2.1 Tigris Basin

The monthly time series of variables used in water budget analysis in the Tigris basin for the reference period are given in Figure 4.10. From the figure, trends and relations between the variables can be seen. For example, it is seen that minimum evapotranspiration (ET) values increase over time. The increase in annual minimum temperature is among the changes observed in the long term and consistently across Türkiye (Yilmaz & Yazicigil, 2011). Therefore, it is normal to observe an increase in minimum ET values. Also, interflow values tend to increase when SWE (snow water equivalent) values are negative, which relates to melting periods. This relation leads to the conclusion that snowmelt and interflow are directly proportional in the reference period.

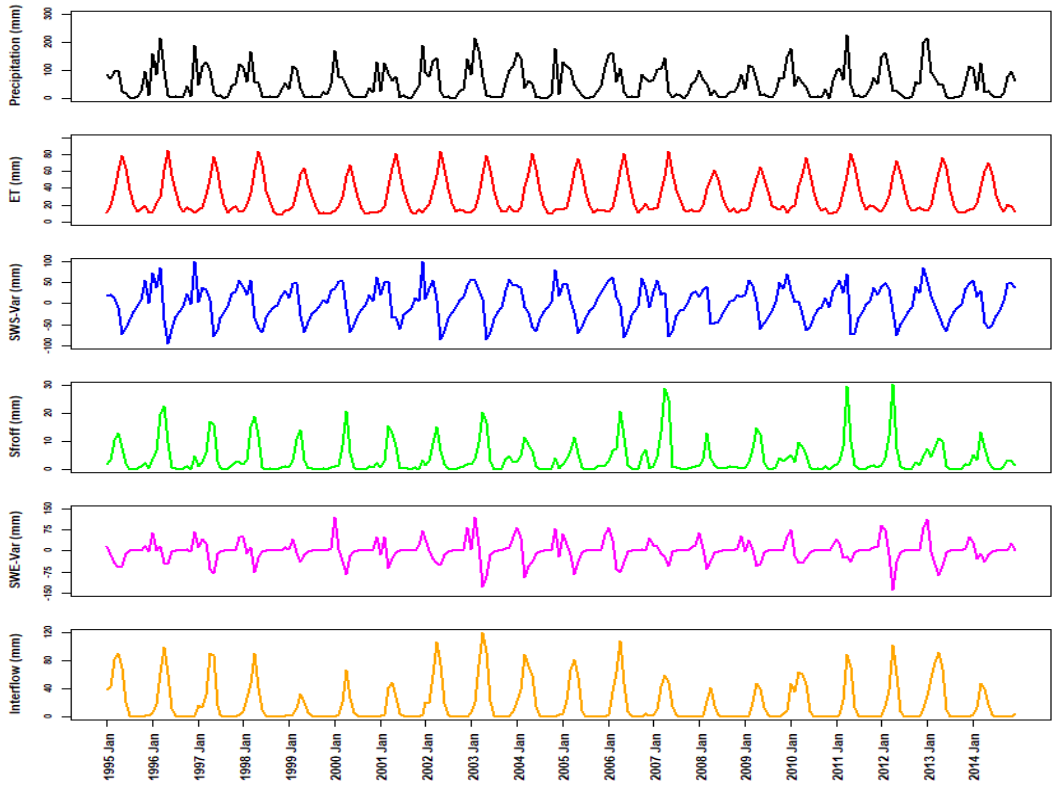


Figure 4.10. Monthly time series of Tigris Basin's water budget components for reference period (1995-2014).

Figures 4.11 and 4.12 show reference period and future period water budget distribution graphs created for the Tigris basin, respectively. From the figures, precipitation occurs mainly in the winter months and continues into mid-spring. In the Tigris basin, one of the basins receiving heavy snow, snow has been showing its effect since November, and most snow fell in January. Although the negative SWE-Var values in March indicate that melting started this month, the maximum melting occurred in April. In addition, it is observed that interflow and surface runoff also increase in the spring months when snow melting increases. It has been determined that precipitation during the winter months is mostly stored in soil. Evapotranspiration increased with increasing temperature, especially from April, and as precipitation decreased, this evaporation began to occur from soil water storage. The amount of water entering the basin during the summer months has decreased significantly, and an evapotranspiration effect appears to increase with temperature.

When the results of the graphs are compared, it is seen that precipitation decreases in winter-spring and increases in summer-autumn periods. Bozkurt & Sen (2013) stated that winter precipitation decreases in the highlands and northern parts of the Euphrates - Tigris basin and increases in the southern parts. There was a significant decrease in the average SWE value. Bozkurt and Sen (2013) supported the decrease in SWE values by stating that warming significantly affects the snow water equivalent in the highlands.

In addition, while the maximum surface runoff values were observed in April in the reference period (see Figure 4.11), it is seen that it will be in March in the future period (see Figure 4.12). Bozkurt & Sen (2013) also reported that the timing of surface runoff in the headwaters region is expected to experience significant temporal shifts to earlier days, ranging from 18 to 39 days.

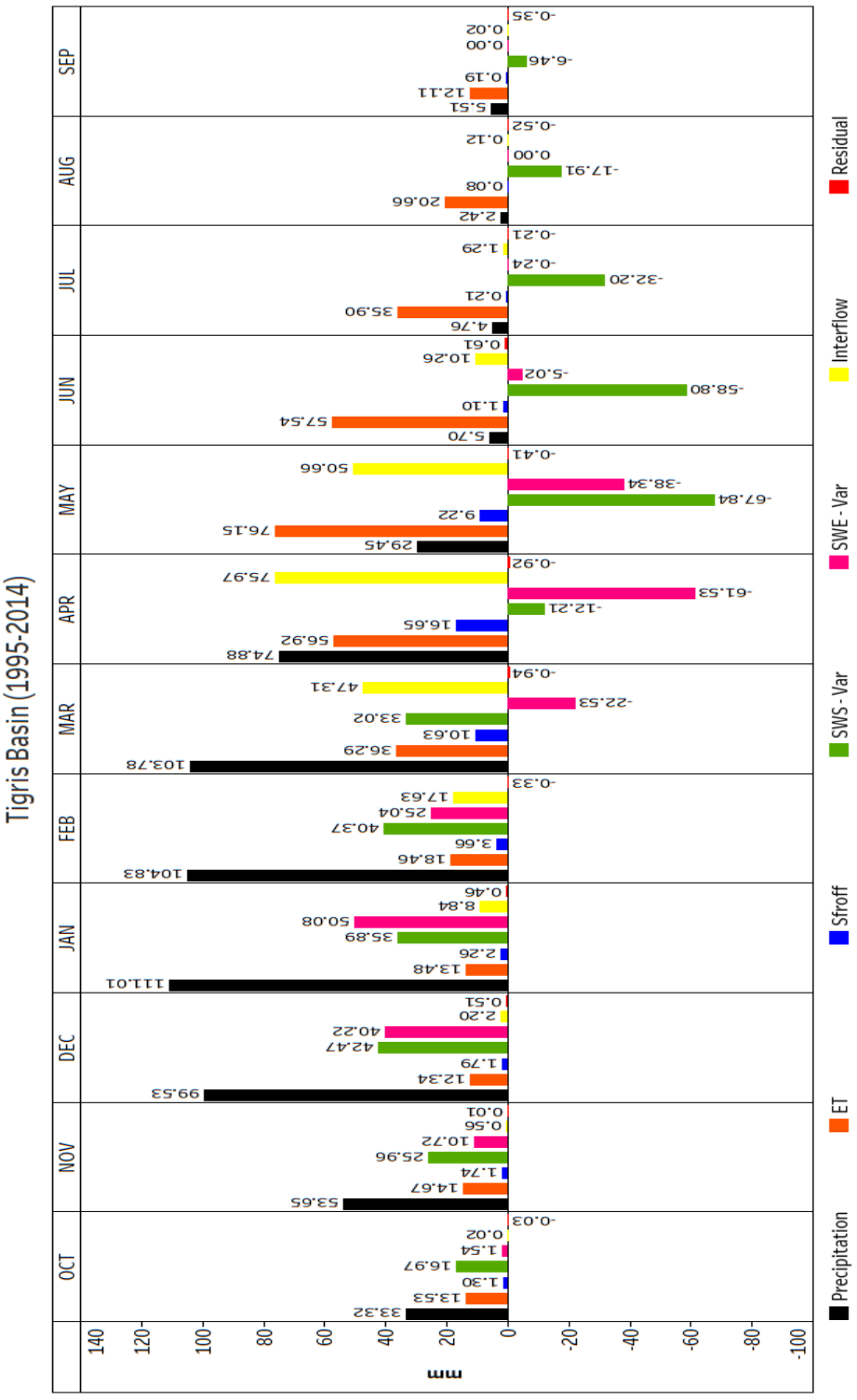


Figure 4.11. Tigris Basin water distribution graph for reference period (1995-2014)

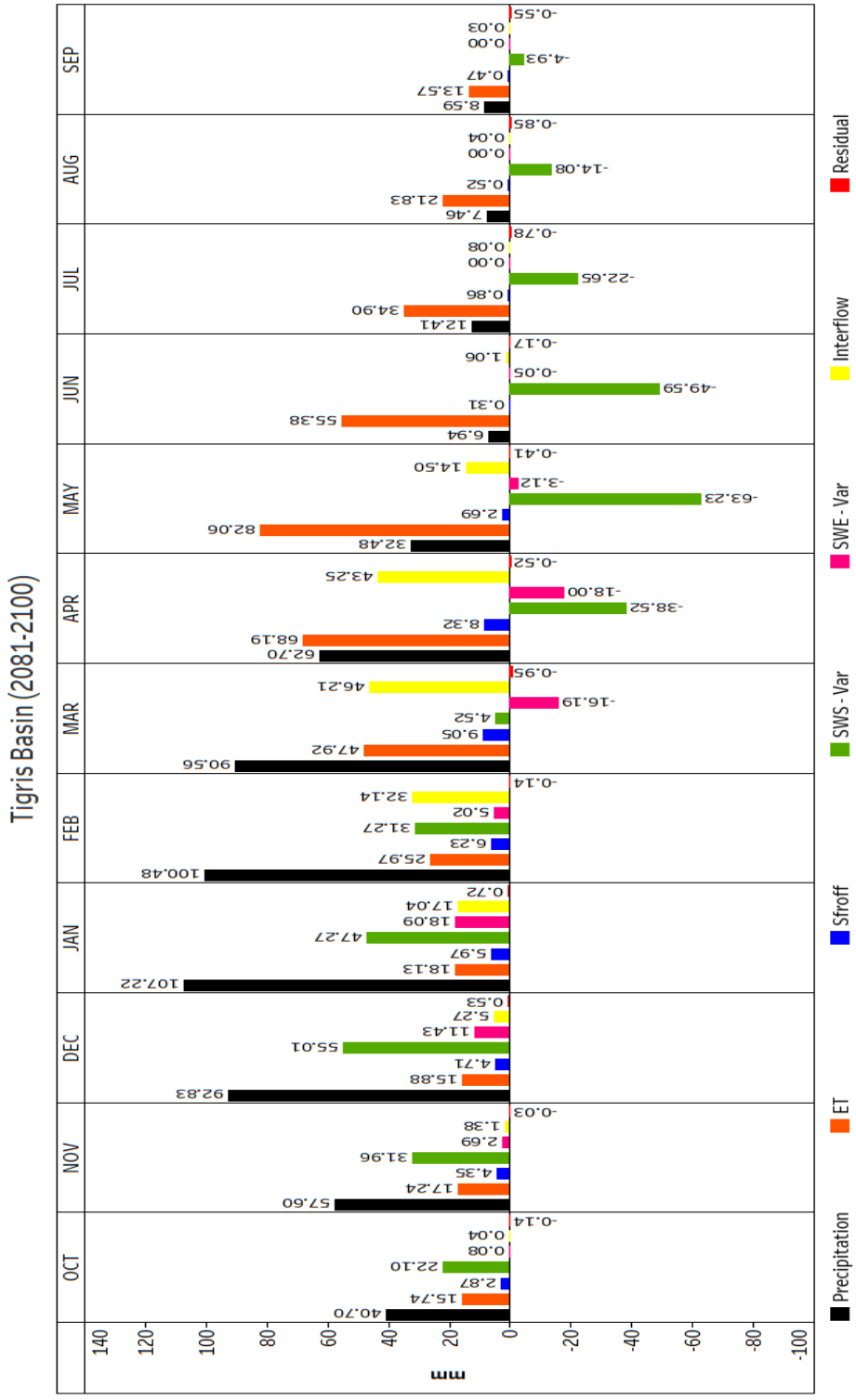


Figure 4.12. Tigris Basin water distribution graph for future period (2081-2100)

Table 4.1 shows the seasonal and annual changes between the future and reference periods for the Tigris basin in percentage and mm. It is apparent from the table that two variables experienced the highest decrease: interflow and SWE. Interflow decreased by approximately 25.06 % (53.84 mm), whereas SWE decreased by around 75.68 % (27.78 mm) annually. While an increase of about 14 mm is expected in precipitation in the summer and spring months, an annual decrease of 8.86 mm is expected due to the decrease in the winter months. (Ohara et al., 2011) stated that because of the dry climate in the lower Tigris-Euphrates river basin, a significant amount of water evaporates from the reservoirs, and Table 4.1 shows that ET was the only value that showed an increase on an annual basis, with a rise of roughly 13.25 %. Moreover, a 5.08 % decrease in surface runoff values is expected. According to research on climate change, it is predicted that there will be significant decreases in precipitation levels in the southern basins of Türkiye, such as the Euphrates and Tigris basins, and this reduction in precipitation will lead to a decrease in surface runoff (Yucel et al., 2015).

Table 4.1. Seasonal and annual changes of water budget components between future and reference period for Tigris Basin

| | **Precipitation % (mm)** | **Sfroff % (mm)** | **Interflow % (mm)** | **ET % (mm)** | **SWE-Mean % (mm)** | **SWS-Mean % (mm)** |
|---|---|---|---|---|---|---|
| **DJF** | -4.70 (-14.84) | 119.19 (9.19) | 89.87 (25.76) | 35.44 (15.69) | -70.23 (-52.16) | 2.25 (13.42) |
| **MAM** | -10.75 (-22.36) | -45.05 (-16.45) | -40.23 (-69.98) | 17.01 (28.81) | -81.06 (-56.81) | -3.62 (-24.26) |
| **JJA** | 108.21 (13.93) | 21.39 (0.29) | -89.83 (-10.44) | -1.75 (-1.99) | -99.59 (-0.58) | -4.36 (-23.52) |
| **SON** | 15.57 (14.40) | 138.59 (4.47) | 145.48 (0.86) | 15.49 (6.24) | -83.30 (-1.56) | -1.99 (-10.12) |
| **ANNUAL** | -1.41 (-8.86) | -5.08 (-2.48) | -25.06 (-53.84) | 13.25 (48.75) | -75.68 (-27.78) | -1.92 (-11.12) |

### 4.2.2 Euphrates Basin

The monthly time series of the Euphrates Basin's water budget components are given in Figure 4.13. It's worth noting that there were significant changes in variables between 1999-2001 and 2006-2008, particularly in the interflow levels, which experienced a significant decrease. Upon further investigation, it was discovered that Türkiye had been severely affected by droughts during those years, which could explain these findings. According to Türkes, Türkiye has experienced several drought events, with the most severe and widespread occurrences happening during specific periods. These periods include 1971-1974, 1983-1984, 1989-1990, and 2007-2008, as well as 1996 and 2001 (Türkes, 2012; Türkes, 1996, 1998ab, 1999, 2003b, 2008abc; Türkes & Erlat, 2003, 2005; Türkes & Tatlı, 2009; Türkes et al., 2009ab).

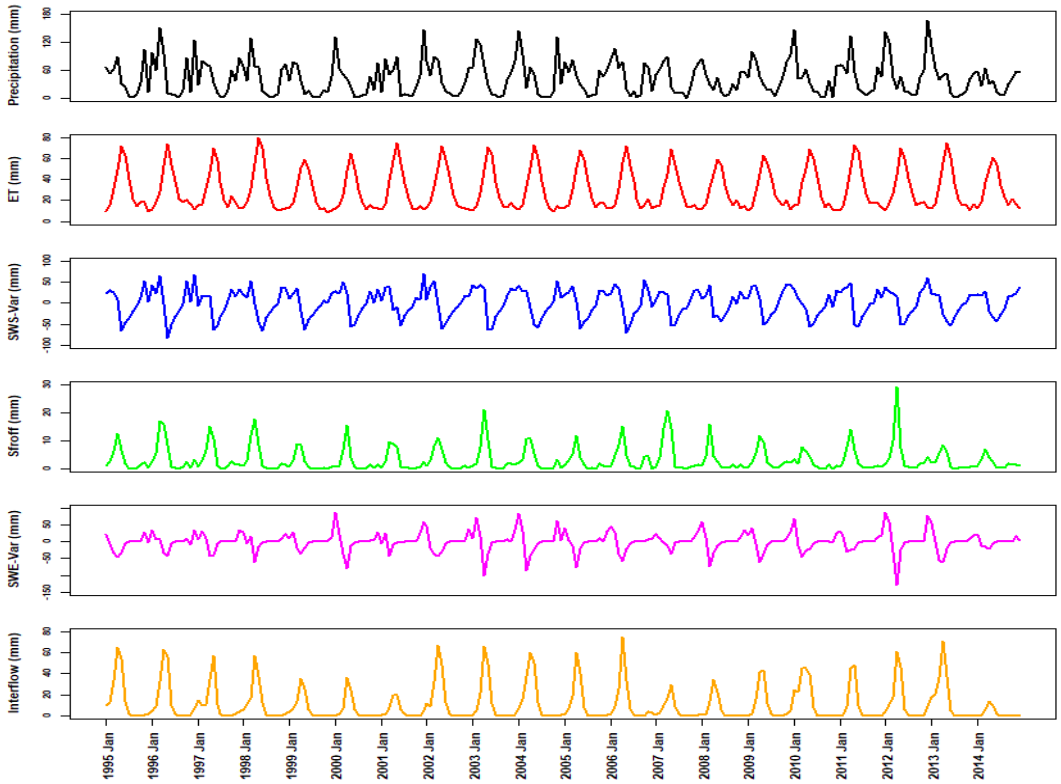


Figure 4.13. Monthly time series of Euphrates Basin's water budget components for reference period (1995-2014)

The Euphrates Basin reference period water distribution graph is given in Figure 4.14, and the future water distribution graph is shown in Figure 4.15. When examining the reference period water budget graph, it becomes evident that it is similar to the Tigris Basin's graph. It is important to note that snowfall significantly impacts interflow in this basin and continues to melt until August. Over the higher altitudes of the Euphrates Basin, precipitation primarily falls as snow, which remains on the ground for almost half of the year (Akyurek et al., 2011). During the spring months, there is a noticeable increase in the surface runoff and interflow values in the Euphrates and Tigris basins (see Figure 4.11 and Figure 4.14), which is linked to the significant rise in snowmelt. In these two snow-dominated basins, snowmelt runoff during the spring and early summer typically makes up 60–70% of the total annual runoff (Yucel et al., 2015; Sorman, 2004).

Additionally, the effect of evapotranspiration becomes more pronounced with the rising temperatures during the summer months, and it continues to rise in future periods (see Figure 4.15). Yilmaz et al. (2019) conducted a study on the upper Euphrates-Tigris basin about the hydroclimatic effects of changes in land use and land cover on the water budget. The authors stated that increased latent heat flux increases evapotranspiration and, as a result, atmospheric water vapor concentration. Moisturization of a shallower boundary layer causes the formation of convective clouds, which increases convective precipitation, especially during the irrigation season. The increased water loss through evapotranspiration can significantly alter the GAP region's water budget (Yilmaz et al., 2019).

Upon comparing the future and reference period graphs, it can be observed that the interflow values have shown a slight decrease owing to the significant decrease in SWE values.

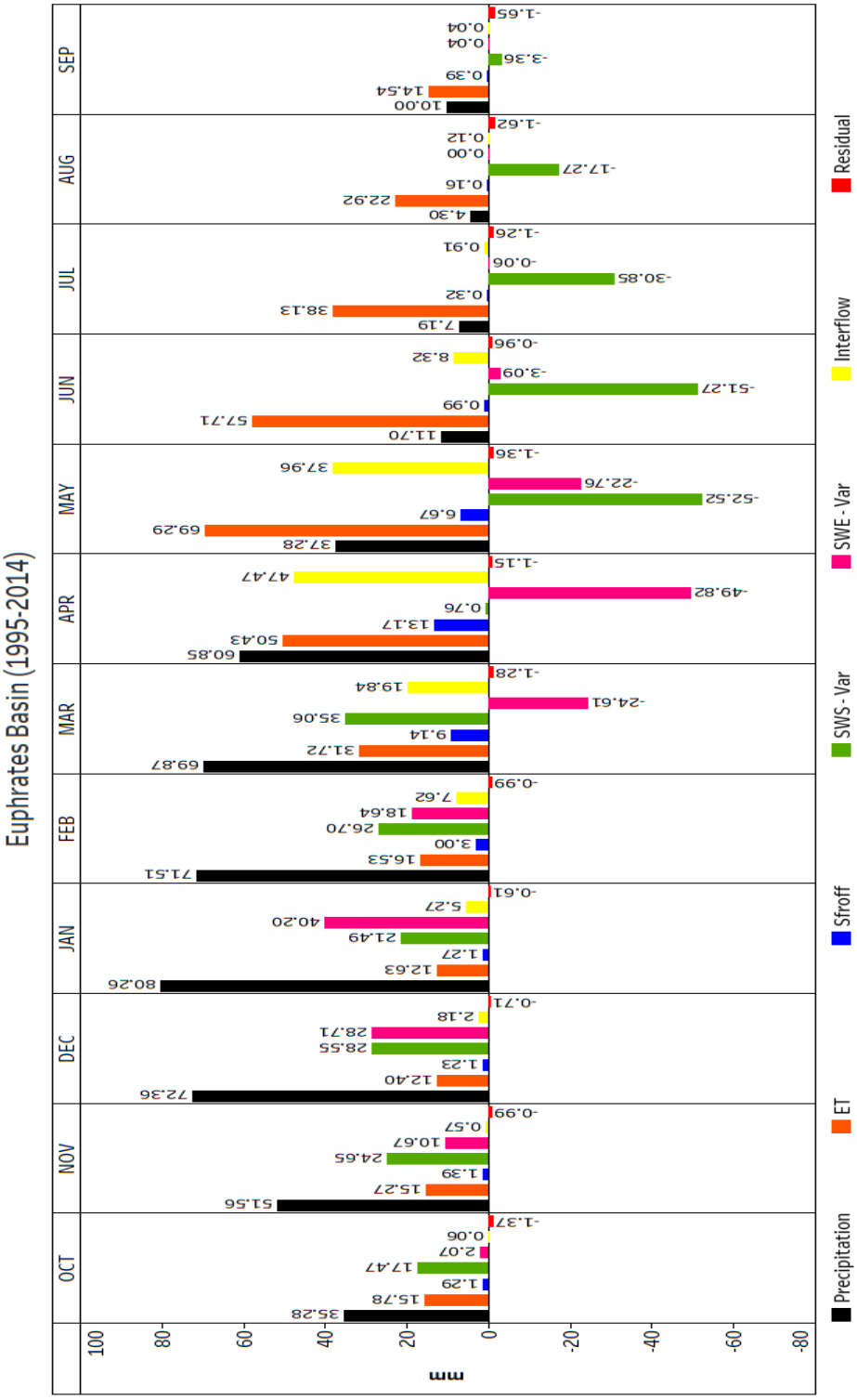


Figure 4.14. Euphrates Basin water distribution graph for reference period (1995-2014)

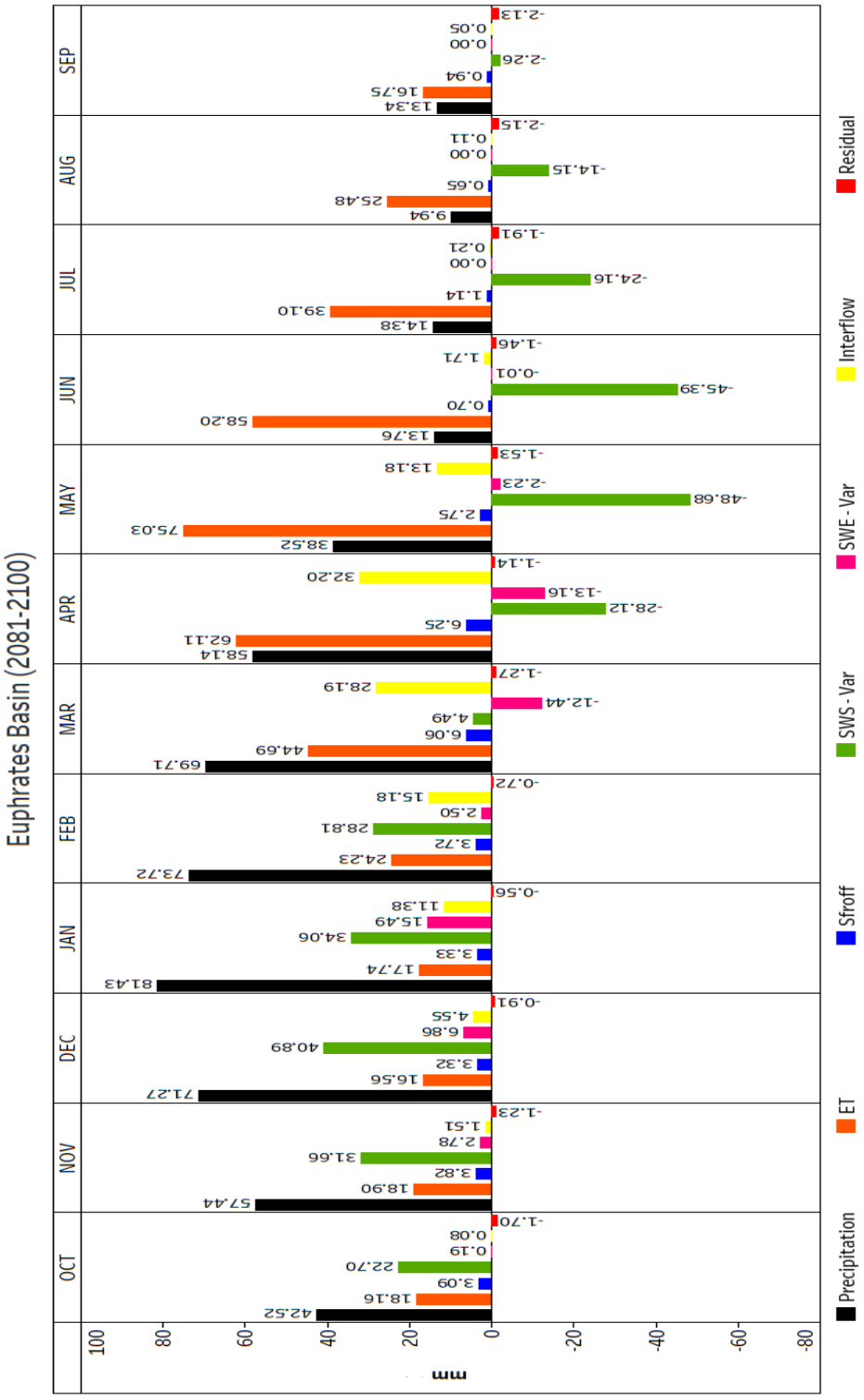


Figure 4.15. Euphrates Basin water distribution graph for future period (2081-2100)

Table 4.2 shows seasonal and annual changes between the future and reference periods for the Euphrates basin. It is seen that total precipitation and ET have increased. When checked from the precipitation maps in Figure 4.2, it is seen that this increase occurs mainly in the northern part of the basin, in the border regions of the Aras and Coruh basins (upper Euphrates). Precipitation in the rain phase, which increased during the winter months, penetrated more into the soil and increased the ET value while also increasing the SWS values. However, increasing ET in the summer months caused the SWS values to decrease.

Table 4.2. Seasonal and annual changes of water budget components between future and reference period for Euphrates Basin

| | **Precipitation % (mm)** | **Sfroff % (mm)** | **Interflow % (mm)** | **ET % (mm)** | **SWE-Mean % (mm)** | **SWS-Mean % (mm)** |
|---|---|---|---|---|---|---|
| **DJF** | 1.03 (2.30) | 88.50 (4.86) | 106.33 (16.03) | 40.83 (16.97) | -71.95 (-42.80) | 2.69 (16.58) |
| **MAM** | -0.97 (-1.63) | -48.02 (-13.92) | -30.11 (-31.70) | 20.07 (30.39) | -80.31 (-39.93) | -2.08 (-14.08) |
| **JJA** | 64.26 (14.89) | 69.90 (1.02) | -78.20 (-7.32) | 3.38 (4.02) | -99.95 (-0.34) | -3.50 (-20.16) |
| **SON** | 16.98 (16.45) | 155.72 (4.77) | 143.91 (0.97) | 18.02 (8.21) | -83.88 (-1.82) | -1.75 (-9.61) |
| **ANNUAL** | 6.25 (32.02) | -8.33 (-3.24) | -16.89 (-22.03) | 16.68 (59.59) | -75.98 (-21.22) | -1.12 (-6.82) |

### 4.2.3 Aras Basin

The monthly time series of Aras Basin for the reference period is given in Figure 4.16. It has been observed that, during the summer months, when the values of ET (evapotranspiration) increase, the precipitation decreases as the temperature increases. Therefore, the SWS (soil water storage) values decrease and become negative.

According to the observations made from 1981 to 2010, it was noted that the basin experienced its driest year in 2001 and its wettest year in 2004 (Aksoy, 2020). Upon analyzing Figure 4.16, it becomes apparent that while the variable values were considerably low in 2001, they experienced a significant surge in 2004.

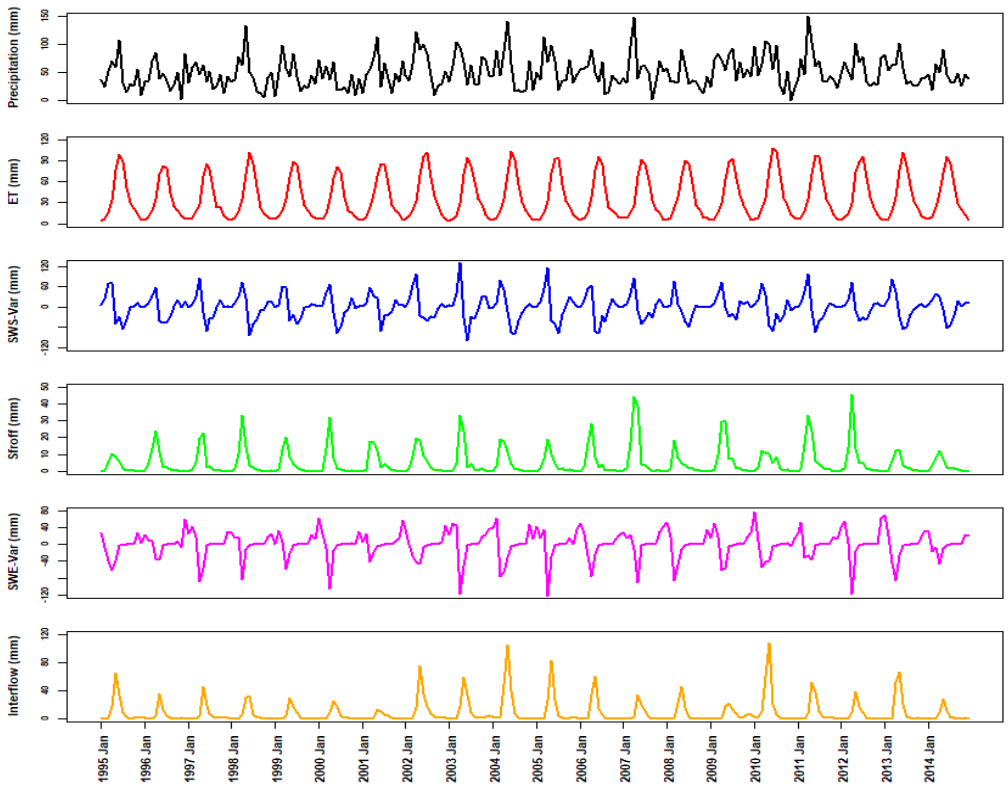


Figure 4.16. Monthly time series of Aras Basin's water budget components for reference period (1995-2014)

Figure 4.17 shows the reference period water distribution graph for Aras Basin. The Aras basin is also where snow density is high, and continentality generally dominates. Therefore, the temperature difference between summer and winter is significant. Figure 4.5 shows that evapotranspiration values are much more effective in summer compared to the other two basins. It is seen that precipitation falls mainly in the spring season, and soil water storage increases in direct proportion. In contrast, the effect of evapotranspiration increases with the temperature increase in May, and soil water storage decreases. Higher surface runoff and interflow are observed in spring with increased precipitation and snowmelt.

Figure 4.18 shows a future-period water distribution graph for the Aras basin. When comparing the future period water budget graph (see Figure 4.18) with the reference period graph (see Figure 4.17), it has been observed that the Aras basin will experience an increase in precipitation, ET, and SWS-Mean values. During the reference period, the precipitation contributed more to surface runoff. However, it was discovered that in the future, since no snowfall fed the interflow, the incoming precipitation contributed more to interflow and soil water storage, resulting in a decrease in surface runoff. Additionally, due to the reduction in SWE values, it is noteworthy that the melting observed even in June during the reference period ended in May in the future period. As a result of the warming effect in eastern Türkiye, the snowmelt runoffs in the basins of the Euphrates, Tigris, and Aras rivers are occurring earlier than usual. This shift in timing is causing changes in the hydrologic regime of the river system, which in turn is leading to alterations in the region's climatic conditions (Güventürk, 2013).

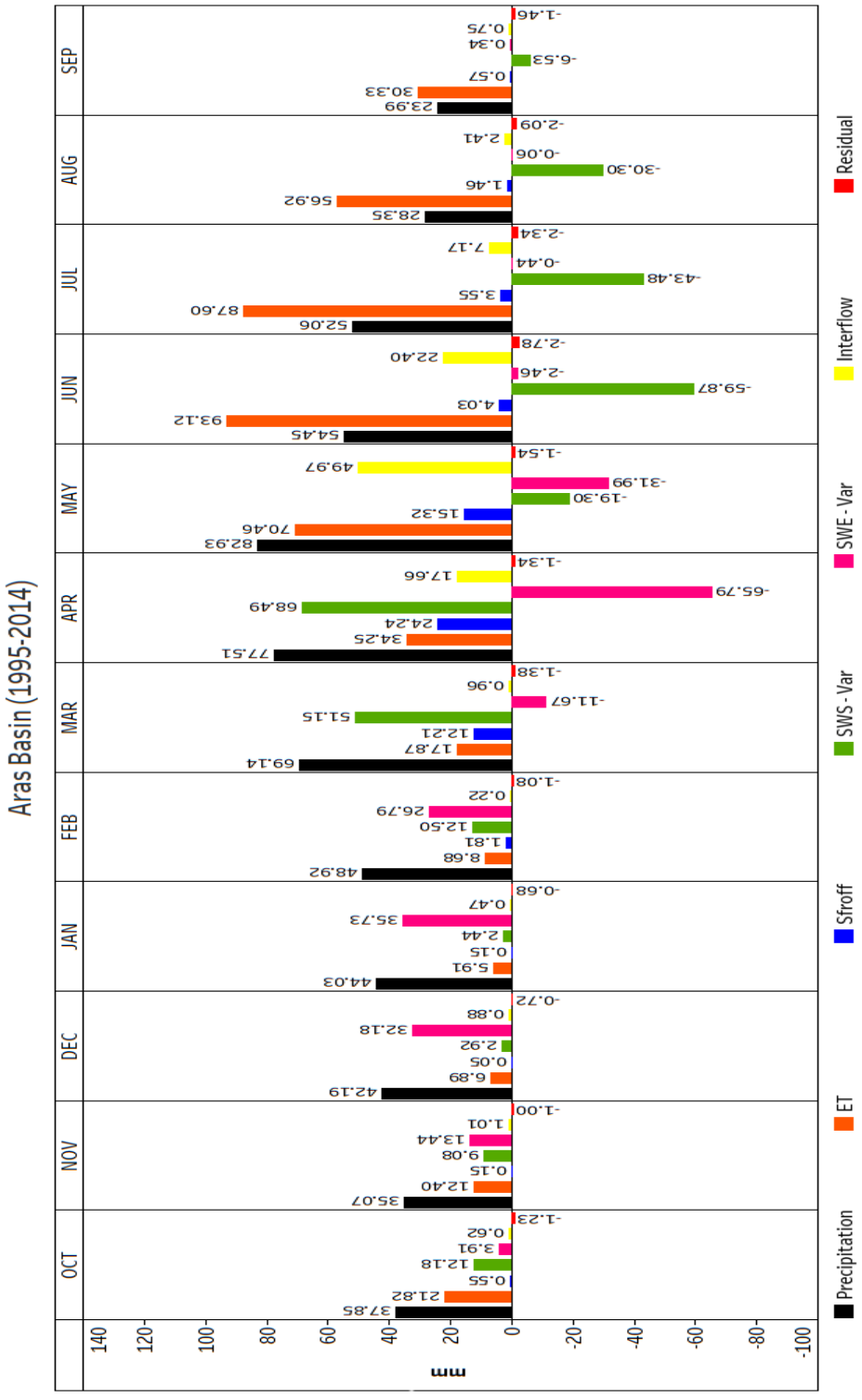


Figure 4.17. Aras Basin water distribution graph for reference period (1995-2014)

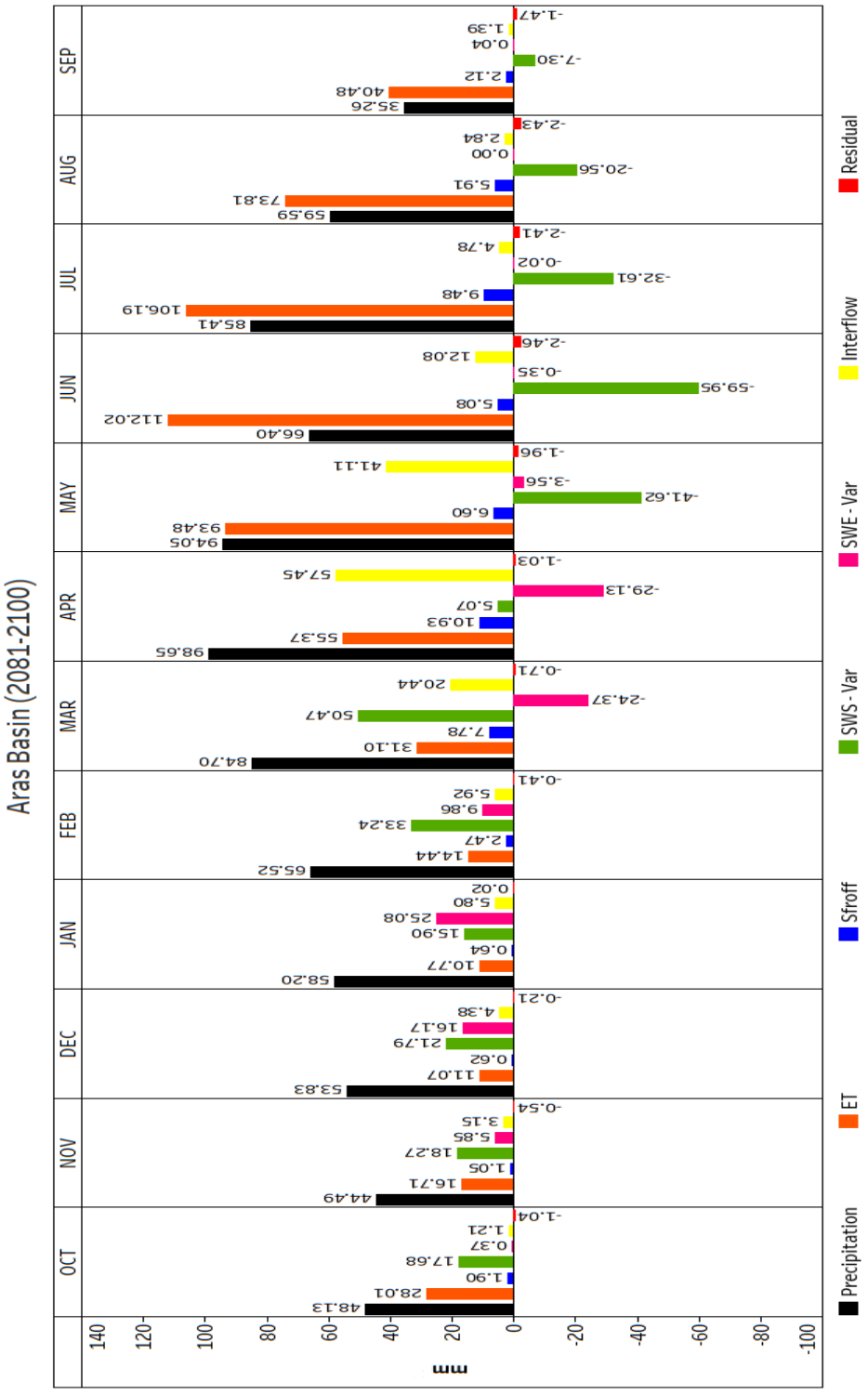


Figure 4.18. Aras Basin water distribution graph for future period (2081-2100)

Seasonal and annual changes between future and reference periods for the Aras basin are shown in Table 4.3. The results show an expected increase of approximately 33.15 % in precipitation, 53.63 % in interflow, 32.98 % in ET, and 6.17 % in SWS-Mean. On the other hand, it was determined that surface runoff would decrease by 14.84 % and SWE-Mean values by 58.72 % annually. According to Yucel et al. (2015), the Aras basin's annual runoff will experience a decline of approximately 11.6 %.

Table 4.3. Seasonal and annual changes of water budget components between future and reference period for Aras Basin

| | **Precipitation % (mm)** | **Sfroff % (mm)** | **Interflow % (mm)** | **ET % (mm)** | **SWE-Mean % (mm)** | **SWS-Mean % (mm)** |
|---|---|---|---|---|---|---|
| **DJF** | 31.39 (42.42) | 85.27 (1.72) | 929.95 (14.54) | 68.89 (14.80) | -48.89 (-32.89) | 11.29 (57.03) |
| **MAM** | 20.83 (47.82) | -51.13 (-26.47) | 73.50 (50.41) | 46.79 (57.36) | -67.87 (-42.79) | 8.17 (48.64) |
| **JJA** | 56.75 (76.54) | 126.41 (11.43) | -38.40 (-12.28) | 22.88 (54.38) | -90.34 (-0.46) | 0.95 (5.10) |
| **SON** | 31.95 (30.97) | 299.87 (3.81) | 142.38 (3.38) | 31.99 (20.65) | -75.64 (-2.59) | 4.20 (20.42) |
| **ANNUAL** | 33.15 (197.75) | -14.84 (-9.51) | 53.63 (56.04) | 32.98 (147.19) | -58.72 (-19.56) | 6.17 (32.80) |

### 4.2.4 Coruh Basin

The monthly time series of the Coruh basin for the reference period is given in Figure 4.19. Similar to the other three basins, the SWE change values in this basin are high due to the heavy snowfall. Aksoy (2020) stated that the basin experienced its driest year in 2001 during the 1981–2010 observation period. The low values in 2001, seen in Figure 4.19, can be evidence of this finding.

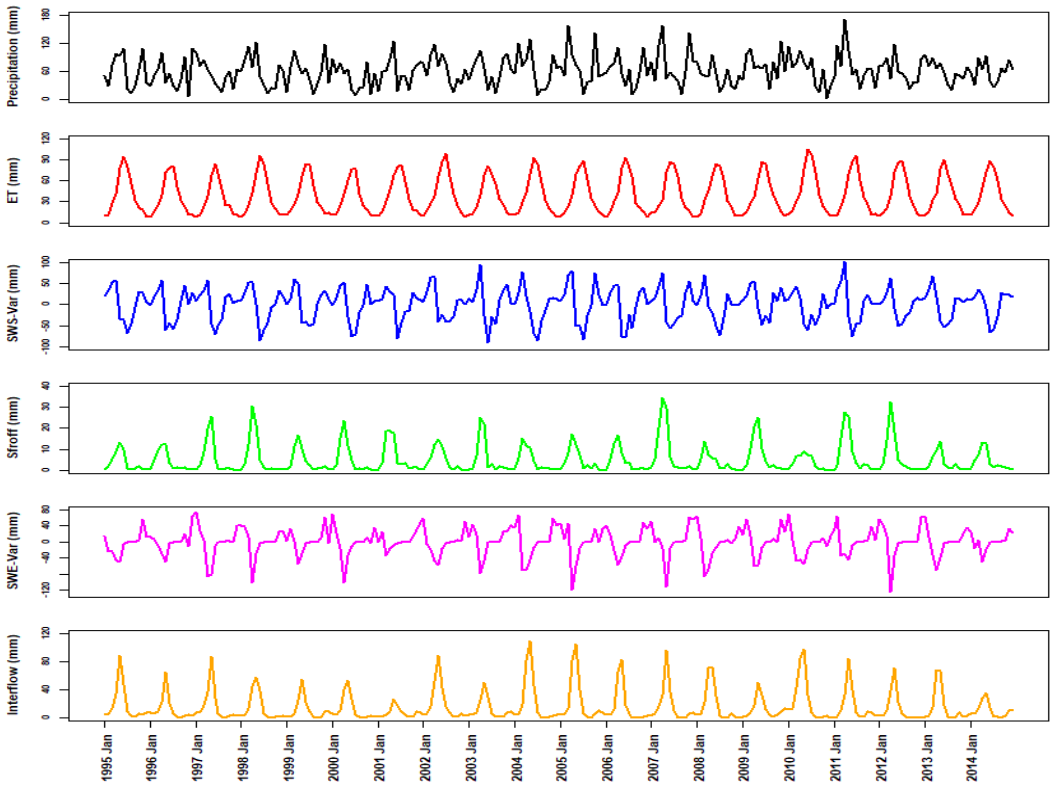


Figure 4.19. Monthly time series of Coruh Basin's water budget components for reference period (1995-2014)

Figure 4.20 shows the reference period water distribution graph of the Coruh basin. Analyzing the graph of the Coruh Basin (see Figure 4.20), it is evident that the region receives higher and more consistent precipitation throughout the year compared to the other basins in the Eastern Anatolia region. In addition to the higher and more consistent precipitation, the Coruh Basin also experiences heavy snowfall and high evapotranspiration in the summer months. These factors indicate that the basin has a

transitional climate between the Black Sea and continental climates. It is worth noting that precipitation in the Coruh Basin mainly increases during spring. As snowmelt occurs during these months in addition to precipitation, there are also significant increases in surface flow values. Since precipitation and snow significantly impact this basin, it is one of the basins with high interflow values, especially with the melting snow in May.

The future period water distribution graph for the Coruh basin is given in Figure 4.21. Among the basins studied, it is the basin where precipitation will increase the most in the future. Based on Figure 4.21, there will be a rise in precipitation and a decrease in SWE values. This implies that the precipitation will predominantly form rain in the future period. As a result, it can be inferred that the increasing interflow and SWS (soil water storage) values in the subsequent period are due to rain, while the effect of snow on these values has decreased. Regarding this issue, Iwata et al. (2011) mentioned that water that permeates the frozen soil increases the temperature of the frozen layer, supplying latent heat and potentially increasing the amount of liquid (i.e., movable) soil water. However, the rate of snowmelt infiltration is decreased by the snowmelt water that refreezes on and in the frozen soil layer (Iwata et al., 2011). In other words, we can say that liquid precipitation has greater penetrating power in the soil and contributes to SWS more.

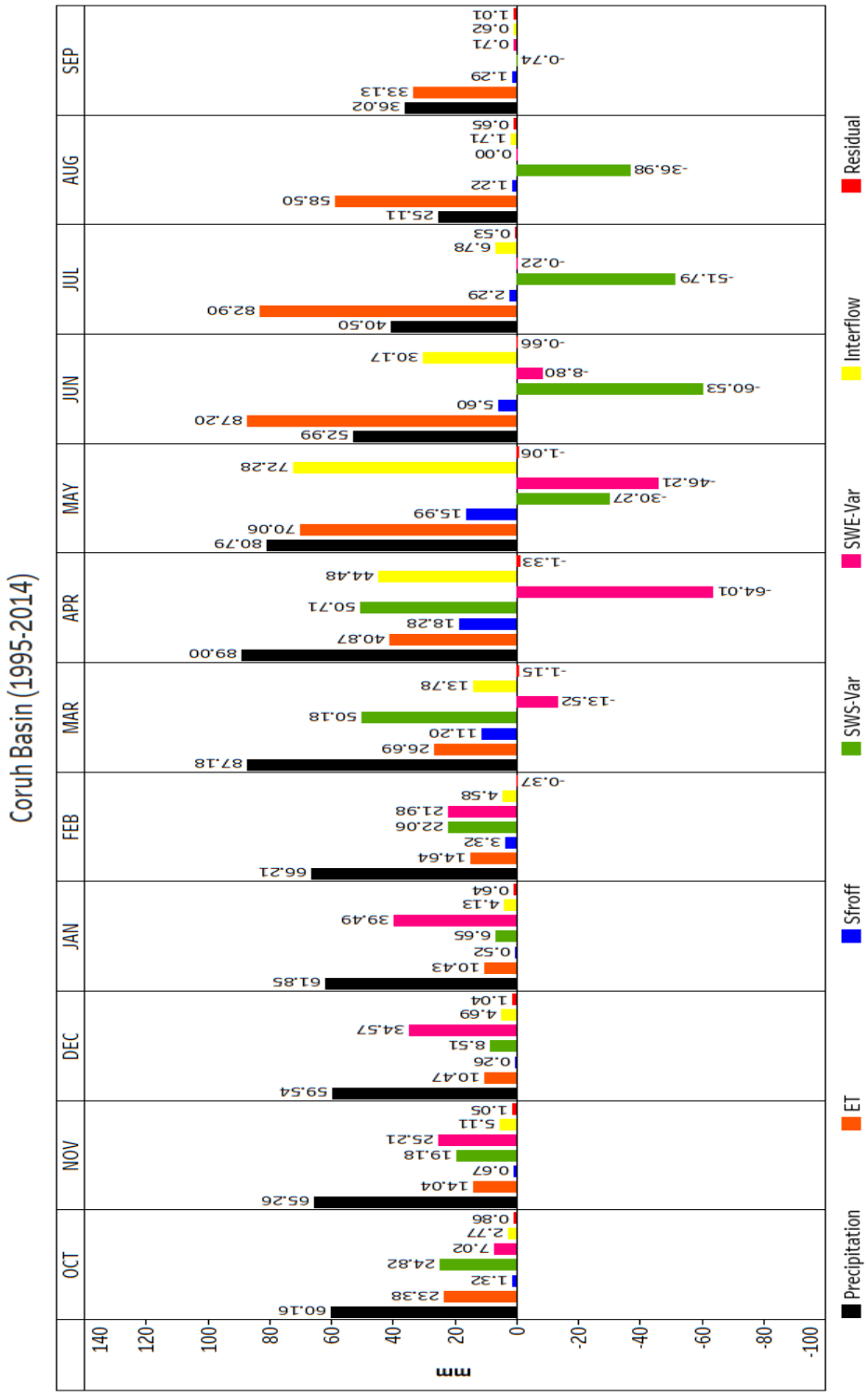


Figure 4.20. Coruh Basin water distribution graph for reference period (1995-2014)

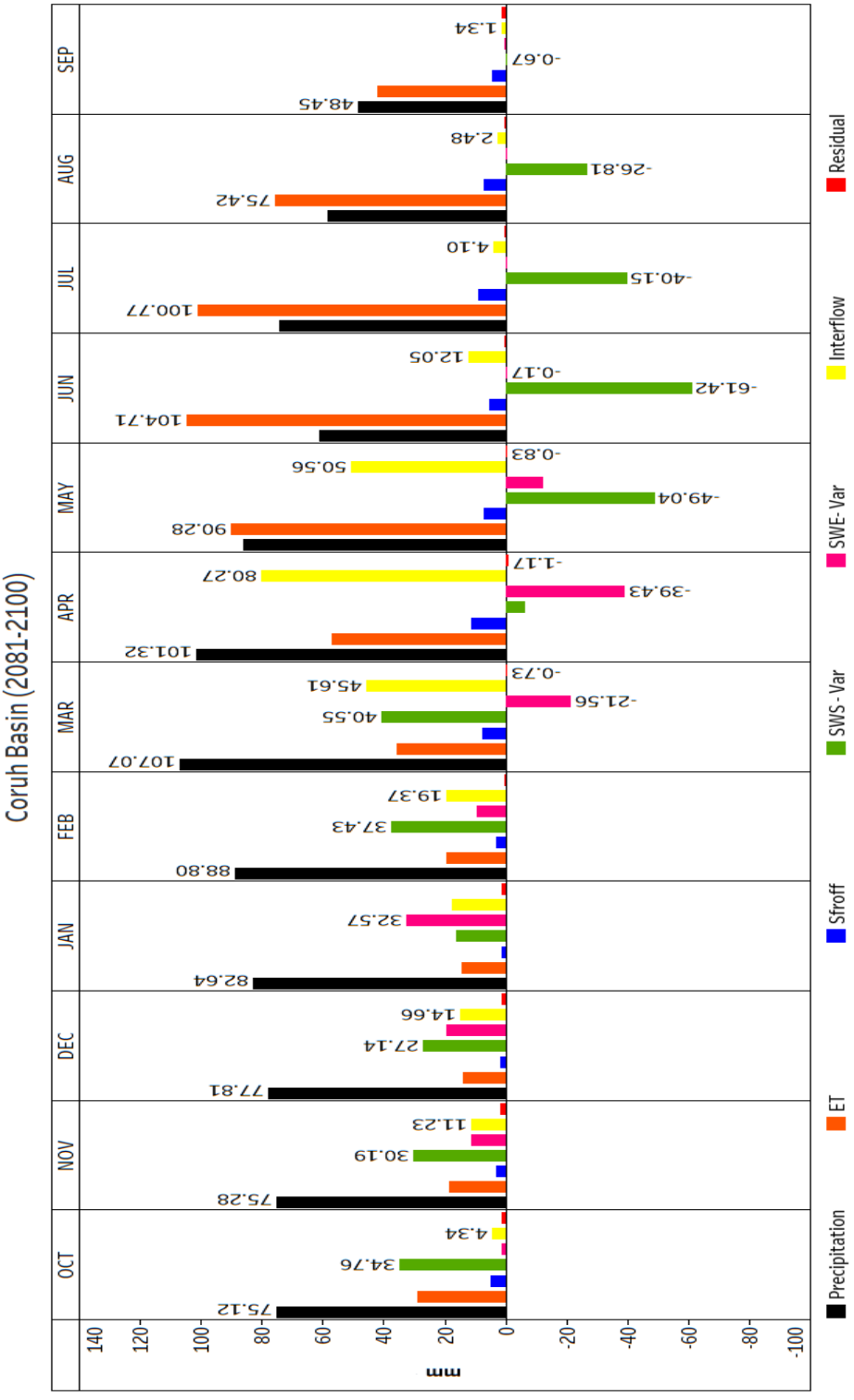


Figure 4.21. Coruh Basin water distribution graph for future period (2081-2100)

Table 4.4 shows the seasonal and annual changes between future and reference period values of the Coruh basin. The figure shows that there has been an annual increase of around 29 % in precipitation due to the absence of any seasonal decrease. As precipitation levels have risen, interflow has increased by about 39.25 % and SWS-Mean by roughly 6 %. Even though the surface runoff values have decreased in the Tigris, Euphrates, and Aras basins, they are expected to increase by 2.62 % in the Coruh basin. According to Yucel et al. (2015), by the end of the current century, a regional climate change simulation based on a high emissions scenario predicts a 10–30% decline in the yearly surface runoffs of the Aras, Euphrates, and Tigris basins and a slight increase of approximately 4 % in the Coruh basin.

Table 4.4. Seasonal and annual changes of water budget components between future and reference period for Coruh Basin

| | **Precipitation % (mm)** | **Sfroff % (mm)** | **Interflow % (mm)** | **ET % (mm)** | **SWE-Mean % (mm)** | **SWS-Mean % (mm)** |
|---|---|---|---|---|---|---|
| **DJF** | 31.14 (59.18) | 34.40 (1.43) | 293.01 (38.29) | 32.43 (11.59) | -46.88 (-40.66) | 11.51 (59.94) |
| **MAM** | 14.59 (37.48) | -44.58 (-20.69) | -35.43 (-46.16) | 33.49 (45.92) | -60.01 (-48.92) | 6.92 (42.18) |
| **JJA** | 64.67 (75.94) | 136.81 (12.34) | -50.43 (-18.95) | 22.93 (52.40) | -99.42 (-1.03) | 0.67 (3.56) |
| **SON** | 23.42 (37.74) | 261.18 (8.57) | 106.60 (8.72) | 26.73 (18.85) | -74.06 (-5.06) | 4.47 (21.44) |
| **ANNUAL** | 28.99 (210.33) | 2.62 (1.65) | 39.25 (74.22) | 27.29 (128.76) | -54.33 (-23.92) | 5.94 (31.78) |

In these four basins located in the eastern part of Türkiye, the snow melt continues until June and even July in the reference period, though to a lesser extent. However, it is also worth mentioning that the duration for which the snow remains on the ground will decrease. Recent studies suggest that streamflow timings in mountainous basins have already shifted earlier by around nine days on average, indicating an earlier spring snowpack melting due to rising temperatures in recent years (Yucel et al., 2015).

### 4.2.5 Western Black Sea Basin

Table 4.22 shows the Western Black Sea basin water budget components' reference period monthly time series. It has been observed that precipitation remains at high values throughout the year. Therefore, SWS value fluctuations are not as dramatic as in other basins. Also, it is seen that SWE variation values are lower than the other four basins.

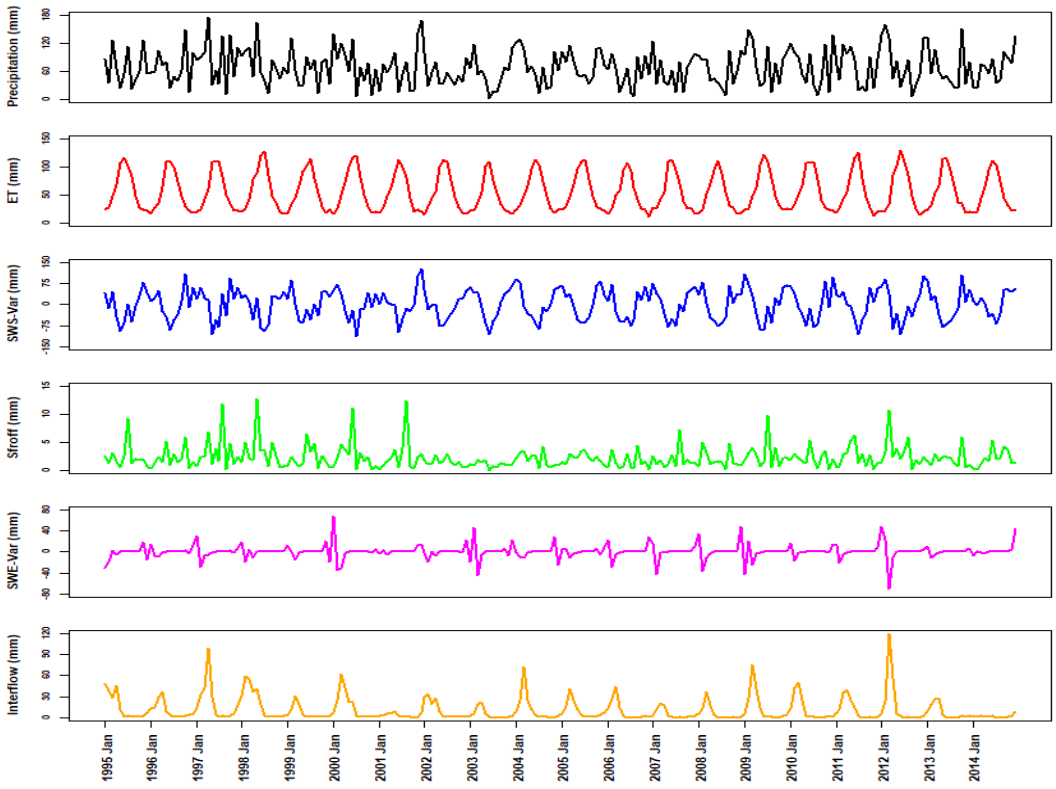


Figure 4.22. Monthly time series of Western Black Sea Basin's water budget components for reference period (1995-2014)

Figure 4.23 displays the water distribution graph for the reference period, while Figure 4.24 illustrates the water distribution graph for the future period of the Western Black Sea basin. Results prove that precipitation happens throughout the year, and Figure 4.2 illustrates that the coastal region experiences higher precipitation levels. According to the report of the General Directorate of Water Management (2023), the average annual total precipitation in the Ereğli, Melen, and

Bartın sub-basins is about 900 mm, which is mainly situated on the coastline in the Western Black Sea Basin. However, the report also suggests precipitation decreases as you move inland and remains below 900 mm in the Devrekani-Sinop and Filyos sub-basins. This results in a decrease in the basin's average.

Snowfall is less frequent in this basin than in the Eastern Anatolian basins. The snow does not remain on the ground for too long, and the melting period ends by April in the reference period. On the other hand, it is seen that the melting period will end in March with a decrease in snowfall and an increase in temperature in the future period (see Figure 4.24).

In the summer months, the ET values also increased due to the increase in precipitation and the temperature in the basin. However, the increase in ET was more significant than the increase in precipitation, which resulted in a decrease in SWS values.

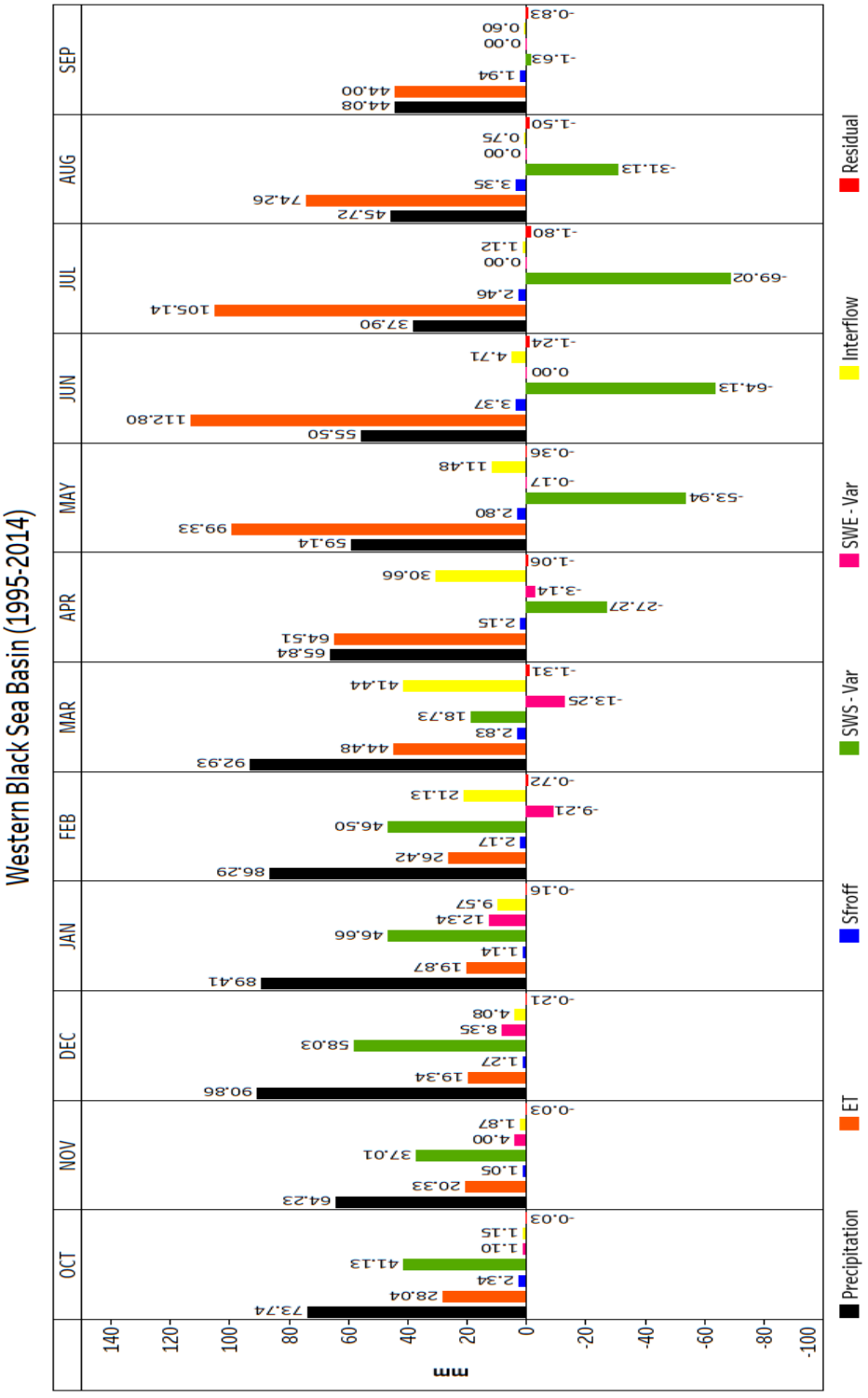


Figure 4.23. Western Black Sea Basin water distribution graph for reference period (1995-2014)

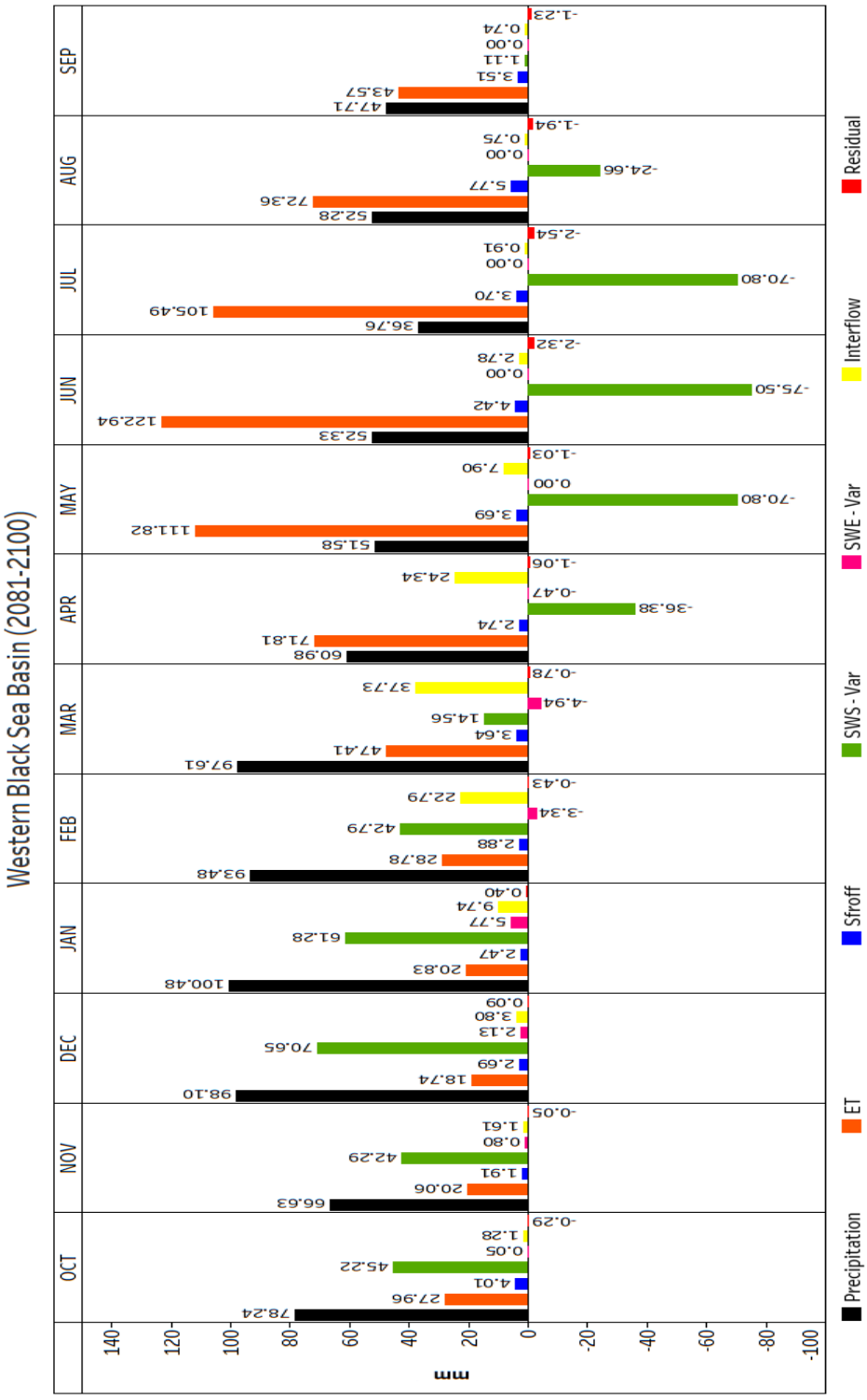


Figure 4.24. Western Black Sea Basin water distribution graph for future period (2081-2100)

Table 4.5 shows the differences between the future and reference periods of the Western Black Sea basin on a seasonal and annual basis. According to Table 4.5, annual increases of 3.79, 54.19, and 5.05 % are expected in precipitation, surface runoff, and ET values, respectively. Regarding increases in precipitation and ET values, Kale (2020) compared the temperature (°C) and precipitation (%) anomalies of the Western Black Sea Basin depending on SRES and RCP scenarios. The author mentioned that the temperature will increase during the 2071-2099 period in both scenarios. However, it is worth noting that while the SRES scenario predicts a decrease in precipitation anomalies, the RCP scenarios predict an increase (Kale, 2020). On the other hand, a decrease of 11.04, 70.09, and 5.24 % is expected in interflow, SWE, and SWS values.

Silkin (2014) compared different scenarios and simulations for 1961-1990 and 2071-2099 and noted that surface runoff in Eastern Anatolia increased during winter but decreased in spring. However, in the Western Black Sea basin, there was an increase in surface runoff during both seasons, and when Tables 4.1 - 4.5 are analyzed, it can be seen that similar findings were obtained.

Table 4.5. Seasonal and annual changes of water budget components between future and reference period for Western Black Sea Basin

| | **Precipitation % (mm)** | **Sfroff % (mm)** | **Interflow % (mm)** | **ET % (mm)** | **SWE-Mean % (mm)** | **SWS-Mean % (mm)** |
|---|---|---|---|---|---|---|
| **DJF** | 9.56 (25.48) | 75.46 (3.46) | 4.46 (1.55) | 4.15 (2.72) | -69.55 (-12.26) | -1.98 (-11.06) |
| **MAM** | -3.55 (-7.73) | 29.48 (2.29) | -16.29 (-13.62) | 10.91 (22.72) | -69. 05 (-3.01) | -2.58 (-16.08) |
| **JJA** | 1.62 (22.5) | 51.41 (4.71) | -32.44 (-2.13) | 2.94 (8.59) | -99.99 (-0.01) | -9.62 (-45.75) |
| **SON** | 5.78 (10.52) | 76.71 (4.09) | 0.43 (0.02) | -0.84 (-0.78) | -81.39 (-1.02) | -8.49 (-36.13) |
| **ANNUAL** | 3.79 (30.53) | 54.19 (14.56) | -11.04 (-14.19) | 5.05 (33.26) | -70.09 (-4.07) | -5.24 (-27.26) |

### 4.2.6 Eastern Mediterranean Basin

The monthly time series of water budget components for the Eastern Mediterranean basin is given in Figure 4.25. The figure shows that there has been a significant increase in some months in the Eastern Mediterranean basin compared to the average. Additionally, it has been discovered that the surface runoff values in this basin are lower than those in other basins.

Aksoy (2020) stated that 2007 was the driest year for the Eastern Mediterranean basin from 1981 to 2010.

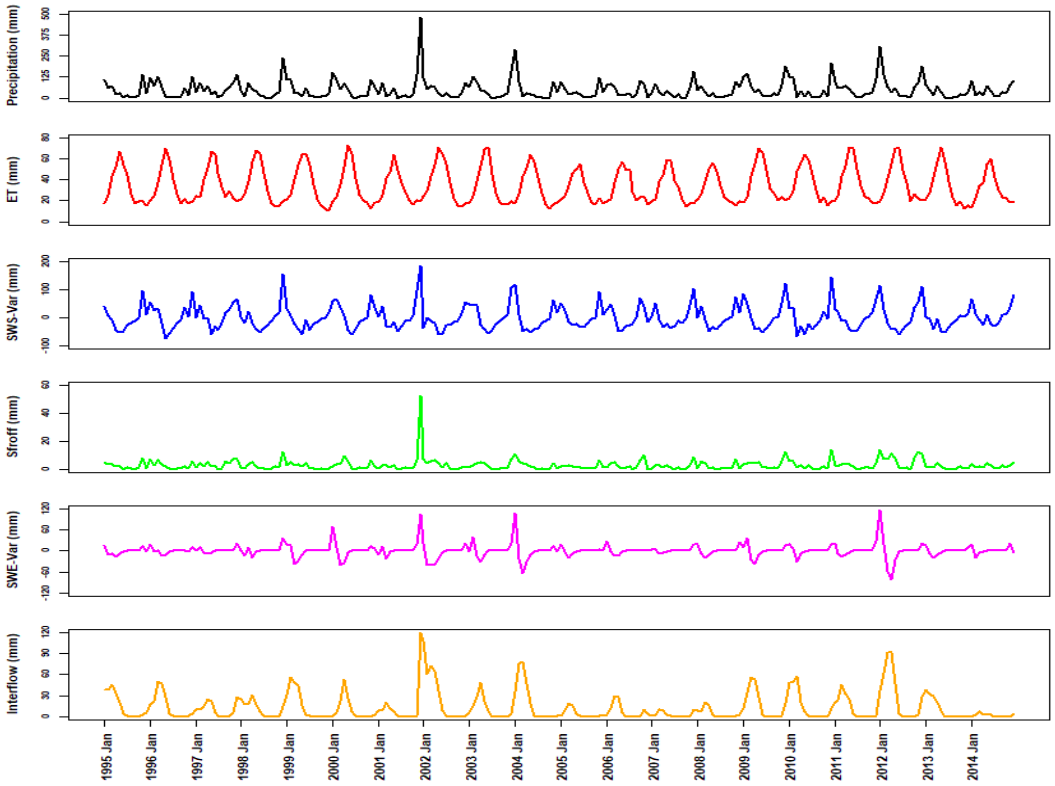


Figure 4.25. Monthly time series of Eastern Mediterranean Basin's water budget components for reference period (1995-2014)

Figure 4.26 shows the reference period water distribution graph, and Figure 4.27 shows the future period water distribution graph for the Eastern Mediterranean basin. According to Figure 4.26, precipitation and surface runoff occur primarily in winter. The snowfall in the Taurus Mountains affects the basin, and with the melting in May, the snow on the ground almost disappears. Again, maximum interflow values are observed in March and April due to snow melt. Unlike other basins where negative values in soil water storage are observed in April-May, in this particular basin, these negative values are observed in March instead. This situation is because evapotranspiration increases with increasing temperature in spring, and decreasing precipitation also contributes to interflow.

When Figures 4.26 and 4.27 are compared, it is seen that the precipitation in this basin will contribute to surface runoff in the future. Also, it is seen that while the amount of precipitation decreases in the winter months, it increases in the spring months.

According to Önol & Semazzi (2009), in the Eastern Mediterranean (which covers the whole area, not only the basin), the temperature rise varies across the seasons. During winter, it can range from 28 to 58 degrees Celsius; in spring, it can be between 28 to 48 degrees Celsius. In the summer, the rise in temperature is more pronounced and can range from 28 to 88 degrees Celsius. Finally, during autumn, the temperature can range from 38 to 58 degrees Celsius (Önol & Semazzi, 2009).

It has been observed that the snow melt seen in May in the reference period will occur in a small amount, even in April in the future period.

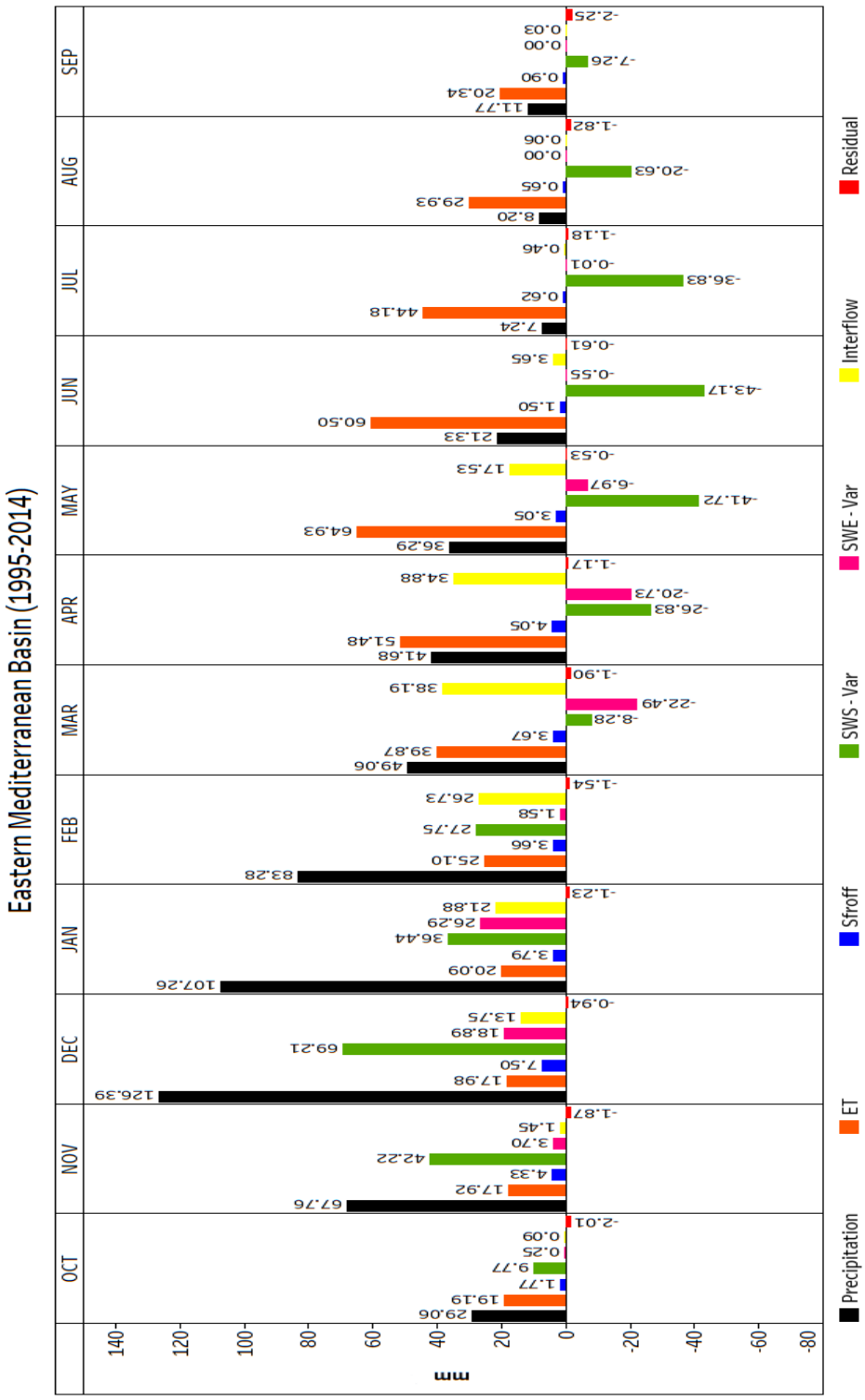


Figure 4.26. Eastern Mediterranean Basin water distribution graph for reference period (1995-2014)

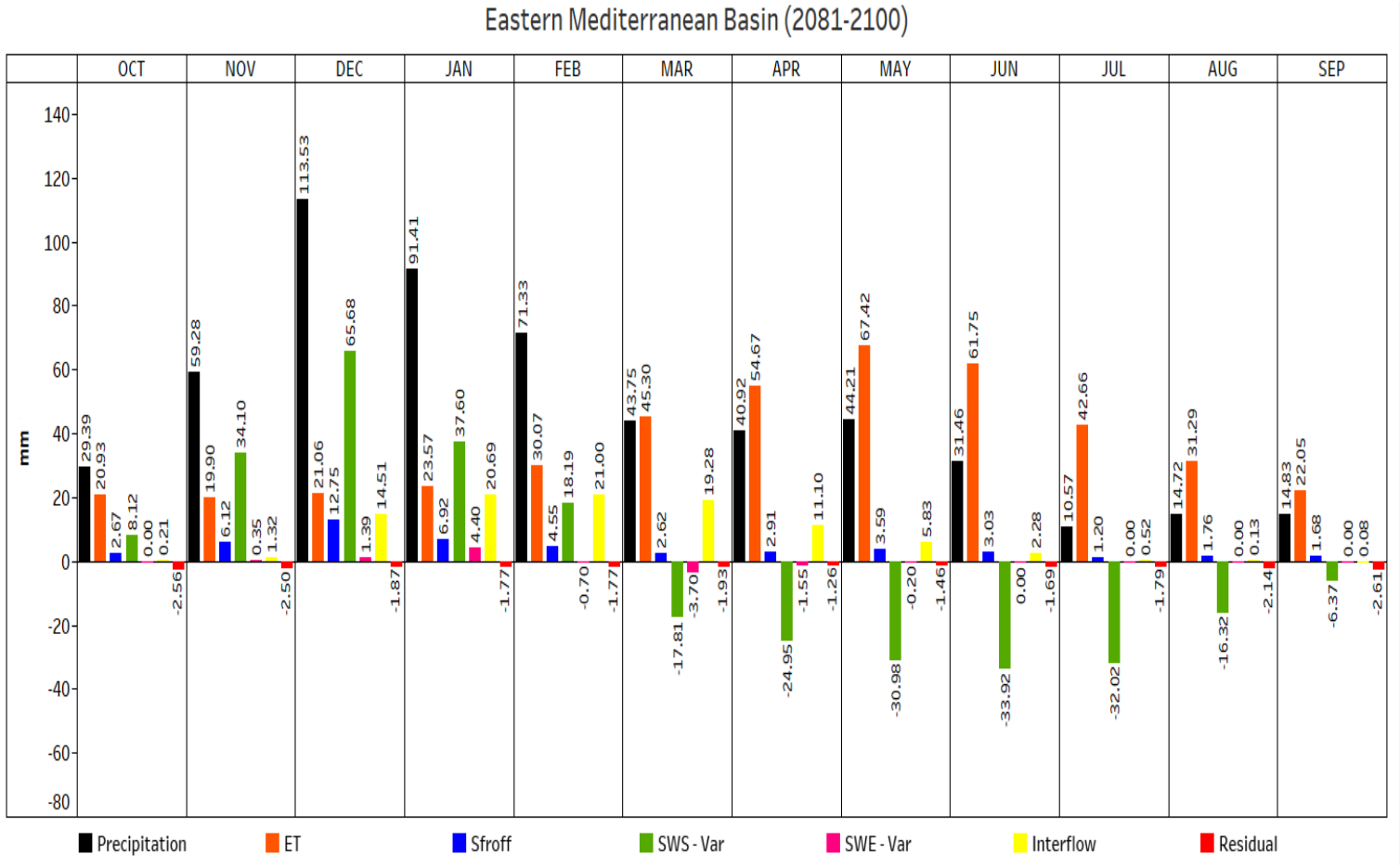


Figure 4.27. Eastern Mediterranean Basin water distribution graph for future period (2081-2100)

Table 4.6 shows seasonal and annual changes between the future and reference periods for the Eastern Mediterranean basin. The decrease in precipitation in the winter months (12.83 %) has outweighed the increase in the summer months, and it is seen that there will be a total decrease (4.05%). Önol & Semazzi (2009) investigated the potential role of global warming in changing the future climate of the Eastern Mediterranean (EM) region. They noted that the southern and southeastern regions of Türkiye and the eastern Mediterranean coasts will experience significant precipitation decreases (20 % - 60 %). Changes associated with the winter season dominate the annual precipitation variation (Önol & Semazzi, 2009).

Table 4.6. Seasonal and annual changes of water budget components between future and reference period for Eastern Mediterranean Basin

| | **Precipitation % (mm)** | **Sfroff % (mm)** | **Interflow % (mm)** | **ET % (mm)** | **SWE-Mean % (mm)** | **SWS-Mean % (mm)** |
|---|---|---|---|---|---|---|
| **DJF** | -12.83 (-40.66) | 61.93 (9.26) | -9.89 (-6.17) | 18.27 (11.54) | -88.68 (-30.04) | -3.84 (-22.81) |
| **MAM** | 1.46 (1.86) | -15.21 (-1.64) | -60.04 (-54.39) | 7.11 (11.10) | -93.03 (-17.93) | -6.05 (-37.54) |
| **JJA** | 54.37 (19.98) | 116.09 (3.22) | -29.95 (-1.25) | 0.81 (1.09) | -99.96 (-0.05) | -3.39 (-17.32) |
| **SON** | -4.69 (-5.09) | 49.47 (3.46) | 2.11 (0.03) | 9.45 (5.43) | -88.86 (-0.65) | -2.44 (-11.56) |
| **ANNUAL** | -4.05 (-23.91) | 40.31 (14.31) | -38.92 (-61.78) | 7.09 (29.17) | -90.25 (-12.17) | -4.06 (-22.31) |

### 4.2.7 Susurluk Basin

The monthly time series of Susurluk Basin's water budget components for the reference period presented in Figure 4.28 shows low values, particularly in 2001 and 2007. According to Aksoy (2020), 2001 was the driest year in the basin during the 1981-2010 observation period.

Although some areas in the Susurluk Basin, such as Uludağ, receive high amounts of snowfall. However, this impact is not significant when averaged across the entire basin.

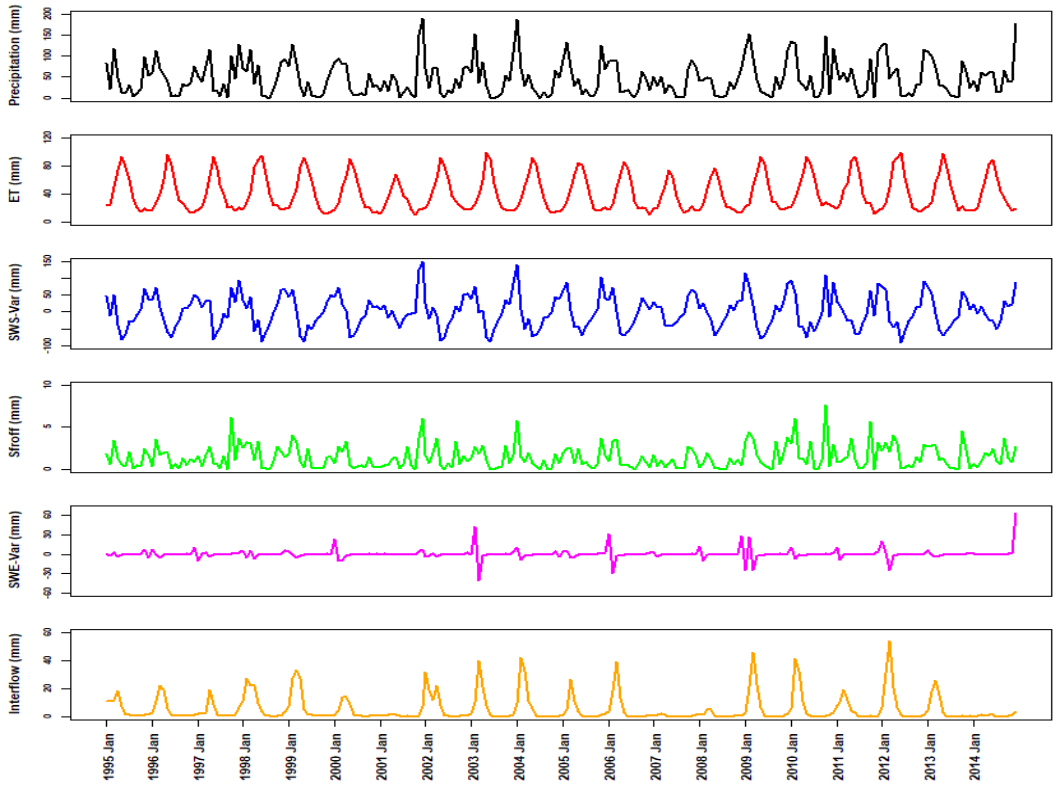


Figure 4.28. Monthly time series of Susurluk Basin's water budget components for reference period (1995-2014)

The reference and future period water distribution graphs for Susurluk Basin are 4.29 and 4.30, respectively.

Koruk et al. (2023) aimed to observe the effects of climate change on the Susurluk basin's monthly precipitation between 1970 and 2019 using Innovative Polygon Trend Analysis (IPTA). According to the authors, precipitation increased in the winter but was almost nonexistent in the summer, and it is also seen in Figure 4.29 and Figure 4.30. The authors emphasized that between September and December, there was an increase in mean precipitation heights, which subsequently decreased. Additionally, they noted that a decrease in precipitation during dry seasons could put a great deal of strain on agricultural water use and impact water quality, while an increase in precipitation during spring could lead to an increase in flood events (Koruk et al., 2023).

San et al. (2024) conducted a study on the Susurluk basin for 1979-2014, 2030-2059 (as a short term), and 2070-2099 (as a long term) under SSPs using CMIP6 GCMs to observe the spatiotemporal variations of wet and dry days transitions. The authors stated that the probability of droughts would rise in the basin as the number of consecutive dry days during the wet season and water year increases and emphasized that for the long term, risks are higher in the western part of the basin (San et al., 2024).

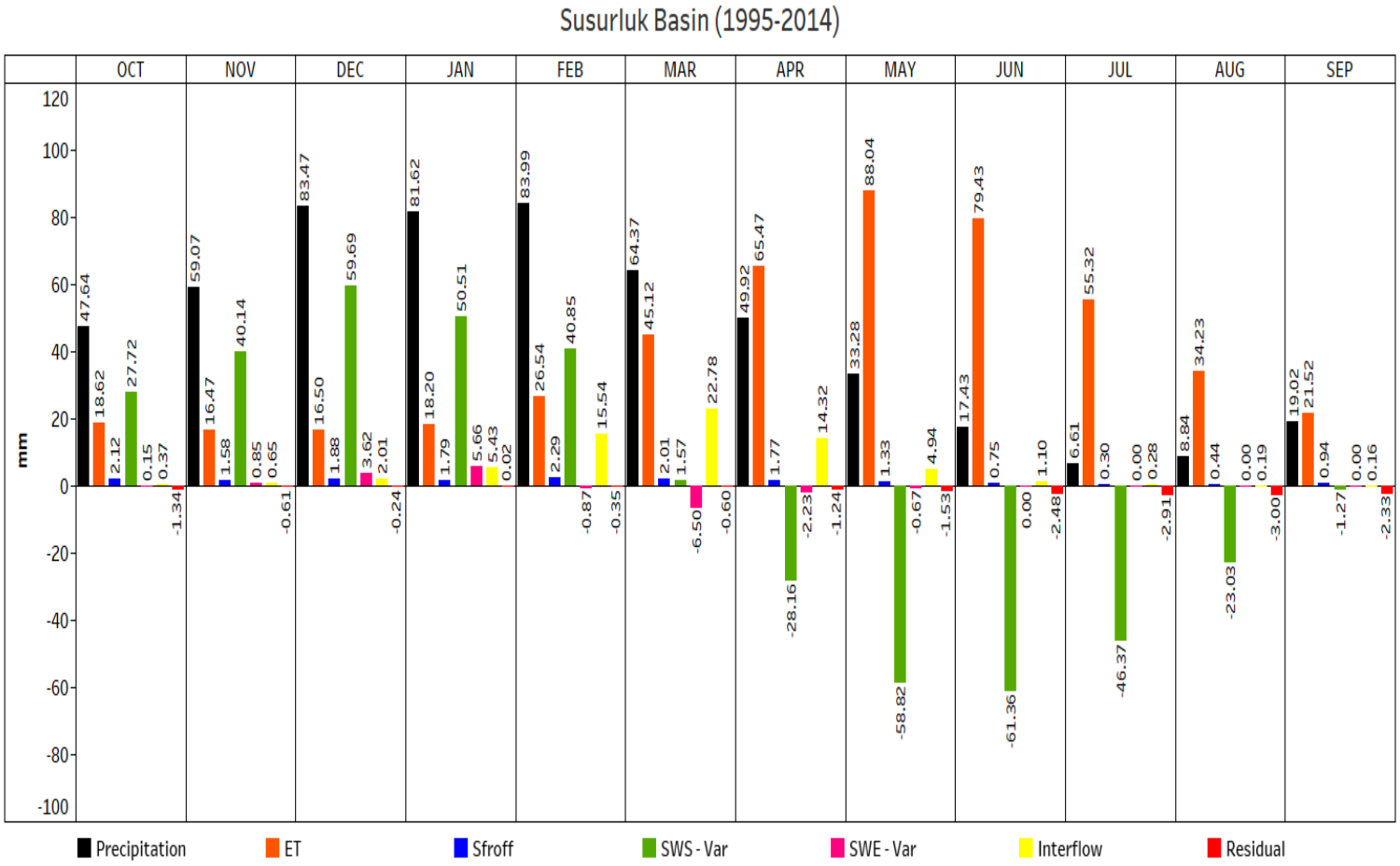


Figure 4.29. Susurluk Basin water distribution graph for reference period (1995-2014)

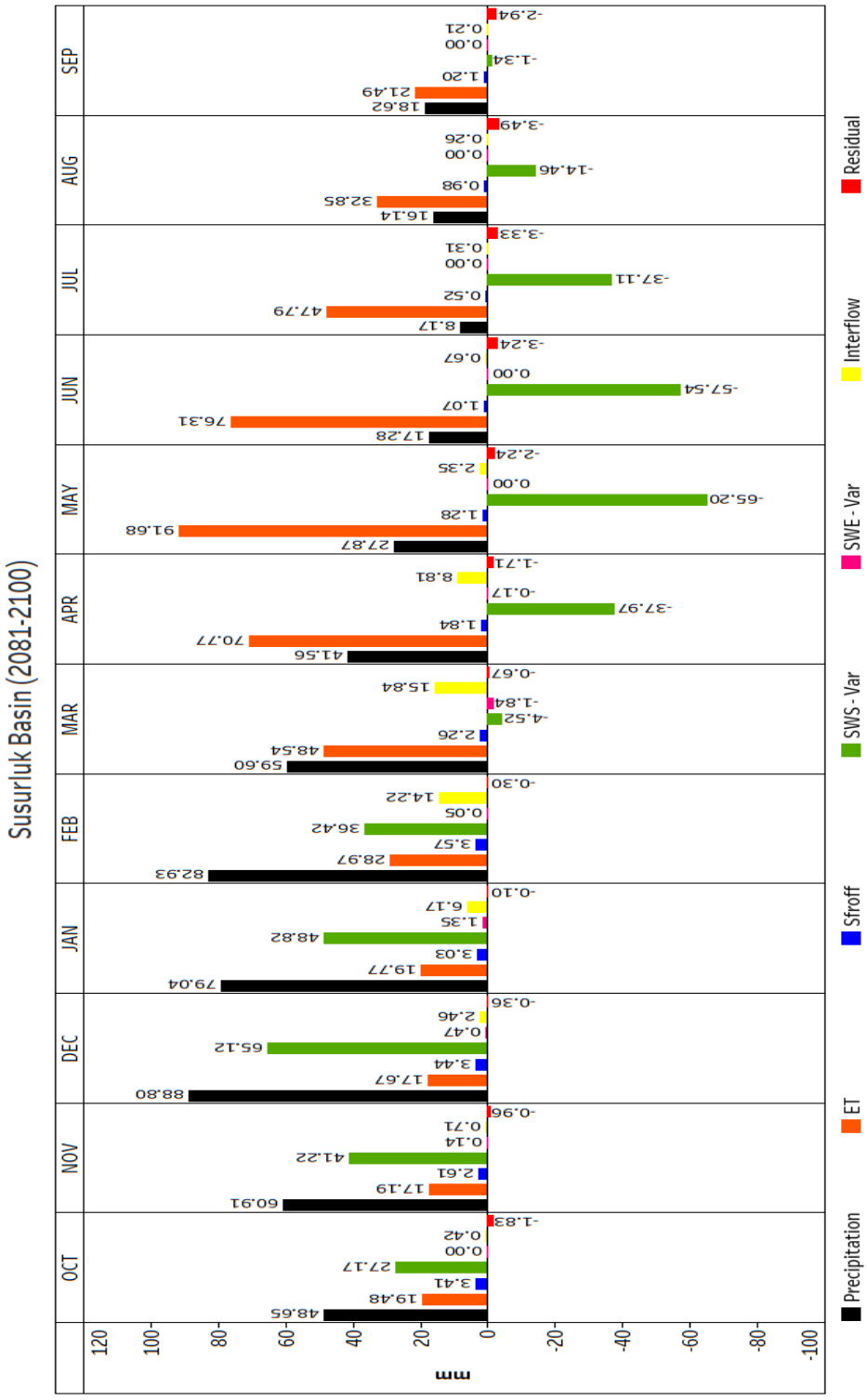


Figure 4.30. Susurluk Basin water distribution graph for future period (2081-2100)

Seasonal and annual changes in water budget components between future and reference periods for the Susurluk basin are given in Table 4.7. It is seen that decreases in precipitation and interflow are 5.69 mm and 15.34 mm, respectively. Since the decrease in precipitation in the spring months was proportionally higher, it also decreased in total. Therefore, while ET values increase, SWS values decrease. Also, it is seen that as surface runoff increases, interflow values will decrease.

According to the Susurluk River Basin report of the Ministry of Agriculture and Forestry, the temperature increases in 2071-2100 will be between 1.6℃ and 4.7℃ compared to the 1971-2000 reference period. From Table 4.7, it is expected that the ET value will increase by almost 7.07 mm annually.

Table 4.7. Seasonal and annual changes of water budget components between future and reference period for Susurluk Basin

| | **Precipitation % (mm)** | **Sfroff % (mm)** | **Interflow % (mm)** | **ET % (mm)** | **SWE-Mean % (mm)** | **SWS-Mean % (mm)** |
|---|---|---|---|---|---|---|
| **DJF** | 0.68 (1.69) | 68.35 (4.08) | -0.60 (-0.13) | 8.44 (5.17) | -78.52 (-5.96) | -1.87 (-10.10) |
| **MAM** | -12.56 (-18.54) | 5.45 (0.28) | -35.76 (-15.04) | 6.22 (12.37) | -86.71 (-2.07) | -4.36 (-25.69) |
| **JJA** | 26.49 (8.71) | 72.26 (1.08) | -20.85 (-0.33) | -7.12 (-12.03) | -98.02 (-0.01) | -6.19 (-27.61) |
| **SON** | 1.94 (2.45) | 55.06 (2.56) | 13.48 (0.16) | 2.77 (1.57) | -81.41 (-0.29) | -3.56 (-14.57) |
| **ANNUAL** | -1.02 (-5.69) | 46.43 (7.99) | -22.63 (-15.34) | 1.45 (7.07) | -80.51 (-2.08) | -3.93 (-19.49) |

## 4.3 Surface Terrestrial Water Storage Changes

A study is done to see discrepancies provided by daily median and daily mean SWE values for the Coruh basin (as an example) in order to reflect central tendency for snow water equivalent. Hourly data for the Coruh basin was used to calculate the daily average and median values. These values were then averaged for the reference and future periods. The dataset was organized, and graphs were made using the literature's statement that the snow year begins on September 1. However, because the snow water equivalent data for September, July, and August is zero or near zero, it is not displayed in the figures. Figure 4.31 shows that the difference between the values is almost negligible, demonstrating that median and mean values can be very similar. Additionally, this suggests that the data is not skewed or clustered on one side since no extreme values are present in the data daily. Since similar results were found in other basins, the analysis was continued based on the daily average.

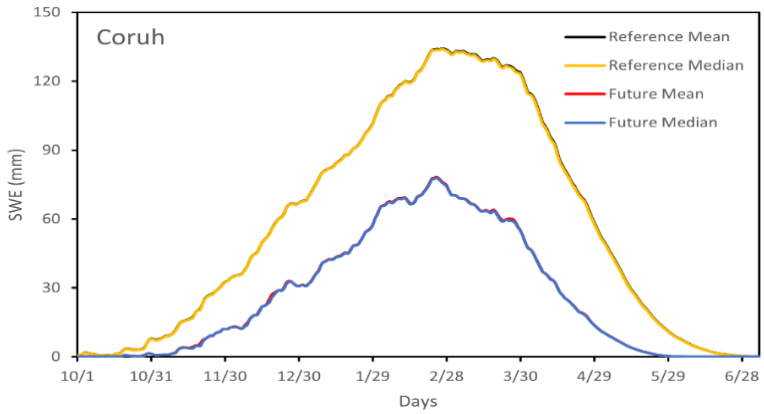


Figure 4.31. Comparison of daily mean and daily median

Figure 4.32 was created by calculating the 20-year average and median of daily average values for both reference and future periods for Türkiye. Although there are no extreme differences, it is observed that the difference between the median and mean widens when analyzed yearly.

The fact that the average values move away from 0 earlier than the median, especially in the beginning part of the graph, proves that most values in the data were 0 at that time. Therefore, while the median value was 0, higher values were obtained on average. It can be inferred from the discrepancy in SWE values between the future and reference period that the amount of snowfall in the future will be severely limited.

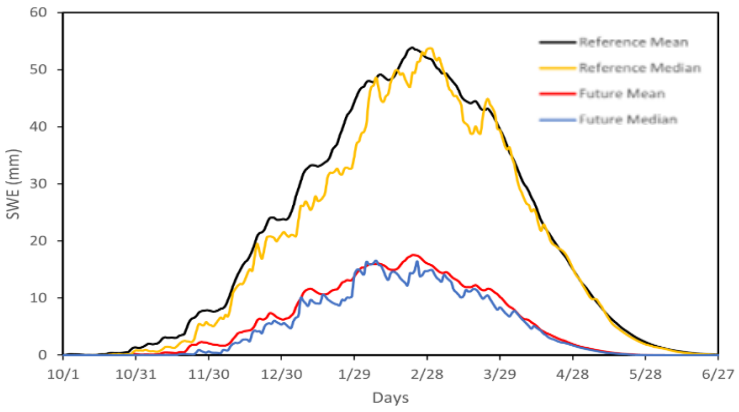


Figure 4.32. Twenty-year mean and median of snow water equivalent (SWE) for Türkiye

Figure 4.33 shows that the average and median values for the basins were analyzed. It was noted that basins with heavy snowfall under the influence of continental climate had higher peak values, and the difference between mean and median was slight. However, both values decreased in the Eastern Mediterranean, Western Black Sea, and Susurluk basins, and the skewness increased. This indicates that these basins experience heavy snowfall in some years and meager snowfall in others.

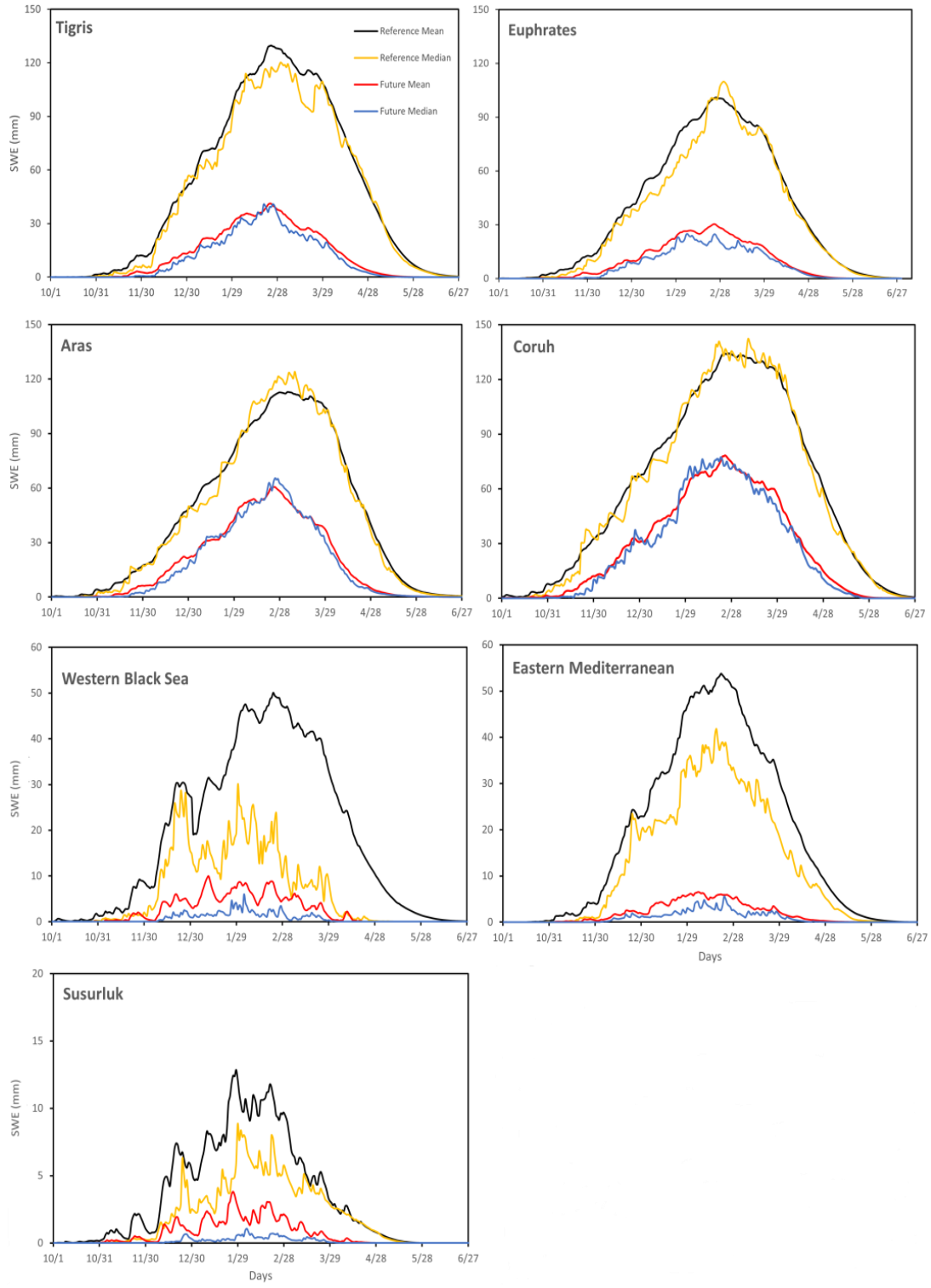


Figure 4.33. Twenty-year mean and median of snow water equivalent (SWE) for selected catchments

Figure 4.34 shows the daily average data for each year in the reference period for Türkiye and the averages and medians of these data over the years. In some years, there is much more snow water equivalent than in other years, and on the days with high values, the total average is higher than the median.

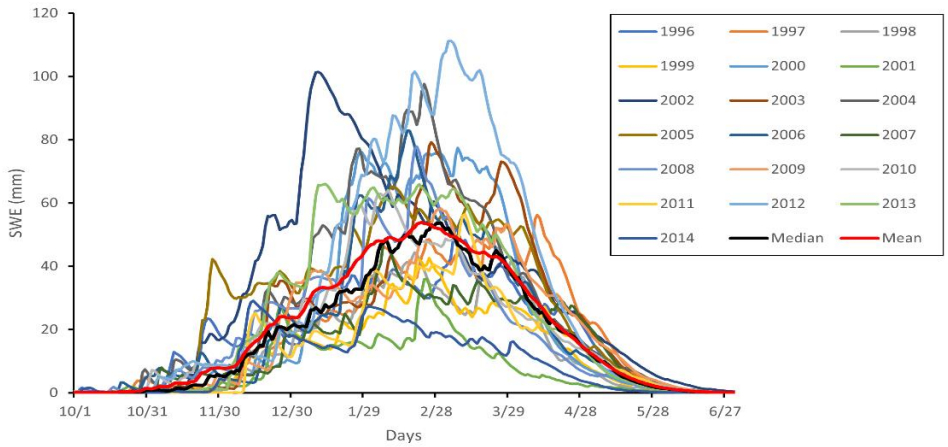


Figure 4.34. Daily mean graphs for each year of reference period (Based on snow-year).

Table 4.8 shows the shifts in peak values, dates of peaks, accumulation start-melting end, and snow year. According to Akyurek et al. (2023), there are two ways that climate change affects the hydrology of the snow-dominated basins. Water scarcity first results from a decrease in runoff amounts brought on by climate change. Second, it causes changes in the melting seasons, which can result in early floods or droughts during the summer (Akyurek et al., 2011). The snowmelt timing also plays a significant role in starting the vegetation cycle; therefore, measuring it is essential to understanding how vegetation responds to climate change (Beniston et al., 2003; Keller and Korner, 2003; Myneni et al., 1997; Prock and Korner, 1996).

Initially, our study focused on analyzing the variations in peak snow water equivalent (SWE) values and the dates on which they occurred across seven basins dominated by snow. Subsequently, we proceeded to estimate the shrinkage of the snow season by reviewing the dates of accumulation and melting. A reference of 1 mm was utilized to determine the dates of accumulation and melting. Whenever the SWE

(snow water equivalent) values surpassed 1 mm, it was considered the start date for accumulation. Conversely, when the SWE values were lower than 1 mm, it was regarded as the end date for melting. Based on Table 4.8, there will be a decrease in peak values, a shift to later accumulation start dates, a shift to earlier melting ending dates, and, therefore, a shrinkage in the snow season for all basins in the future. Stewart (2009) stated that in this field since the end of the snow season (spring) is more affected by this than the beginning (autumn), it is reasonable to assume that snow melt will occur much earlier in the season than it does under the current circumstances (Stewart, 2009). According to our analysis, the snow season is expected to shrink by 25.43%, 25.88%, 21.99%, 20.48%, 34.10%, 38.73%, and 41.03% in the Tigris, Euphrates, Aras, Coruh, Western Black Sea, Eastern Mediterranean, and Susurluk basins, respectively.

Sensoy et al. (2023) conducted a study to show the impact of climate change across runoff regimes and snow dynamics for future periods (2024–2099) of two snow-dominated headwaters, namely Karasu and Murat, which are in the Euphrates basin. According to the findings of the study that involved the use of GCMs downscaled with RCMs provided from the CMIP5 EURO-CORDEX under RCP 4.5 and 8.5 scenarios, there is a significant reduction in snow cover extents (over 65%) and snow duration (about 25%). Additionally, the authors stated that there is a decrease in snow water equivalent by more than 50% and a shift in peak runoff through early spring in the runoff hydrograph for the last future period (2075–2099) by up to a month (Sensoy et al., 2023). Table 4.8 also shows that the decrease in SWE is 69.92% for the Euphrates basin.

Table 4.8. Shifts in peak values and date of peak, accumulation start-melting end dates, and snow year for reference and future periods.

| Basins | Period | Peak SWE (mm) | Peak Date | Accumulation Start Date | Melting End Date | Snow Year (days) |
|---|---|---|---|---|---|---|
| Tigris | Reference | 129.72 | 24-Feb | 30-Oct | 18-Jun | 232 |
| | Future | 41.27 | 23-Feb | 22-Nov | 13-May | 173 |
| | Difference | 68.19% decrease | 1 day shift to earlier | 23 days shift to later | 36 days shift to earlier | 25.43% shrinkage |
| Euphrates | Reference | 100.9 | 25-Feb | 29-Oct | 13-Jun | 228 |
| | Future | 30.35 | 24-Feb | 22-Nov | 9-May | 169 |
| | Difference | 69.92% decrease | 1 day shift to earlier | 24 days shift to later | 35 days shifts to earlier | 25.88% shrinkage |
| Aras | Reference | 112.78 | 5-Mar | 20-Oct | 17-Jun | 241 |
| | Future | 60.64 | 25-Feb | 11-Nov | 17-May | 188 |
| | Difference | 46.23% decrease | 28 days shift to earlier | 22 days shift to later | 31 days shifts to earlier | 21.99% shrinkage |
| Coruh | Reference | 134.24 | 26-Feb | 17-Oct | 22-Jun | 249 |
| | Future | 78.32 | 24-Feb | 8-Nov | 24-May | 198 |
| | Difference | 41.66% decrease | 2 days shift to earlier | 22 days shift to later | 29 days shifts to earlier | 20.48% shrinkage |
| Western Black Sea | Reference | 50.04 | 22-Feb | 29-Oct | 2-Jun | 217 |
| | Future | 9.96 | 11-Jan | 22-Nov | 13-Apr | 143 |
| | Difference | 80.10% decrease | 42 days shift to earlier | 24 days shift to later | 50 days shift to earlier | 34.10% shrinkage |
| Eastern Mediterranean | Reference | 53.77 | 20-Feb | 4-Nov | 26-May | 204 |
| | Future | 6.48 | 5-Feb | 10-Dec | 13-Apr | 125 |
| | Difference | 87.95% decrease | 15 days shift to earlier | 36 days shift to later | 43 days shift to earlier | 38.73% shrinkage |
| Susurluk | Reference | 12.85 | 28-Jan | 21-Nov | 25-Apr | 156 |
| | Future | 3.82 | 26-Jan | 12-Dec | 13-Mar | 92 |
| | Difference | 70.27% decrease | 2 days shift to earlier | 21 days shift to later | 43 days shift to earlier | 41.03 % shrinkage |

Figure 4.35 shows the mean SWE map with contours for the reference period (1995-2014), and Figure 4.36 shows the mean SWE map with contours for a future period (2081-2100) under the SSP5-8.5 emission scenario. The elevation map is given separately in Figure 4.37. According to Beniston et al. (2003), any significant changes in the mountain snowpack would significantly impact the flow of numerous large river basins. These changes would also affect the timing and amount of runoff, the possibility of increased flooding, erosion, and related natural hazards (Beniston et al., 2003). Also, Stewart (2009) stated that studies have shown that mountain snowpacks have changed worldwide with the rise in temperature and precipitation. However, the extent and nature of these changes differ significantly based on geographical factors such as elevation, latitude, and others (Stewart, 2009).

While it is possible to see snow at lower elevations in the reference period, it will generally be seen at elevations above 2500 m in the future. Stewart (2009) observed that while high-elevation areas that remain well below freezing throughout the winter have not been impacted, warmer temperatures at mid-elevations have reduced snowpack and caused an earlier meltdown despite increases in precipitation (Stewart, 2009).

Akyurek et al. (2023) used the ERA5-Land reanalysis product to study the country's snow cover dynamics spatially and temporally from 1970 to 2022. They discovered an increasing trend of 0.4 C/decade and a decreasing trend in snow duration due to early melting. This trend is even more pronounced at elevations less than 2000 m (Akyurek et al., 2023). Additionally, they discovered that the duration of snow was trending downward at elevations lower than 500 meters, suggesting a change in precipitation types from snow to rain. The authors noted that the greatest number of snow cover days are found at higher elevations, with an average of about 54 days. At lower altitudes, the variability is smaller, about five days, but at higher altitudes, it increases to about 21 days (Akyurek et al., 2011).

Also, Beniston et al. (2003) studied snow accumulation in the Swiss Alps. They discovered that, in response to the current climate, an average warming of 4 °C

predicted for the years 2071–2100 implies that the amount of snow in the Alps may decrease by at least 90% at elevations near 1000 m, 50% at 2000 m, and 35% at 3000 m. According to the authors, snow cover duration is significantly reduced in warmer climates. At high elevations above 2000-2500 m, the season ends around 50-60 days earlier, while at medium elevation locations near 1000 m, it ends 110-130 days earlier (Beniston et al., 2003).

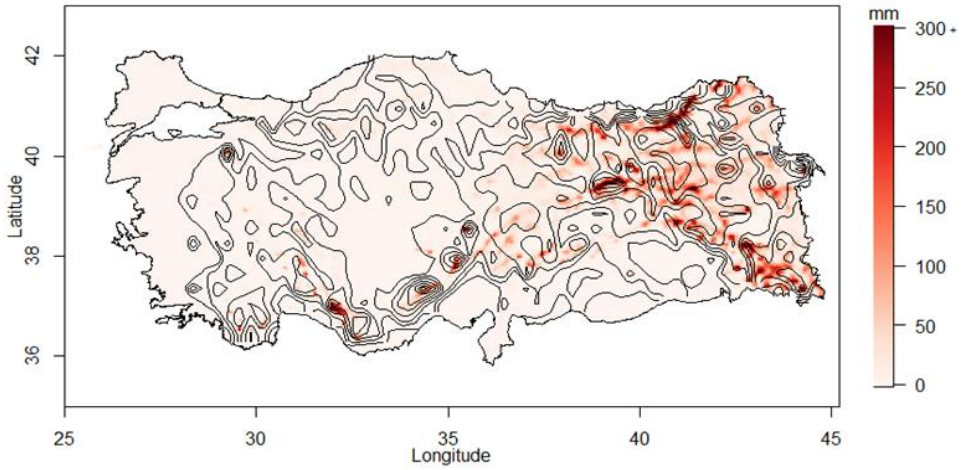


Figure 4.35. Mean SWE map with contours under the SSP5-8.5 emission scenario reference period (1995-2014).

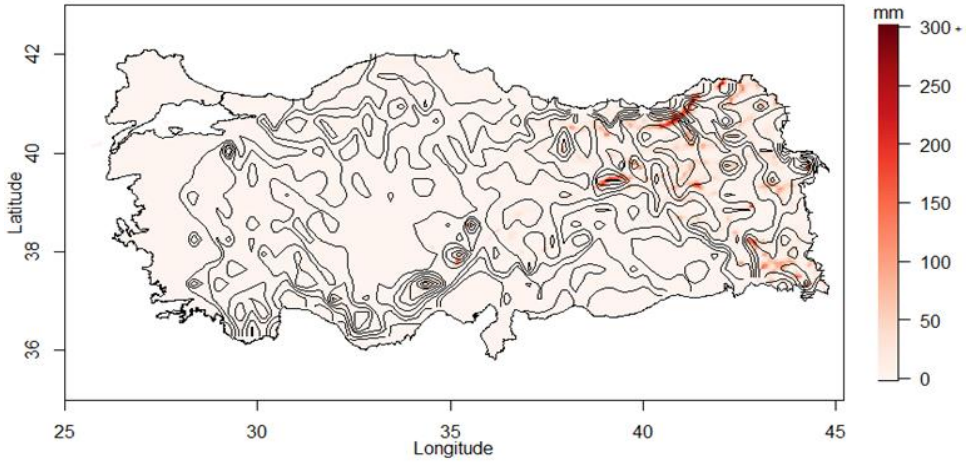


Figure 4.36. Mean SWE map with contours under SSP5-8.5 emission scenario for future period (2081-2100).

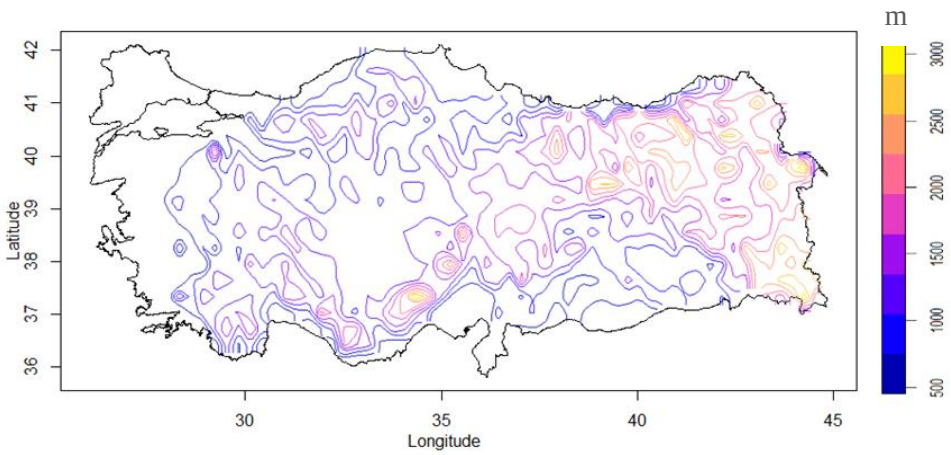


Figure 4.37. Elevation map with contours

Table 4.9 indicates total annual precipitation and ET, differences between precipitation and ET for future and reference periods, and differences in percentage, and Figure 4.38 displays these differences as a bar graph. One of the main components of the water cycle is the net flow of water on Earth's surface, which is the difference between precipitation and evapotranspiration and, on continents, equals the total of surface and subsurface runoff (Ferreira et al., 2023; Byrne Eth et al., n.d.). Souza et al. (2017) and Jesus et al. (2017) stated that the analysis of the intensity, distribution, and frequency of water deficits greatly benefits from quantitative data on the variables precipitation (P), reference evapotranspiration (ETo), and climatic water balance (Ferreira et al., 2023). The information mentioned above plays a crucial role in evaluating the water availability and the occurrence of extreme events such as floods and droughts. Therefore, it is necessary for efficient management of water resources (Moreira et al., 2019).

It can be interpreted that where this difference is positive, the water balance is maintained, and where it is negative, there will be water scarcity. The P-ET value increases by 34.21% and 30.71%, respectively, with the expected rainfall increases in the Aras and Coruh basins in the future period. In contrast, it was observed that the gap between precipitation and evapotranspiration reduced in other basins. Specifically, the reduction amounted to 22.16% in the Tigris, 19.18% in the Euphrates, 2.08% in the Western Black Sea, 31.69% in the Eastern Mediterranean,

and 19.25% in Susurluk. It can be concluded that the water budget will be negatively affected in these basins in the future period.

Table 4.9. Annual total precipitation, ET, and their differences for future and reference periods

| Basins | Period | Precipitation (mm) | ET (mm) | Differences (P-ET) (mm) | Changes of differences (Future-Reference) |
|---|---|---|---|---|---|
| Tigris | Reference | 628.78 | 369.22 | 259.56 | 22.16 % decrease |
| | Future | 620.89 | 418.86 | 202.03 | |
| Euphrates | Reference | 510.95 | 357.80 | 153.15 | 19.18 % decrease |
| | Future | 541.46 | 417.69 | 123.77 | |
| Aras | Reference | 593.16 | 446.26 | 146.90 | 34.21 % increase |
| | Future | 790.08 | 592.93 | 197.15 | |
| Coruh | Reference | 724.61 | 472.29 | 252.32 | 30.74 % increase |
| | Future | 930.21 | 600.32 | 329.89 | |
| Western Black Sea | Reference | 808.73 | 660.37 | 148.36 | 2.08 % decrease |
| | Future | 840.57 | 695.30 | 145.27 | |
| Eastern Mediterranean | Reference | 586.87 | 411.22 | 175.65 | 31.69 % decrease |
| | Future | 560.69 | 440.71 | 119.98 | |
| Susurluk | Reference | 557.67 | 486.95 | 70.72 | 19.25 % decrease |
| | Future | 550.60 | 493.50 | 57.10 | |

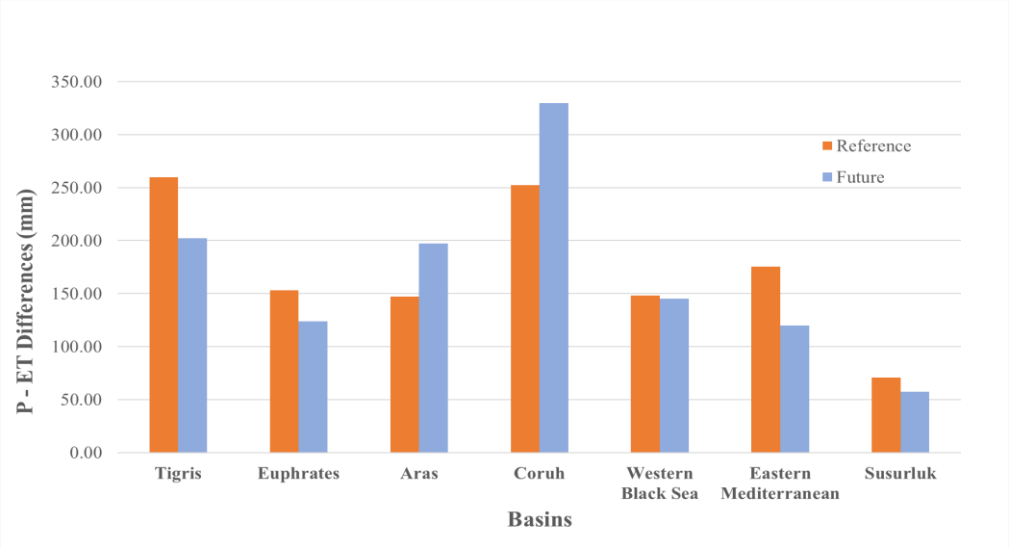


Figure 4.38. Differences between P – ET for future and reference periods

The contribution of SWEA and SWSA to TWSA in the reference and future period for the Tigris, Euphrates, Aras, and Coruh basins is shown in Figure 4.39. In contrast, the contribution of the Western Black Sea, Eastern Mediterranean, and Susurluk basins is shown in Figure 4.40.

TWSA calculations are made by Equation 4. It is essential to note that the calculations did not include groundwater variables since, as previously mentioned, Noah LSM was used in this study and is considered deep drainage in Noah LSM. Therefore, the aim is to see how much snow water equivalent (SWE) and soil water storage (SWS) contribute to TWS in these snow-dominated basins and their distribution within themselves. Since these graphs are anomaly graphs, positive values show storage values above average and negative values below normal.

Figures 4.39 and 4.40 show that the TWSA values, which were initially positive in January, became negative during May, June, and July. This indicates snow water equivalent (SWE) and soil moisture storage (SWS) levels typically rise during winter with increased precipitation. The availability of precipitation plays a crucial role in providing nourishment to TWS and its constituents (Koycegiz et al., 2023; Zhang et al., 2019). Therefore, TWSA and precipitation are closely related (Koycegiz et al., 2023). However, storage values tend to decrease during spring months as temperatures rise, snow melts, and soil moisture evaporates. Also, Zheng et al. (n.d) stated that TWSA peaks in the spring, falls off quickly in the summer, reaches a minimum in the fall, and rises again in the winter.

Magotra et al. (2024) also conducted a study on TWSA in a rain-fed region of southern India, Kudige, Cauvery River basin (Magotra et al., 2024). The authors showed the distribution of the variables (soil moisture, groundwater storage, surface water storage) for seasons with bar graphs as in Figures 4.39 and 4.40. They noted that surface water storage (SWS) accounts for 8% of the variability in terrestrial water storage (TWS) worldwide and included it in the study. In their final observations, the authors noted that during periods of low precipitation in winter and summer, the terrestrial water storage was insufficient compared to the long-term

monthly average. However, during the monsoon season, there was surplus water storage, and this pattern of water storage was consistent with the basin climate.

When the graphs are examined in more detail, one of the first striking observations is that the contribution of SWEA to TWSA is more significant in the Eastern Anatolia Region basins (Tigris, Euphrates, Aras, and Coruh). It is seen that the surplus period (positive anomaly) of terrestrial water storage is projected to decrease for the Tigris, Euphrates, Aras, and Eastern Mediterranean basins in the future. At the same time, the Coruh, Western Black Sea, and Susurluk basins are expected to remain relatively stable. The highest reductions in storage peak value observed in March were 36% for the Eastern Mediterranean and 25% for the Tigris basins. The contribution of snow to water storage in these snow-fed basins is expected to decrease significantly due to the impact of future climate change. Among the snow-fed basins of the Euphrates, Tigris, Aras, and Coruh basins, only Aras and Coruh maintain their historically more significant portions of snow accumulation (in January and February) for total water storage under future climate change. Soil moisture contributions to water storage in the Euphrates, Tigris, and Aras basins are expected to increase with future warming climate during accumulation periods, specifically in January and February. Moreover, the peak occurrence of surplus storage in April is shifted to March with the future climate in the Coruh basin. Changes in the partition of soil and snow water storage to the total water storage in these basins between the historical and future periods also indicate a shift in precipitation type from snow to rain. In addition, the deficit in water storage during summer is expected to increase significantly due to evaporative losses in these basins fed by snow, according to future climate projections. With the already disappeared snow amount in the surplus period under future climate change, the Eastern Mediterranean and Susurluk basins show decreased evaporative losses in the deficit period compared to the deficit months in the historical period.

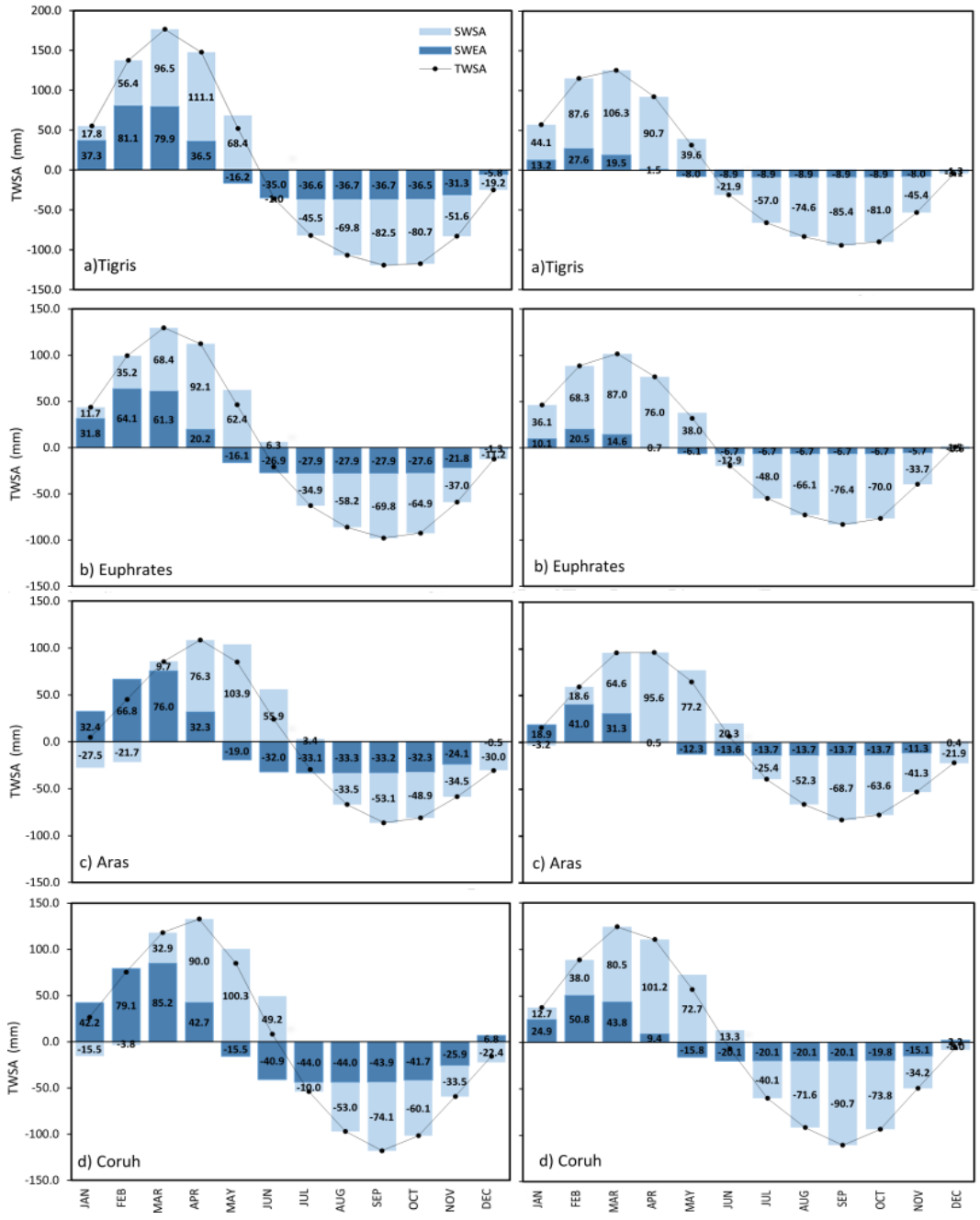


Figure 4.39. Contribution of SWEA and SWSA to TWSA for Tigris, Euphrates, Aras, and Coruh basins. The first column shows the reference period, and the second column shows the corresponding future period TWSA graphs.

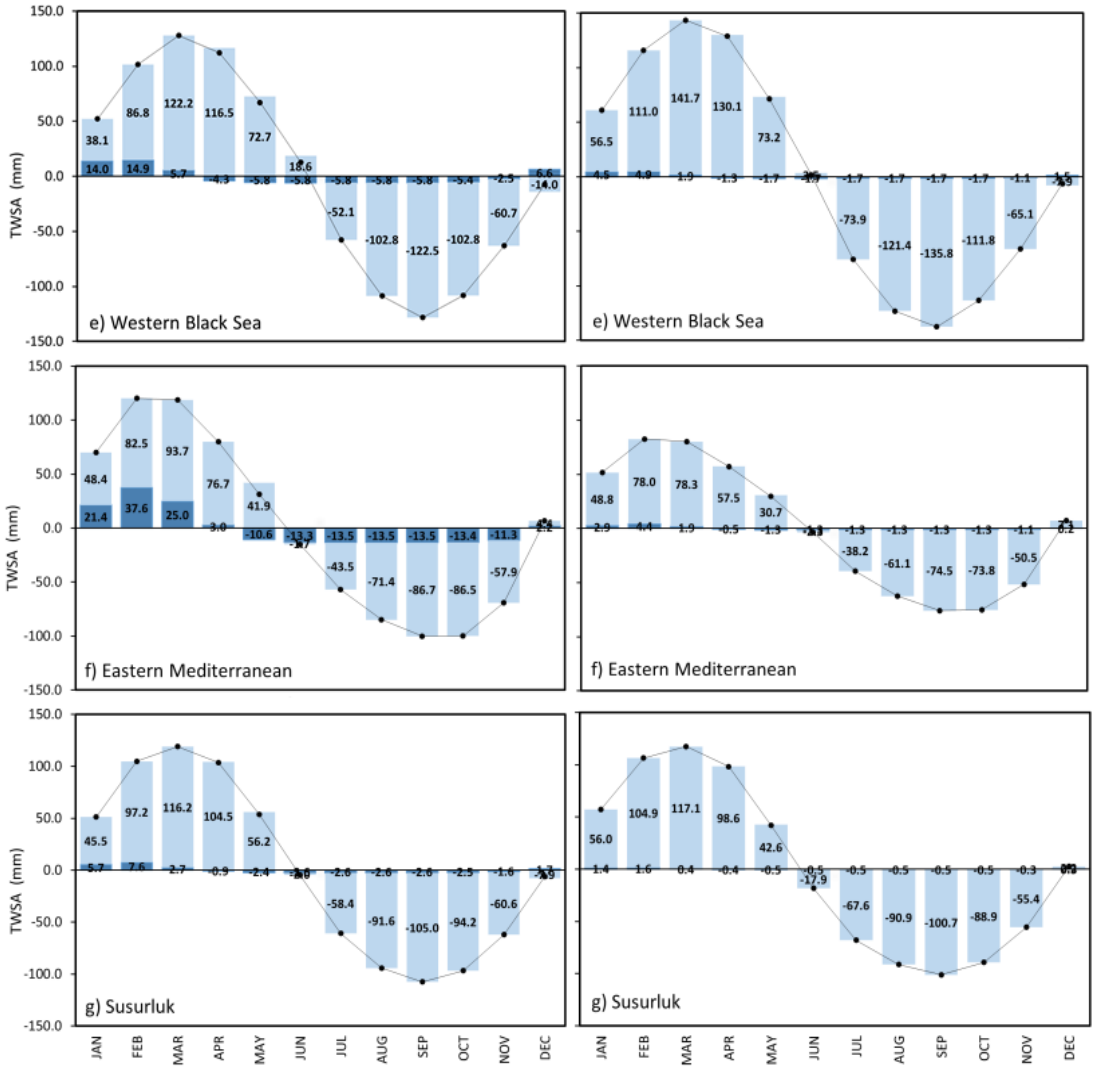


Figure 4.40. Contribution of SWEA and SWSA to TWSA for Western Black Sea, Eastern Mediterranean, and Susurluk basins. The first column shows the reference period, and the second column shows the corresponding future period TWSA graphs.

In Figure 4.41, the TWSA graphs of all studied basins for the reference and future periods are presented together to examine the difference between these two periods. Peak value changes and changes in surplus-deficit transition times, which were explained before, are seen more clearly.

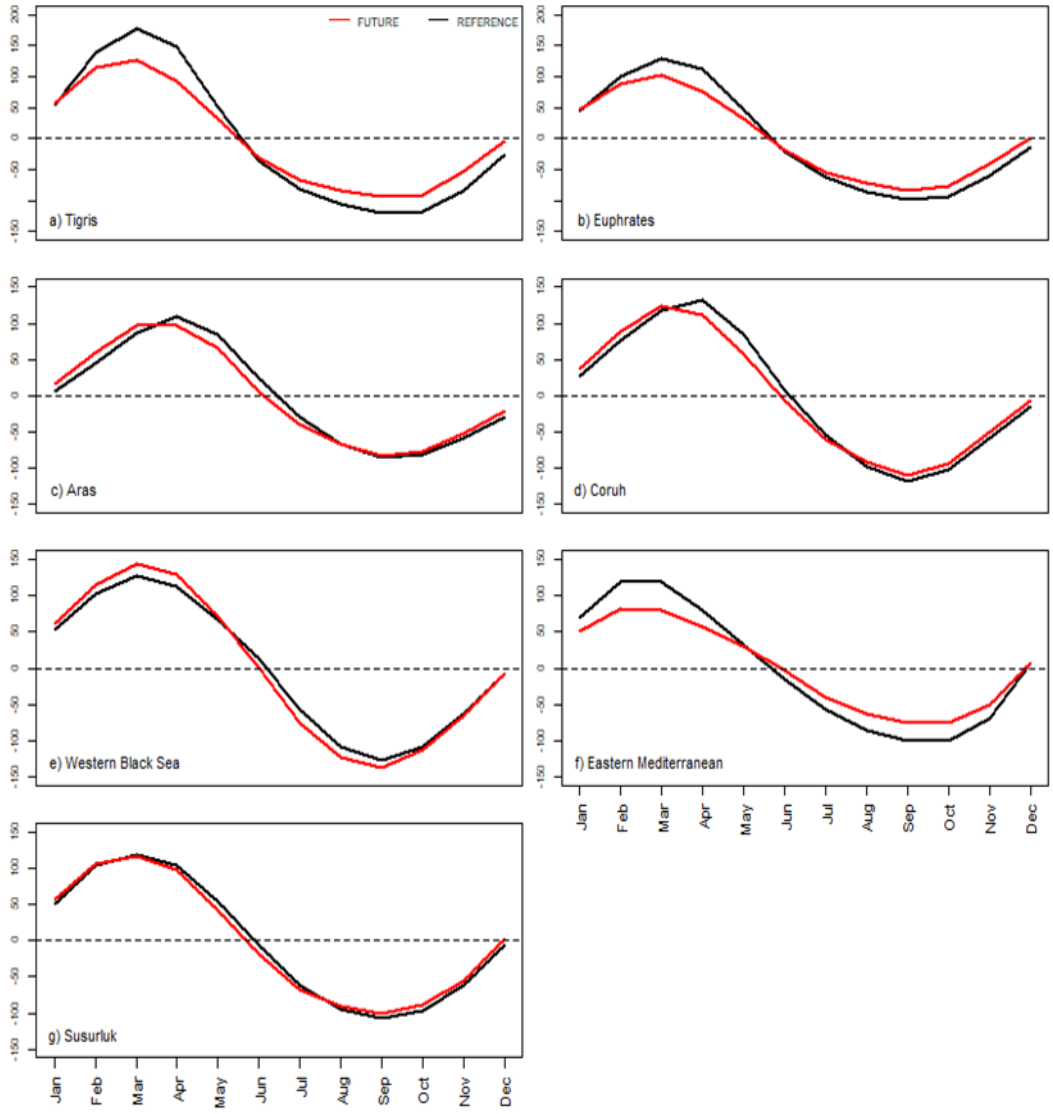


Figure 4.41. Reference and corresponding future period TWSA graphs for all studied catchments

## 4.4 Changes in Surface Runoff Fractions

Figure 4.42 shows the ratio of monthly surface runoffs of basins to annual surface runoffs for reference and future periods. It shows that the surface runoff values of four basins (Tigris, Euphrates, Aras, Coruh) in Eastern Anatolia, where snowfall is more dominant than other basins, are higher. Yucel et al. (2015) stated that the mountainous region of Türkiye's eastern Anatolia consists of basins that can hold 31% of the country's total surface flow, 193 billion $m^3$ per year (DSI, 2009).

Based on the results, it can be inferred that all basins' runoff values in the future winter, summer, and fall seasons are expected to be higher than the reference period. On the other hand, the runoff values during the spring season are anticipated to be lower. This decrease in the spring months, when surface runoff values peak with snow melt in the reference period, indicates that snowfall in all basins will decrease. While the highest flow value in the Eastern Anatolia basins (Tigris, Euphrates, Aras, and Coruh) occurred in April in the reference period, the same peak flow value is less and expected to occur in March in the future period for Tigris and Euphrates. This change proves that snowmelt will occur at earlier times in the future.

As seen in Figure 4.42, Aras and Coruh basins are among the basins where the precipitation will increase the most in the summer months for future periods. Therefore, the runoff increase in the summer months in these two basins is notably higher than in other basins.

Although the snowfall is heavy in the Western Black Sea, Eastern Mediterranean, and Susurluk basins, the changes are less since it is more local and not as much as the other four basins.

Yucel et al. (2015) also stated that, regarding this issue, there will be a transition from snow to rain, and the melting time of the snow will shift earlier due to the increase in temperatures in the future period.

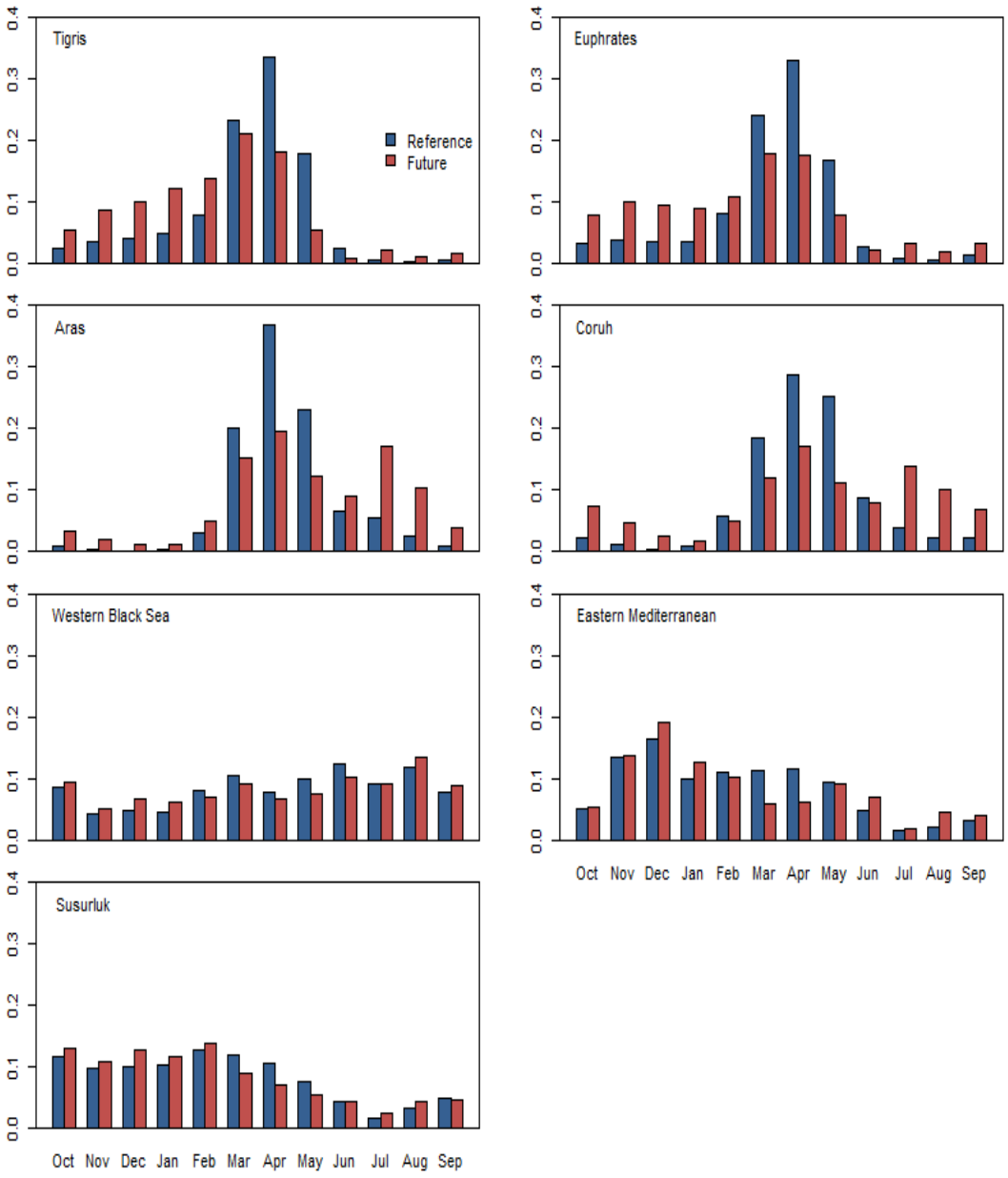


Figure 4.42. Surface runoff fractions for reference and future periods (monthly surface runoff over annual surface runoff).

# CHAPTER 5

# CONCLUSION

## 5.1 Summary

This thesis aimed to comprehensively assess the impacts of climate change on surface water budgets in seven snow-dominated basins (Tigris, Euphrates, Aras, Coruh, Western Black Sea, Eastern Mediterranean, and Susurluk) of Türkiye. Utilizing the most recent CMIP6 (13 GCMs) models, the study employed high-resolution (4 km grid resolution) regional climate simulations to examine a number of variables, including precipitation, snow water equivalent, soil moisture, evapotranspiration, surface runoff, and interflow. These high-resolution data are the outputs of the study conducted by Bagcaci (2023). Bagcaci (2023) obtained the data through two WRF simulations. For the historical period (1995–2014), one simulation used ERA5 reanalysis data; for the future period (2081-2100), the second simulation used dynamic downscaling with the pseudo-global warming approach. The perturbed version of ERA5 analysis data was used under the SSP5-8.5 emission scenario during the latter simulation (Bagcaci, 2023).

Within the scope of the study, firstly, inter-annual changes in precipitation, evapotranspiration, and snow water equivalent (SWE) were scrutinized for the reference period throughout Türkiye. Then, the mean historical distributions of these variables for the reference period on a seasonal and annual basis are produced, together with their anomalous differences from the future projection period. A comparative analysis between historical and pseudo-future periods under climate change scenarios sheds light on the potential effects of climate change.

For both the reference and future periods, the study estimated the residual values of a water budget analysis for seven basins dominated by snow. As a result, the study analyzed the changes in water-budget variables between the two periods and their interrelationships.

Snow water equivalents (SWE) for the reference and subsequent periods were analyzed by creating 20-year averages and median graphs. The graphs were analyzed to identify any differences between the reference and future periods in accumulation-melt periods, peak value, and snow season. In addition, annual average snow water equivalent graphs and 20-year average and median graphs were created and examined for the reference period. Finally, to determine the expected retreat of snow in the upcoming period, contour lines were incorporated into average SWE maps for two periods.

Analyzing the difference between evapotranspiration and precipitation is one method of tracking changes in basin water balances in the future. This research looked at how this disparity changed in the reference and subsequent periods.

Terrestrial water storage anomaly graphs were created and compared for two periods, revealing the varying effectiveness of snow water equivalent (SWE) and soil water storage (SWS) in selected basins.

Ultimately, an analysis was conducted on the proportions between the monthly and annual total surface runoffs.

As a result of the study, the following conclusions were drawn:

- According to precipitation maps, an increase in precipitation is anticipated in the future, particularly in the Eastern Black Sea region. At the same time, a significant decrease is observed in the Eastern Mediterranean-Antalya basins.
- ET maps reveal increased evapotranspiration values in the northeastern part of the country (encompassing the Aras and Coruh basins). In contrast, a decrease is noted in the western and southeastern Anatolian regions.

- Average SWE maps indicate a general decrease in snowfall in almost every region for the future.
- Water budget analyses have reached reasonable residual levels (successful closure); all of them are smaller than 4 mm.
- Examining variable time series during the reference period reveals a proportional relationship between precipitation and surface runoff, as well as between SWE and interflow, with an inverse correlation between ET and soil water storage (SWS).
- Looking at future period water budgets, the relationship among variables appears less pronounced due to a significant decrease in SWE values. The distribution among them changes, even in areas where precipitation is reduced.
- Interflow and soil water storage (SWS) values increase in the future despite decreased precipitation in some places with less snow accumulation, indicating a change from snow to rain.
- Based on the water budget analysis, it has been predicted that the Tigris, Eastern Mediterranean, and Susurluk basins will experience a reduction in precipitation by 1.4%, 4%, and 1%, respectively. In contrast, it was found that the Euphrates, Aras, Coruh, and Western Black Sea basins are expected to experience an increase of 6.3%, 33%, 29%, and 3.8%, respectively.
- The snow water equivalent (SWE) analysis has revealed that there will be a substantial reduction in peak SWE values and a decrease in snow period of about 20-40% in all the selected basins during the snow season.
- Comparing 20-year mean and median values for snow water equivalent (SWE) due to skewness in SWE values, it is observed that the mean and median values are closer in the eastern Anatolian basins, where snowfall reduction is evident in the future. In other basins, the difference between mean and median values increases, possibly due to outliers or clustering in the dataset.

- TWSA analysis suggests that peak surface runoff values during the future decrease due to reduced snowfall, and melt-evaporation periods occur earlier. Additionally, it was found that the Eastern Mediterranean and Tigris basins will encounter the most significant decline in peak storage values in the month of March, with a reduction of 36% and 25%, respectively.
- A significant decrease in peak values of surface runoff and an earlier onset of the melting period are notable particularly in the Tigris and Euphrates basins.

The results provide essential information for water resources management, agriculture, infrastructure planning, and climate policies. Through analyses based on water budget equations, the research provides a comprehensive understanding of future precipitation patterns, snow accumulation, and their impacts on water resources. Identifying snow accumulation-melting periods and evaluating changes in snowmelt runoff timing provided insights into the future hydrological dynamics. This research contributes valuable knowledge for understanding and adapting to the evolving water resource scenarios in Türkiye's mountainous regions under the influence of climate change.

Modern water monitoring systems are essential for tracking and assessing water resources in different climatic zones. They can help manage existing water assets and monitor the effects of climate change. Developing planning strategies based on climate change scenarios and updating water resource management strategies regularly using the latest climate projections, such as those from CMIP6 models, is recommended. These recommendations aim to assist Türkiye in strengthening its water resource management and taking proactive measures to tackle the challenges posed by climate change.

## 5.2 Limitations

- This study solely focused on climate change effect on water balance elements of the basins without conducting an accuracy assessment of these elements in the historical period. The impact of the model errors on the changes in these elements is ignored.
- It has been noted in various studies that the Noah Land Surface Model (LSM) tends to underestimate SWE values. Because there is a lack of knowledge about the processes and characteristics of the surface layer, LSMs contain avoidable uncertainties (Lim et al., n.d.). To address this issue, it is recommended to combine Noah LSM with other parameterization models to achieve more precise and reliable outcomes.

## 5.3 Recommendations

- This study aims to evaluate climate change on average at the basin level. However, since there may be different climate impacts within basins, it would not be appropriate to generalize the findings of this study for smaller regional areas. Therefore, the study should be repeated by narrowing the area to obtain more accurate results for local regions. For example, if a water budget analysis were made around Uludağ, snow effects would be much more evident than in the entire Susurluk basin.
- In order to display the contribution of the surface water mass elements rather than the precise TWSA value, only SWE and SWS were utilized in the TWSA graphs in this study. Assume, however, that the primary objective is to obtain the most accurate TWSA changes. It is then advised to include factors in the analysis such as surface water, groundwater, canopy, etc.

## REFERENCES


Aksoy, H. (2020). *World Water Resources Water Resources of Turkey*. http://www.springer.com/series/15410

Akyurek, Z., Surer, S., & Beser, Ö. (2011). Investigation of the snow-cover dynamics in the Upper Euphrates Basin of Turkey using remotely sensed snow-cover products and hydrometeorological data. *Hydrological Processes*, *25*(23), 3637–3648. https://doi.org/10.1002/hyp.8090

Bagcaci, S. Ç. (2023). *The Analysis of Current and Future Climate Projections of Türkiye and the Large-Scale Eastern Mediterranean Black Sea Region in the Coarse and High Resolutions*.

Bagcaci, S. Ç., Yucel, I., Duzenli, E., & Yilmaz, M. T. (2021). Intercomparison of the expected change in the temperature and the precipitation retrieved from CMIP6 and CMIP5 climate projections: A Mediterranean hot spot case, Turkey. *Atmospheric Research*, *256*. https://doi.org/10.1016/j.atmosres.2021.105576

Balasubramanian, A. (n.d.). *Surface Water Runoff*. https://www.researchgate.net/publication/320331329

Barlage, M., Chen, F., Tewari, M., Ikeda, K., Gochis, D., Dudhia, J., Rasmussen, R., Livneh, B., Ek, M., & Mitchell, K. (2010). Noah land surface model modifications to improve snowpack prediction in the Colorado Rocky Mountains. *Journal of Geophysical Research Atmospheres*, *115*(22). https://doi.org/10.1029/2009JD013470

Bell, B., Hersbach, H., Simmons, A., Berrisford, P., Dahlgren, P., Horányi, A., Muñoz-Sabater, J., Nicolas, J., Radu, R., Schepers, D., Soci, C., Villaume, S., Bidlot, J. R., Haimberger, L., Woollen, J., Buontempo, C., & Thépaut, J. N. (2021). The ERA5 global reanalysis: Preliminary extension to 1950. *Quarterly Journal of the Royal Meteorological Society*, *147*(741), 4186–4227. https://doi.org/10.1002/qj.4174

Beniston, M., Keller, F., Koffi, B., & Goyette, S. (2003). Estimates of snow accumulation and volume in the Swiss Alps under changing climatic conditions. *Theoretical and Applied Climatology*, *76*(3–4), 125–140. https://doi.org/10.1007/s00704-003-0016-5

Bozkurt, D., & Sen, O. L. (2013). Climate change impacts in the Euphrates-Tigris Basin based on different model and scenario simulations. *Journal of Hydrology*, *480*, 149–161. https://doi.org/10.1016/j.jhydrol.2012.12.021

Brogli, R., Heim, C., Mensch, J., Sorland, S. L., & Schar, C. (2023). The pseudo-global-warming (PGW) approach: Methodology, software package PGW4ERA5 v1.1, validation, and sensitivity analyses. *Geoscientific Model Development*, *16*(3), 907–926. https://doi.org/10.5194/gmd-16-907-2023

Byrne Eth, M. P., Urich, Z., & O'gorman, P. A. (n.d.). *The Response of Precipitation Minus Evapotranspiration to Climate Warming: Why the "'Wet-Get-Wetter, Dry-Get-Drier'" Scaling Does Not Hold over Land**. https://doi.org/10.1175/JCLI-D-15-0369.s1

Campbell, P. C., Bash, J. O., & Spero, T. L. (2019). Updates to the Noah Land Surface Model in WRF-CMAQ to Improve Simulated Meteorology, Air Quality, and Deposition. *Journal of Advances in Modeling Earth Systems*, *11*(1), 231–256. https://doi.org/10.1029/2018MS001422

Carroll, R. W. H., Deems, J. S., Niswonger, R., Schumer, R., & Williams, K. H. (2019). The Importance of Interflow to Groundwater Recharge in a Snowmelt-Dominated Headwater Basin. *Geophysical Research Letters*, *46*(11), 5899–5908. https://doi.org/10.1029/2019GL082447

Ceribasi, G., Ceyhunlu, A. I., & Ahmed, N. (2021). Innovative trend pivot analysis method (ITPAM): a case study for precipitation data of Susurluk

Basin in Turkey. *Acta Geophysica*, *69*(4), 1465–1480. https://doi.org/10.1007/s11600-021-00605-6

Chen, F., & Dudhia, J. (2001). *Coupling an Advanced Land Surface-Hydrology Model with the Penn State-NCAR MM5 Modeling System. Part I: Model Implementation and Sensitivity*.

Chen, H., Sun, J., Lin, W., & Xu, H. (2020). Comparison of CMIP6 and CMIP5 models in simulating climate extremes. In *Science Bulletin* (Vol. 65, Issue 17, pp. 1415–1418). Elsevier B.V. https://doi.org/10.1016/j.scib.2020.05.015

Cho, E., Vuyovich, C. M., Kumar, S. V., Wrzesien, M. L., Kim, R. S., & Jacobs, J. M. (2022). Precipitation biases and snow physics limitations drive the uncertainties in macroscale modeled snow water equivalent. *Hydrology and Earth System Sciences*, *26*(22), 5721–5735. https://doi.org/10.5194/hess-26-5721-2022

Claessens, L., Hopkinson, C., Rastetter, E., & Vallino, J. (2006). Effect of historical changes in land use and climate on the water budget of an urbanizing watershed. *Water Resources Research*, *42*(3). https://doi.org/10.1029/2005WR004131

Dong, N., Prentice, I. C., Harrison, S. P., Song, Q. H., & Zhang, Y. P. (2017). Biophysical homoeostasis of leaf temperature: A neglected process for vegetation and land-surface modelling. *Global Ecology and Biogeography*, *26*(9), 998–1007. https://doi.org/10.1111/geb.12614

DSI. 2009. Turkey Water Report. Republic of Turkey, Retrieved

February 20, 2014. http://www.dsi.gov.tr.

Dudhia, J. (2015). *Overview of WRF Physics*.

Durdu, Ö. F. (2010). Effects of climate change on water resources of the Büyük Menderes river basin, Western Turkey. *Turkish Journal of Agriculture and Forestry*, *34*(4), 319–332. https://doi.org/10.3906/tar-0909-402

Duzenli, E. (2022). *Evaluation of the WRF & WRF-Hydro Modeling System to Better Understand the Hydrometerological Interactions over Humid and Semi-arid Climate Conditions*.

Elmastas, N. (2000). *Su Potansiyeli Açısından bir Araştırma: Dicle Havzası*.

Ferreira, F. L. V., Rodrigues, L. N., Althoff, D., & Amorim, R. S. S. (2023). Spatial–Temporal Variability of Climatic Water Balance in the Brazilian Savannah Region River Basins. *Water (Switzerland)*, *15*(10). https://doi.org/10.3390/w15101820

Fersch, B., Senatore, A., Adler, B., Arnault, J., Mauder, M., Schneider, K., Völksch, I., & Kunstmann, H. (2020). High-resolution fully coupled atmospheric-hydrological modeling: A cross-compartment regional water and energy cycle evaluation. *Hydrology and Earth System Sciences*, *24*(5), 2457–2481. https://doi.org/10.5194/hess-24-2457-2020

Fontrodona-Bach, A., Schaefli, B., Woods, R., Teuling, A. J., & Larsen, J. R. (2023). NH-SWE: Northern Hemisphere Snow Water Equivalent dataset based on in situ snow depth time series. *Earth System Science Data*, *15*(6), 2577–2599. https://doi.org/10.5194/essd-15-2577-2023

Frederick, K. D., & Major, D. C. (1997). *Climate Change and Water Resources*.

Fujihara, Y., Tanaka, K., Watanabe, T., Nagano, T., & Kojiri, T. (2008). Assessing the impacts of climate change on the water resources of the Seyhan River Basin in Turkey: Use of dynamically downscaled data for hydrologic simulations. *Journal of Hydrology*, *353*(1–2), 33–48. https://doi.org/10.1016/j.jhydrol.2008.01.024

Girotto, M., & Rodell, M. (2019). Terrestrial water storage. In *Extreme Hydroclimatic Events and Multivariate Hazards in a Changing Environment: A Remote Sensing Approach* (pp. 41–64). Elsevier. https://doi.org/10.1016/B978-0-12-814899-0.00002-X

Gonzalez, R., Ouarda, T. B. M. J., Marpu, P. R., Allam, M. M., Eltahir, E. A. B., & Pearson, S. (2016). Water Budget Analysis in Arid Regions, Application to the United Arab Emirates. *Water (Switzerland)*, *8*(9). https://doi.org/10.3390/W8090415

Grose, M. R., Narsey, S., Delage, F. P., Dowdy, A. J., Bador, M., Boschat, G., Chung, C., Kajtar, J. B., Rauniyar, S., Freund, M. B., Lyu, K., Rashid, H., Zhang, X., Wales, S., Trenham, C., Holbrook, N. J., Cowan, T., Alexander, L., Arblaster, J. M., & Power, S. (2020). Insights From CMIP6 for Australia's Future Climate. *Earth's Future*, *8*(5). https://doi.org/10.1029/2019EF001469

Gumus, B., Oruc, S., Yucel, I., & Yilmaz, M. T. (2023). Impacts of Climate Change on Extreme Climate Indices in Türkiye Driven by High-Resolution Downscaled CMIP6 Climate Models. *Sustainability (Switzerland)*, *15*(9). https://doi.org/10.3390/su15097202

Guo, J., Liang, X., & Ruby Leung, L. (2004). Impacts of different precipitation data sources on water budgets. *Journal of Hydrology*, *298*(1–4), 311–334. https://doi.org/10.1016/j.jhydrol.2003.08.020

Guo, L., Li, T., Chen, D., Liu, J., He, B., & Zhang, Y. (2021). Links between global terrestrial water storage and large-scale modes of climatic variability. *Journal of Hydrology*, *598*. https://doi.org/10.1016/j.jhydrol.2021.126419

Güventürk, A. (2013). *Impacts of Climate Change on Water Resources on Eastern Mountainous Region of Turkey*.

Haddeland, I., Heinke, J., Biemans, H., Eisner, S., Flörke, M., Hanasaki, N., Konzmann, M., Ludwig, F., Masaki, Y., Schewe, J., Stacke, T., Tessler, Z. D., Wada, Y., & Wisser, D. (2014). Global water resources affected by human interventions and climate change. *Proceedings of the National Academy of Sciences of the United States of America*, *111*(9), 3251–3256. https://doi.org/10.1073/pnas.1222475110

Healy, R., Winter, T., LaBaugh, J., & Franke, O. (2007). *Water Budgets: Foundations for Effective Water-Resources and Environmental Management USGS/Circular 1308*.

Hersbach, H., Bell, B., Berrisford, P., Hirahara, S., Horányi, A., Muñoz-Sabater, J., Nicolas, J., Peubey, C., Radu, R., Schepers, D., Simmons, A., Soci, C., Abdalla, S., Abellan, X., Balsamo, G., Bechtold, P., Biavati, G., Bidlot, J., Bonavita, M., … Thépaut, J. N. (2020). The ERA5 global reanalysis. *Quarterly Journal of the Royal Meteorological Society*, *146*(730), 1999–2049. https://doi.org/10.1002/qj.3803

Iwata, Y., Nemoto, M., Hasegawa, S., Yanai, Y., Kuwao, K., & Hirota, T. (2011). Influence of rain, air temperature, and snow cover on subsequent spring-snowmelt infiltration into thin frozen soil layer in northern Japan. *Journal of Hydrology*, *401*(3–4), 165–176. https://doi.org/10.1016/j.jhydrol.2011.02.019

Jin, S., & Zhang, T. (2016). Terrestrial Water Storage Anomalies Associated with Drought in Southwestern USA from GPS Observations. In *Surveys in Geophysics* (Vol. 37, Issue 6, pp. 1139–1156). Springer Netherlands. https://doi.org/10.1007/s10712-016-9385-z

Kale, M. M. (2020). İklim Değişikliği Çerçevesinde Ankara İli Ana Su Havzaları Gelecek Projeksiyonu: Sakarya ve Batı Karadeniz Havzaları. *Coğrafi Bilimler Dergisi*, *18*(2), 191–215. https://doi.org/10.33688/aucbd.732831

Karimi, P., & Bastiaanssen, W. G. M. (2015). Spatial evapotranspiration, rainfall and land use data in water accounting - Part 1: Review of the accuracy of the remote sensing data. In *Hydrology and Earth System Sciences* (Vol. 19, Issue 1, pp. 507–532). Copernicus GmbH. https://doi.org/10.5194/hess-19-507-2015

Khan, A., Hillaire Saquib Najmus Woodard, T., Paul Shipman, C., Haas Frank Qian, J., Van Lienden, B., & Namvar Woodard, R. (2018). *Groundwater Resources Association of California 2018 Annual Groundwater Congress*.

Koçyigit, M. B., Akay, H., & Babaiban, E. (2021). Evaluation of morphometric analysis of flash flood potential of Eastern Mediterranean Basin using principle component analysis. *Journal of the Faculty of Engineering and Architecture of Gazi University*, *36*(3), 1669–1685. https://doi.org/10.17341/gazimmfd.829390

Koruk, A. E., Kankal, M., Yıldız, M. B., Akçay, F., Şan, M., & Nacar, S. (2023). Trend analysis of precipitation using innovative approaches in northwestern Turkey. *Physics and Chemistry of the Earth*, *131*. https://doi.org/10.1016/j.pce.2023.103416

Koycegiz, C., Sen, O. L., & Buyukyildiz, M. (2023). An analysis of terrestrial water storage changes of a karstic, endorheic basin in central Anatolia, Turkey. *Ecohydrology and Hydrobiology*. https://doi.org/10.1016/j.ecohyd.2023.07.002

Kundzewicz, Z. W. (2008). Climate change impacts on the hydrological cycle. *Ecohydrology and Hydrobiology*, *8*(2–4), 195–203. https://doi.org/10.2478/v10104-009-0015-y

Levin, S. B., Briggs, M. A., Foks, S. S., Goodling, P. J., Raffensperger, J. P., Rosenberry, D. O., Scholl, M. A., Tiedeman, C. R., & Webb, R. M. (2023). Uncertainties in measuring and estimating water-budget components:

Current state of the science. *Wiley Interdisciplinary Reviews: Water*, *10*(4). https://doi.org/10.1002/wat2.1646

Li, Q., Liu, X., Zhong, Y., Wang, M., & Zhu, S. (2021). Estimation of terrestrial water storage changes at small basin scales based on multi-source data. *Remote Sensing*, *13*(16). https://doi.org/10.3390/rs13163304

Li, Y., Li, Z., Zhang, Z., Chen, L., Kurkute, S., Scaff, L., & Pan, X. (2019). High-resolution regional climate modeling and projection over western Canada using a weather research forecasting model with a pseudo-global warming approach. *Hydrology and Earth System Sciences*, *23*(11), 4635–4659. https://doi.org/10.5194/hess-23-4635-2019

Liang, X. Z., Xu, M., Yuan, X., Ling, T., Choi, H. I., Zhang, F., Chen, L., Liu, S., Su, S., Qiao, F., He, Y., Wang, J. X. L., Kunkel, K. E., Gao, W., Joseph, E., Morris, V., Yu, T. W., Dudhia, J., & Michalakes, J. (2012). Regional climate-weather research and forecasting model. *Bulletin of the American Meteorological Society*, *93*(9), 1363–1387. https://doi.org/10.1175/BAMS-D-11-00180.1

Lim, S., Gim, H.-J., Lee, E., Lee, S.-Y., Lee, W. Y., Lee, Y. H., Cassardo, C., & Park, S. K. (n.d.). *Optimization of Snow-Related Parameters in Noah Land Surface Model (v3.4.1) Using Micro-Genetic Algorithm (v1.7a)*. https://doi.org/10.5194/gmd-2021-333

Ma, X., Li, Y., & Li, Z. (2022). The projection of canadian wind energy potential in future scenarios using a convection-permitting regional climate model. *Energy Reports*, *8*, 7176–7187. https://doi.org/10.1016/j.egyr.2022.05.122

Magotra, B., Prakash, V., Saharia, M., Getirana, A., Kumar, S., Pradhan, R., Dhanya, C. T., Rajagopalan, B., Singh, R. P., Pandey, A., & Mohapatra, M. (2024). Towards an Indian land data assimilation system (ILDAS): A coupled hydrologic-hydraulic system for water balance assessments.

*Journal of Hydrology*, *629*, 130604. https://doi.org/10.1016/j.jhydrol.2023.130604

Maxwell, R. M., & Miller, N. L. (2005). Development of a coupled land surface and groundwater model. *Journal of Hydrometeorology*, *6*(3), 233–247. https://doi.org/10.1175/JHM422.1

Meinshausen, M., Nicholls, Z. R. J., Lewis, J., Gidden, M. J., Vogel, E., Freund, M., Beyerle, U., Gessner, C., Nauels, A., Bauer, N., Canadell, J. G., Daniel, J. S., John, A., Krummel, P. B., Luderer, G., Meinshausen, N., Montzka, S. A., Rayner, P. J., Reimann, S., … Wang, R. H. J. (2020). The shared socio-economic pathway (SSP) greenhouse gas concentrations and their extensions to 2500. *Geoscientific Model Development*, *13*(8), 3571–3605. https://doi.org/10.5194/gmd-13-3571-2020

Mintz, Y., & Serafini, Y. V. (1992). Glimai¢ Dynamles A global monthly climatology of soil moisture and water balance. In *Climate Dynamics* (Vol. 8).

Molina, O., Luong, T. T., & Bernhofer, C. (2020). Projected changes in the water budget for Eastern Colombia due to climate change. *Water (Switzerland)*, *12*(1). https://doi.org/10.3390/w12010065

Mollema, P., Antonellini, M., Gabbianelli, G., Laghi, M., Marconi, V., & Minchio, A. (2012). Climate and water budget change of a Mediterranean coastal watershed, Ravenna, Italy. *Environmental Earth Sciences*, *65*(1), 257–276. https://doi.org/10.1007/s12665-011-1088-7

Moreira, A. A., Ruhoff, A. L., Roberti, D. R., Souza, V. de A., da Rocha, H. R., & de Paiva, R. C. D. (2019). Assessment of terrestrial water balance using remote sensing data in South America. *Journal of Hydrology*, *575*, 131–147. https://doi.org/10.1016/j.jhydrol.2019.05.021

Nair, A. S., & Indu, J. (2016). Enhancing noah land surface model prediction skill over indian subcontinent by assimilating smops blended soil moisture. *Remote Sensing*, *8*(12). https://doi.org/10.3390/rs8120976

Ni, S., Chen, J., Wilson, C. R., Li, J., Hu, X., & Fu, R. (2018). Global Terrestrial Water Storage Changes and Connections to ENSO Events. In *Surveys in Geophysics* (Vol. 39, Issue 1). Springer Netherlands. https://doi.org/10.1007/s10712-017-9421-7

Ohara, N., Asce, A. M., Kavvas, ; M L, Asce, F., Anderson, ; M L, Asce, M., Chen, ; Z Q Richard, & Yoon, J. (2011). *Water Balance Study for the Tigris-Euphrates River Basin*. https://doi.org/10.1061/(ASCE)HE

O'Neill, B. C., Tebaldi, C., Van Vuuren, D. P., Eyring, V., Friedlingstein, P., Hurtt, G., Knutti, R., Kriegler, E., Lamarque, J. F., Lowe, J., Meehl, G. A., Moss, R., Riahi, K., & Sanderson, B. M. (2016). The Scenario Model Intercomparison Project (ScenarioMIP) for CMIP6. *Geoscientific Model Development*, *9*(9), 3461–3482. https://doi.org/10.5194/gmd-9-3461-2016

Önol, B., & Semazzi, F. H. M. (2009). Regionalization of climate change simulations over the eastern Mediterranean. *Journal of Climate*, *22*(8), 1944–1961. https://doi.org/10.1175/2008JCLI1807.1

Özdoğan, M. (2011). Climate change impacts on snow water availability in the euphrates-tigris basin. *Hydrology and Earth System Sciences*, *15*(9), 2789–2803. https://doi.org/10.5194/hess-15-2789-2011

Pan, H.-L., & Mahrt, L. (1987). *Interaction between Soil Hydrology and Boundary-layer Development*.

Pokhrel, Y., Felfelani, F., Satoh, Y., Boulange, J., Burek, P., Gädeke, A., Gerten, D., Gosling, S. N., Grillakis, M., Gudmundsson, L., Hanasaki, N., Kim, H., Koutroulis, A., Liu, J., Papadimitriou, L., Schewe, J., Müller Schmied, H., Stacke, T., Telteu, C. E., … Wada, Y. (2021). Global terrestrial water storage and drought severity under climate change. *Nature*

*Climate Change*, *11*(3), 226–233. https://doi.org/10.1038/s41558-020-00972-w

Riahi, K., van Vuuren, D. P., Kriegler, E., Edmonds, J., O'Neill, B. C., Fujimori, S., Bauer, N., Calvin, K., Dellink, R., Fricko, O., Lutz, W., Popp, A., Cuaresma, J. C., KC, S., Leimbach, M., Jiang, L., Kram, T., Rao, S., Emmerling, J., … Tavoni, M. (2017). The Shared Socioeconomic Pathways and their energy, land use, and greenhouse gas emissions implications: An overview. *Global Environmental Change*, *42*, 153–168. https://doi.org/10.1016/j.gloenvcha.2016.05.009

Rijtema, P. E. (1965). *An analysis of actual evapotranspiration V^ LANDB01 WAGENINGi*.

Samuel, J. B., & Chakraborty, A. (2023). Integration of a Groundwater Model to the Noah Land Surface Model for Aquifer-Soil Interaction. *Journal of Advances in Modeling Earth Systems*, *15*(7). https://doi.org/10.1029/2022MS003153

San, M., Nacar, S., Kankal, M., & Bayram, A. (2024). Spatiotemporal analysis of transition probabilities of wet and dry days under SSPs scenarios in the semi-arid Susurluk Basin, Türkiye. *Science of the Total Environment*, *912*. https://doi.org/10.1016/j.scitotenv.2023.168641

Sari, C., & Demirkaya, H. (2012). *October 9th, 2011 Flood Disaster in Haskızılören (Serik-Antalya)*. https://www.researchgate.net/publication/339068511

Şensoy, A., Uysal, G., Doğan, Y. O., & Civelek, H. S. (2023). The Future Snow Potential and Snowmelt Runoff of Mesopotamian Water Tower. *Sustainability (Switzerland)*, *15*(8). https://doi.org/10.3390/su15086646

Skamarock, W. C., Klemp, J. B., Dudhia, J., Gill, D. O., Barker, D. M., Duda, M. G., Huang, X.-Y., Wang, W., & Powers, J. G. (2008). *A Description of the Advanced Research WRF Version 3*.

Stewart, I. T. (2009). Changes in snowpack and snowmelt runoff for key mountain regions. In *Hydrological Processes* (Vol. 23, Issue 1, pp. 78–94). https://doi.org/10.1002/hyp.7128

Taylor, K. E., Stouffer, R. J., & Meehl, G. A. (2012). An overview of CMIP5 and the experiment design. In *Bulletin of the American Meteorological Society* (Vol. 93, Issue 4, pp. 485–498). https://doi.org/10.1175/BAMS-D-11-00094.1

Tokarska, K. B., Stolpe, M. B., Sippel, S., Fischer, E. M., Smith, C. J., Lehner, F., & Knutti, R. (2020). Past warming trend constrains future warming in CMIP6 models. In *Sci. Adv* (Vol. 6). https://www.science.org

TSMS. (2010). *2009 Climate Data Evaluation Report*.

Türkes, M. (2012). Türkiye'de Gözlenen ve Öngörülen Đklim Değişikliği, Kuraklık ve Çölleşme Observed and Projected Climate Change, Drought and Desertification in Turkey Murat TÜRKEŞ. In *Ankara Üniversitesi Çevrebilimleri Dergisi* (Vol. 4, Issue 2).

*Understanding shared socio-economic pathways (ssps)*. Climate Data Canada. (2023b, July 20). https://climatedata.ca/resource/understanding-shared-socio-economic-pathways-ssps/

Weatherl, R. K., Salgado, M. J. H., Ramgraber, M., Moeck, C., & Schirmer, M. (2021). *Estimating surface runoff and groundwater recharge in an urban catchment using a water balance approach*.

Yao, H., Field, T., McConnell, C., Beaton, A., & James, A. L. (2018). Comparison of five snow water equivalent estimation methods across categories. *Hydrological Processes*, *32*(12), 1894–1908. https://doi.org/10.1002/hyp.13129

Ye, B., Yang, D., & Ma, L. (2012). Effect of precipitation bias correction on water budget calculation in Upper Yellow River, China. *Environmental Research Letters*, *7*(2). https://doi.org/10.1088/1748-9326/7/2/025201

Yilmaz, A. G., & Imteaz, M. A. (2014). Climate change and water resources in Turkey: A review. In *International Journal of Water* (Vol. 8, Issue 3, pp. 299–313). Inderscience Publishers. https://doi.org/10.1504/IJW.2014.064222

Yilmaz, K., & Yazicigil, H. (2011). *Climate Change and its Effects on Water Resources*. http://www.nato.int/science

Yilmaz, T., & Bulut, B. (2015). *Dicle Üniversitesi Mühendislik Fakültesi mühendislik dergisi Türkiye'deki 2000-2015 yılları arasındaki buharlaşma ve terlemenin NOAH hidrolojik modeli ile incelenmesi Öz*.

Yilmaz, Y. A., Sen, O. L., & Turuncoglu, U. U. (2019). Modeling the hydroclimatic effects of local land use and land cover changes on the water budget in the upper Euphrates – Tigris basin. *Journal of Hydrology*, *576*, 596–609. https://doi.org/10.1016/j.jhydrol.2019.06.074

Yoon, Y., Kumar, S. V., Forman, B. A., Zaitchik, B. F., Kwon, Y., Qian, Y., Rupper, S., Maggioni, V., Houser, P., Kirschbaum, D., Richey, A., Arendt, A., Mocko, D., Jacob, J., Bhanja, S., & Mukherjee, A. (2019). Evaluating the uncertainty of terrestrial water budget components over high mountain Asia. *Frontiers in Earth Science*, *7*. https://doi.org/10.3389/feart.2019.00120

Yucel, I., Güventürk, A., & Sen, O. L. (2015). Climate change impacts on snowmelt runoff for mountainous transboundary basins in eastern Turkey. *International Journal of Climatology*, *35*(2), 215–228. https://doi.org/10.1002/joc.3974

Zhang, Y., Pan, M., Sheffield, J., Siemann, A. L., Fisher, C. K., Liang, M., Beck, H. E., Wanders, N., MacCracken, R. F., Houser, P. R., Zhou, T.,

Lettenmaier, D. P., Pinker, R. T., Bytheway, J., Kummerow, C. D., & Wood, E. F. (2018). A Climate Data Record (CDR) for the global terrestrial water budget: 1984-2010. In *Hydrology and Earth System Sciences* (Vol. 22, Issue 1, pp. 241–263). Copernicus GmbH. https://doi.org/10.5194/hess-22-241-2018

Zheng, H., Fei, W., Yang, Z.-L., Wei, J., Zhao, L., & Li, L. (n.d.). *An ensemble of 48 physically perturbed model estimates of the 1/8° terrestrial water budget over the conterminous United States, 1980-2015*. https://doi.org/10.5281/zenodo.7109816